Structural and Functional analysis of mTORβ

Christopher Fu

A thesis submitted to the University College of London in fulfilment with the requirements for the degree of Master of Philosophy

London, August 2012

Research Department of Structural and Molecular Biology
University College, London
Gower Street
London WC1E 6BT
United Kingdom

DECLARATION

I, Christopher Fu declare that all work presented in this thesis is the result of my own work. The work presented here does not constitute part of any other thesis. Where information has been derived from other sources, I confirm this has been indicated in the thesis. The work herein was carried out while I was a graduate student at the University College London, Research Department of Structural and Molecular Biology under the supervision of Professor Ivan Gout and Dr Andrew Martin.

Christopher Fu

Abstract

mTOR is a serine/threonine protein kinase that has been shown to be a key player in the regulation of cell growth and proliferation. Furthermore, mTOR forms the catalytic core of two known mTOR complexes, mTORC1 and mTORC2. These complexes sense various intra and extracellular signals, and regulate cellular processes that are critical for cell growth and proliferation. However, when conventional mTOR signalling is deregulated, cellular homeostasis is disrupted, resulting in a wide range of human diseases such as diabetes, neurodegeneration and cancer. Due to its involvement in tumorigenesis, mTOR has attracted enormous interest as a therapeutic target. Initially, the classical mTOR inhibitor rapamycin was tested as a potential treatment. However, when the compound was assessed in clinical trials, it proved to be of limited efficacy. This led to the design of novel types of inhibitors, which are currently being evaluated. The results obtained with rapamycin clearly indicated that our understanding of the mTOR signalling pathway is far from complete.

In addition, mTOR is currently known to exist in two isoforms, which are generated by alternative splicing of the transcript. These are known as mTORα and mTORβ respectively. The mTORα protein was the first isoform discovered and is 2,549 residues long. mTORβ is approximately one third of the length at 706 amino acids. Both proteins share identical C-terminal domains, but mTORβ lacks the N-terminal HEAT and FAT repeats that mTORα possesses. Work done in our lab has shown that mTORβ is capable of forming complexes with Raptor and Rictor, which are the key components of mTORC1 and mTORC2. Furthermore, overexpression of mTORβ transforms immortal cells and causes tumour formation in nude mice. It is

thought that modulation of cell proliferation via the mTOR signalling pathway could be achieved through mTORβ, which behaves as a protooncogene. Thus, mTORβ has the potential to be used as a target for anti-cancer therapies.

The first chapter of my thesis consisted of comparative modelling of mTORβ's C-terminal region from the FRB domain to the kinase domain. The model that was generated could then be used to give us insight into potential mechanisms for the inhibition of mTOR by either rapamycin or ATP-competitive inhibitors.

The second chapter examined the effects of two different mutations in mTOR's kinase domain on its activity. A point mutation (S2215Y) and a deletion of 12 amino acids (12del) were introduced into the kinase domain of mTORβ. Mutant proteins were expressed in HEK293 mammalian cells and the phosphorylation status of various mTOR substrates was assessed under different experimental conditions.

The final chapter of my thesis described how a TAP-tag fusion protein was created. This would have been used to search for novel mTORβ binding partners in mammalian cells had I chosen to complete my PhD studies.

Acknowledgements

A big thank you must go to my supervisors Professor Ivan Gout and Dr Andrew Martin for all their help and guidance during the production of my thesis, as well as everything that they taught me in the time that I worked with them. I am also grateful to Prof Helen Hailes and Dr Carolyn Moores for chairing my PhD committee. Thanks must also go to Prof Kaila Srai and Helen Notter for helping me with the thesis submission process.

What made the two years bearable at times when it was truly frustrating were my friends and colleagues. To Nadeem, Zeyad, the Dashas, Alex, Lena, Pascale, Yugo, Pei, Kamil, Nouf, Anja, Benoit and Mahmoud thank you for all your help, humour and support. Prof Saggerson has also been a source of ideas whenever I have encountered him in our lab common room, so I am grateful to him as well. I would also like to thank Max, Sandra, Anoup, Phil and Mina for lending me reagents and for help with cell culture. The trio of Mike, Ian and Rob also deserve a mention for their banter and always managing to make my trips to stores enjoyable. Do you remember antibody Chris?

Also, thanks to all the girls and guys I bumped into around the department and shared a joke with from time to time. You made life a bit more enjoyable.

Last of all I would like to thank my family, in particular my mother for spurring me on to complete this thesis and for all her support during my studies.

Rapanui – Where the m(s)TOR(y) all started

Contents

List of Figures

Abbreviations

4E-BP1	Eukaryotic initiation factor 4E binding protein 1
AB	Antibody
AMPK	AMP-activated protein kinase
ATP	Adenosine Triphosphate
BLAST	Basic Local Alignment Search Tool
Cryo-EM	Cryo-Electron Microscopy
DEPTOR	DEP-domain-containing mTOR-interacting protein
DMSO	Dimethyl Sulfoxide
DNA	Deoxyribonucleic Acid
DSSP	Dictionary of Secondary Structure Prediction
EBI	European Bioinformatics Institute
eIF4A	Eukaryotic translation initiation factor 4A
eIF4E	Eukaryotic translation initiation factor 4E
eIF4G	Eukaryotic translation initiation factor 4G
E-value	Expectation Value
FAT	FRAP, ATM and TRRAP
FAT	FRAP-ATM-TRRAP domain

FATC	FRAP-ATM-TRRAP-C-terminal domain
FATN	FRAP, ATM and TRRAP N-terminal
FATN	FRAP-ATM-TRRAP-N-terminal domain
FIT	Found in TOR
FKBP12	12-kDa FK506-binding protein
FRB	FKBP12-rapamycin binding domain
GS-TAP Tag	Protein G/Streptavidin Binding Peptide TAP Tag
HEK293	Human Embryonic Kidney 293 Cells
KOG1	Kontroller of Growth
LB	Luria Broth
LKB1	Liver Kinase B1
MAPK	Mitogen-activated protein kinase
mLST8	Mammalian lethal with SEC13 protein 8; aka GβL
mRNA	Messenger Ribonucleic Acid
mSIN1	Mammalian stress-activated MAP kinase-interacting protein 1
mTOR	Mammalian Target of Rapamycin
mTORC1	Mammlian Target of Rapamycin Complex 1
mTORC2	Mammalian Target of Rapamycin Complex 2
MW	Molecular Weight
NMR	Nuclear Magnetic Resonance
PDB	Protein Data Bank

PI3K	Phosphoinositide 3-kinase
PI3Kγ	Phosphoinositide 3-kinase Gamma
PI3Kδ	Phosphoinositide 3-kinase Delta
PI4K	Phosphatidylinositol 4-kinase
PIKK	Phosphatidyl inositol 3’ kinase-related kinases
PP2A	Protein Phosphatase 2
PRAS40	Prolone-rich AKT substrate 40kDa
PROTOR1	Protein observed with Rictor
Rag	Recombination Activation protein
RNA	Ribonucleic Acid
S6K1	S6 Kinase 1
TAE	Tris-acetate-EDTA
TAP	Tandem affinity purification
TBST	Tris-Buffered Saline and Tween 20
TNFα	Tumour Necrosis Factor-Alpha
TOR	Target of Rapamycin
TRAAP	Transformation domain-associated protein
UV	Ultra-violet

Chapter 1

General Introduction

Chapter 1: General Introduction

Overview of mTOR

Target of Rapamycin (TOR) first rose to prominence as the cellular target for the macrocylic lactone, rapamycin in yeast cells. Further studies in higher eukaryotes revealed that a similar protein existed in mammals, which was named the mammalian target of rapamycin (mTOR). mTOR, also known as FRAP, RAFT1, SEPT and RAPT1 (Harris & Lawrence, Jr. 2003b), is an evolutionarily conserved 289-kDa serine/threonine kinase that belongs to the phosphatidylinositol kinase-related kinase (PIKK) family (Laplante & Sabatini 2009). Other members of this family include ATM, ATR, DNA-PK, SMG1 and TRRAP (Sengupta, Peterson, & Sabatini 2010); (Hall 2008) Robitaille & Hall 2008). All the PIKK proteins possess a C-terminal protein kinase domain that shares significant sequence similarity to the catalytic domains of PI3Ks and PI4Ks (Wullschleger, Loewith, & Hall 2006). However, unlike the PI3Ks and PI4Ks, mTOR does not display lipid kinase activity. Instead, mTOR is capable of phosphorylating cellular proteins at two specific sites; a threonine or serine residue followed by a proline (Thr/Ser-Pro), and a threonine or serine adjacent to a large hydrophobic (Φ) amino acid (Φ-Ser/Thr-Φ) (Hall 2008). Besides its kinase activity, mTOR has no other known enzymatic functions (Yip et al. 2010).

mTOR forms the catalytic core of two known, distinct signalling complexes; mTORC1 and mTORC2. As the key components of the mTOR signalling pathway, these complexes sense various intracellular and extracellular signals, and respond by modulating the appropriate cellular processes to maintain cellular homeostasis. As such, abundant experimental evidence suggests that deregulation of mTOR signalling results in a host of human diseases ranging from diabetes to cancer and cardiac

hypertrophy (**Fig. 1.1**). Due to its critical involvement in tumorigenesis, mTOR has attracted enormous interest as a therapeutic target for the treatment of cancer.

It has also been shown that several isoforms of mTOR exist. mTORα was the first mTOR isoform discovered, but a second isoform, denoted mTORβ has recently been revealed (Panasyuk et al. 2009). The focus of my studies was to to elucidate the mTORβ signalling pathway in both normal and cancerous cells.

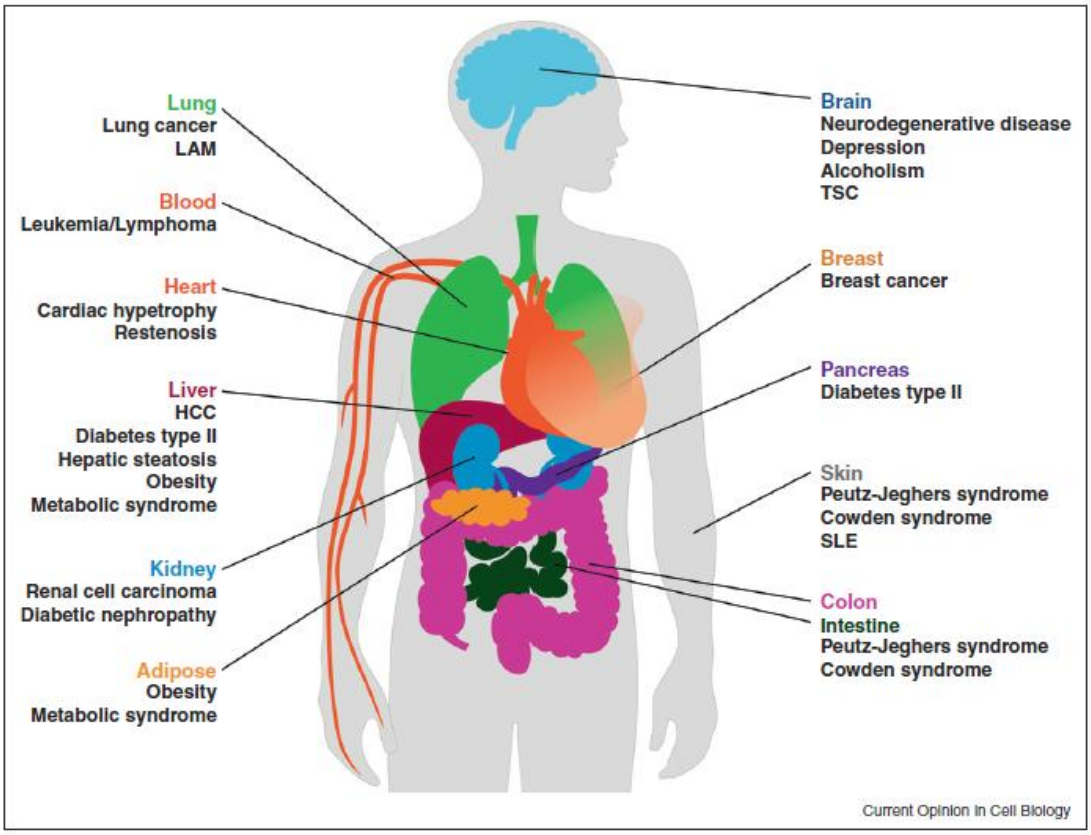

Fig. 1.1, Diseases linked to dysregulated mTOR signalling and the corresponding affected organs. (Dazert & Hall 2011)

Subcellular localisation of mTOR and its importance in mTOR signalling

Work conducted by several groups has led to the conclusion that mTOR is primarily cytosolic. However, mTOR has also been found on the membranes of several intracellular organelles such as the Golgi, endoplasmic reticulum and mitochondria (Desai, Myers, & Schreiber 2002), (Drenan et al. 2004), (Liu & Zheng 2007), (Sabatini et al. 1999), (Tirado et al. 2003), (Withers et al. 1997). These results are consistent with the multitude of cellular activities that are regulated by the mTOR complexes. Indeed, there is mounting evidence which suggests that mTOR signalling could be regulated by membrane trafficking. For example, it appears that amino acids are essential in the shuttling of mTORC1 to the lysosomal surface, where it is able to respond to growth factors. The localisation of mTORC1 to the lysosome also implies that it may play a direct role in the regulation of autophagy. This is possible because autophagic membranes fuse with lysosomes, where their contents are then degraded. The proximity of mTORC1 to the region of degradation places it in an ideal position to phosphorylate and cause the inhibition of proteins that promote autophagy. Unfortunately, the precise subcellular location(s) of mTORC2 is currently unknown. Nevertheless, a recent study suggested that yeast TORC2 localises to specific, dot-like domains on the plasma membrane (Berchtold & Walther 2009).

Also of interest is the existence of a Golgi/ER localisation sequence in mTOR's HEAT repeats. When GFP was fused to the HEAT repeats, it was later detected at the Golgi/ER (Liu & Zheng 2007). Furthermore, Phosphatidic acid (PA) is able to bind to mTOR's FRB domain, which suggests that PA may mediate movement of mTOR to cellular membranes. Finally, mTOR translocates between the cytoplasm and the nucleus, but the mechanism for this process remains unknown.

The structure of mTOR and the different mTOR isoforms

mTORα

In humans, the mTOR gene encodes a protein of 2,549 amino acids and is composed of several conserved structural domains. At the extreme N-terminus of mTOR, there are a series of 20 HEAT repeats (Andrade & Bork 1995). Each of the HEAT motifs is ~39 amino acids in length and possesses three highly conserved positions consisting of the residues Proline, Aspartic acid and Arginine. Every HEAT repeat also contains several conserved hydrophobic amino acids. It is thought that the structure of mTOR's HEAT repeats could resemble those of PP2A's A subunit. In PP2A, each individual HEAT repeat is formed from a pair of antiparallel α helices that stack alongside other repeats to create an ordered array (Groves et al. 1999). The HEAT region is postulated to mediate protein-protein interactions, due to the extensive surface formed by its stacked helices. For example, the protein Gephyrin which is required for the clustering of glycine receptors in neurons, interacts with one of mTOR's HEAT repeats. (Sabatini et al. 1999)

Adjacent to the HEAT motifs is the relatively large helical FAT (for *F*RAP, *A*TM, *T*RAP) domain, which is common amongst the PIKKs. Overexpression of this domain in yeast led to arrest of the G_1 phase of the cell cycle (Alarcon et al. 1999). It was thought that this could be due to the sequestration of requisite interacting proteins away from TOR1. Downstream of the FAT domain is the FRB (for FKBP12-rapamycin binding) domain. This portion of the mTOR protein is able to bind the FKBP12-rapamycin complex, which inhibits mTOR kinase activity. A crystal structure of the FRB domain bound to the FKBP12-rapamycin complex has been elucidated (Choi et al. 1996). This model showed that there were numerous interactions between rapamycin and FRB, but a smaller number of interactions

between FKBP12 and FRB. These results suggest that FKBP12 presents rapamycin to mTOR in a conformation that facilitates interaction with FRB. In addition to the FRB domain, the C-terminal half of mTOR also contains the catalytic domain, followed by a putative negative regulatory domain (RD) (Sekulic et al. 2000) and a FATC domain. The potential negative regulatory domain is phosphorylated in response to growth factors and insulin (Scott et al. 1998), (Nave et al. 1999), (Sekulic et al 2000). It has been shown that the FATC domain is crucial for mTOR's kinase activity. Deletion of just one amino acid from this domain, or the addition of an epitope tag to the C-terminus virtually abolishes the kinase activity of mTOR (Takahashi et al. 2000). Furthermore, it is thought that FATC and FATN may interact and fold in a manner that facilitates exposure of the catalytic domain. Moreover, a NMR study revealed that the FATC domain forms a disulphide bridge between two conserved cysteine residues (Dames et al. 2005). mTOR contains numerous phosphorylation sites: **Ser2448, Ser2481, Thr2446** and **Ser1261**. These are shown in **Fig. 1.2**.

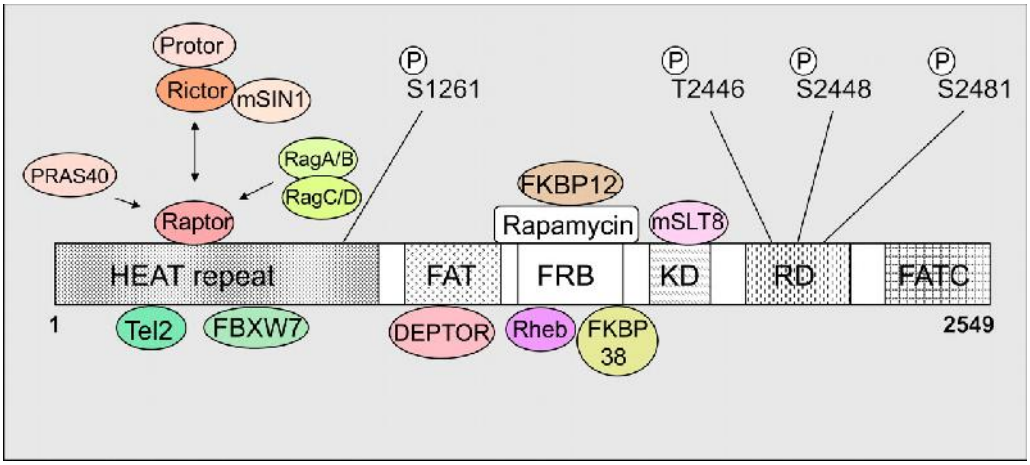

Fig. 1.2, Schematic diagram of mTOR domains: The 2549-amino acid mTOR protein is depicted above a scale indicating amino acid residue number. The different mTOR domains are shown in grey and white. Other proteins that mTOR is known to interact with or form complexes with have been shaded in various colours (Watanabe et al. 2011) .

mTORβ

mTORβ is 706 residues in length and is a splicing iso form of mTOR (see **Fig. 1.3** for a detailed schematic). The sole difference between the two isoforms is that mTORβ lacks mTORα's HEAT as well as the majority of its FATN domains. Furthermore, mTORβ is a protein kinase that has the ability to stimulate cellular proliferation and to control the cell cycle progression via the G1/S phase (Panasyuk et al 2009). Downstream signalling is effected by mTORβ when it forms complexes with the Rictor and Raptor proteins. In vitro, mTORβ has also been shown to phosphorylate several mTORα substrates such as S6K1, PKB/AKT and 4EBP1 (Panasyuk et al 2009). Moreover, it has been demonstrated that overexpression of mTORβ transforms immortal cells and causes tumour formation in nude mice (Panasyuk et al 2009). It is thought that modulation of cell proliferation via the mTOR signalling pathway could be achieved through mTORβ, which behaves as a protooncogene. Thus, mTORβ has the potential to be used as a target for anti-cancer therapies.

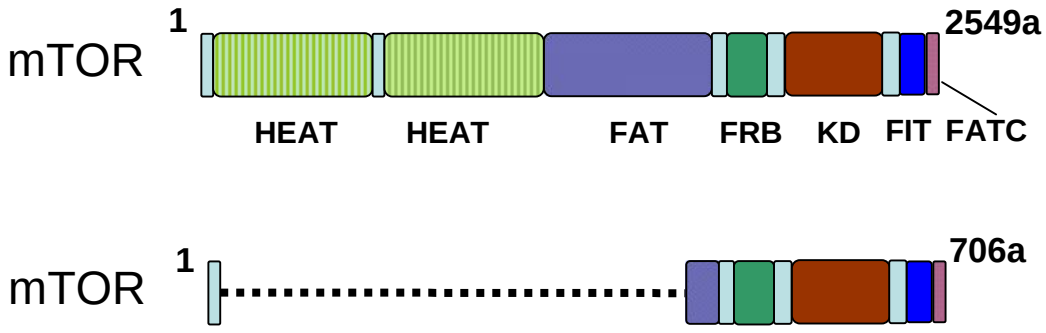

Fig. 1.3, Comparison of the mTORα and mTORβ proteins: The domains have been colour coded in both proteins, so common domains share the same coloration.

Comparative Modelling of mTOR

At present, no crystal structures exist for either the full-length mTOR protein or for its kinase domain. In the interim, before the acquisition of crystallographic data, in silico models may help us to develop more potent and effective mTOR inhibitors. In 2009, Sturgill and Hall used homology modelling to produce a model of TOR's catalytic region from its FAT domain to near the end of the FATC domain (Sturgill & Hall 2009). In human TOR, this corresponded to amino acid residues 1906-2526. The model was based on PI3KCγ's crystal structure and is shown in **Fig. 1.4**. The creation of this model allowed visualisation of the ATP-binding pocket, and use of molecular docking software (MGL tools 1.6.0 with AutoGrid4 and AutoDock4 (Scripps)) revealed how ATP binds to mTOR. Furthermore, the model also showed that activating mutations in TOR are located in the catalytic, helical and FIT domains. Interestingly, oncogenic mutations in PI3KCα were also centred in the helical and catalytic domains, as well as in helix kα11 of the C-terminus. Helix kα11 corresponds to part of the FIT domain in TOR. The location of mutations in similar regions in the two proteins provided further evidence that they also shared structural similarities. Crucially, the model shed new light on potential mechanisms for the regulation of TOR.

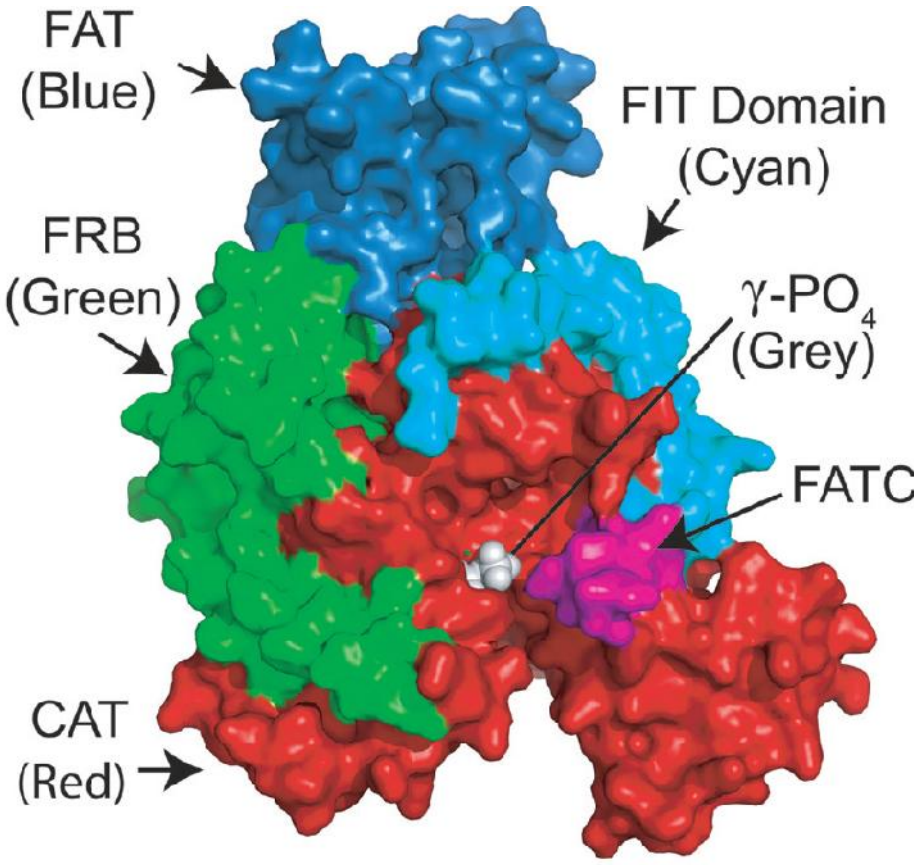

Fig. 1.4, The model of TOR's catalytic portion generated by using PI3KCγ as the homologue. The different domains have been highlighted and clearly labelled. The γ-PO_4 of ATP is visible in the ATP-binding pocket of TOR's catalytic domain. (Sturgill & Hall 2009)

Overview of the mTOR Complexes

mTOR is known to nucleate at least two distinct protein complexes, which have been denoted mTORC1 and mTORC2. Both mTORC1 and mTORC2 share common subunits (mTOR, mLST8/GβL and deptor), but are differentiated by unique components. Rapamycin in complex with the immunophilin FKBP12 is capable of inhibiting mTORC1 by binding to the FRB domain of the mTOR subunit (Loewith et al. 2002). In contrast to mTORC1, mTORC2 does not directly bind FKBP12-rapamycin. The activity of the complex is unaffected by acute treatment with rapamycin. Nevertheless, in approximately 20% of cancer cell lines, the assembly of mTORC2 is disrupted by prolonged exposure to rapamycin. This has the consequence of diminishing the cellular quantities of functional mTORC2. Why this phenomenon is only observed in a subset of cancerous cell lines remains to be elucidated.

mTORC1 is sensitive to intracellular and extracellular signals such as the cell's energy status, growth factors and nutrients. When these are present in abundance, mTORC1 stimulates anabolic and inhibits catabolic cellular processes. However, when the cell is subjected to stress signals or starvation, mTORC1 activity is curtailed. This ensures that biosynthetic rates in the cell are maintained at a level that corresponds to a limited supply of raw materials for cell growth (Dunlop & Tee 2009), (Ma & Blenis 2009), (Reiling & Sabatini 2006). mTORC1 is known to play a pivotal role in the regulation of protein synthesis via its downstream substrates 4E-BP1 and S6K1. It has also been shown that mTORC1 stimulates the biogenesis of ribosomes by augmenting the transcription of ribosomal RNAs and proteins. The result is that the cell's protein biosynthetic capacity is markedly increased (Inoki et al. 2005). Moreover, diminished mTORC1 signalling has the effect of promoting macroautophagy. This is a process whereby certain intracellular components are

degraded to yield amino acids and other biological materials for the continuation of anabolic activities such as energy production and protein synthesis. In effect, it is a mechanism that enables the cell to survive when faced with a dearth of nutrition. The function of several transcription factors that are involved in mitochondrial metabolism and lipid synthesis are also modulated by mTORC1.

The modulation of actin cytoskeleton organisation was the first cellular function that was attributed to mTORC2. It has now come to light that mTORC2 is also involved in the control of cell cycle progression and cell size (Rosner et al. 2009). It is currently known that mTORC2 phosphorylates and activates three substrates; protein kinase C (PKC), serum- and glucocorticoid-regulated kinase (SGK) and Akt. These three proteins are all members of the AGC kinase family and regulate anabolism, cell cycle progression and cell survival (Facchinetti et al. 2008), (Garcia-Martinez & Alessi 2008), (Ikenoue et al. 2008), (Sarbassov et al. 2005). From a therapeutic perspective, the study of Akt is particularly important due to its involvement in cancer and diabetes. However, when compared with mTORC1, our knowledge of mTORC2 signalling pales in comparison. This is largely due to the lack of mTORC2 inhibitors, especially its indifference to the classical mTOR inhibitor rapamycin. A diagram illustrating the different cellular functions that are regulated by mTORC1 and mTORC2 is shown in **Fig. 1.5**.

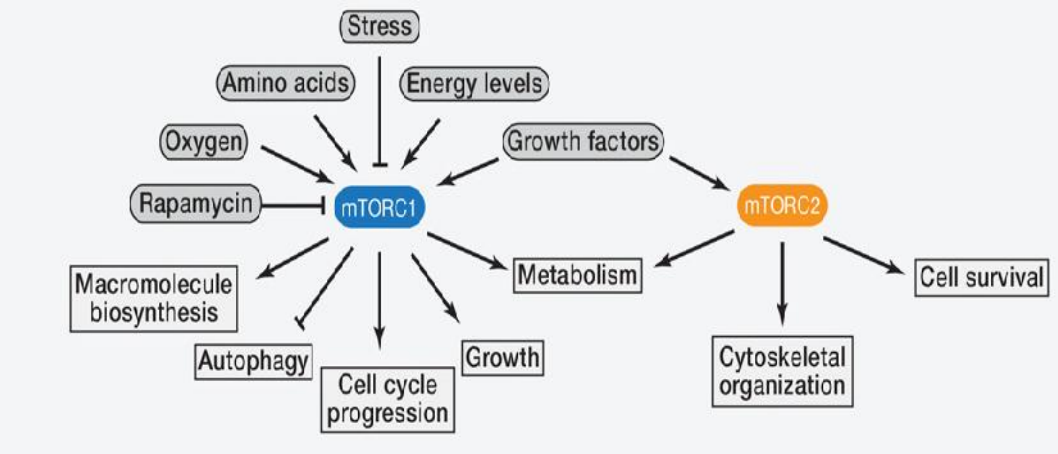

Fig. 1.5, Cellular functions regulated by mTORC1 and mTORC2. The mTOR kinase nucleates two distinct protein complexes termed mTORC1 and mTORC2. mTORC1 responds to amino acids, stress, oxygen, energy and growth factors and is acutely sensitive to rapamycin. It promotes cell growth by inducing and inhibiting anabolic and catabolic processes, respectively, and also drives cell-cycle progression. mTORC2 responds to growth factors and regulates cell survival and metabolism, as well as the cytoskeleton. mTORC2 is insensitive to acute rapamycin treatment but chronic exposure to the drug can disrupt its structure. (Laplante & Sabatini 2012)

The Structure of mTORC1

mTORC1 is composed of at least 5 different protein subunits. These include **mTOR**, which acts as the catalytic subunit of the complex; proline-rich AKT substrate 40kDa (**PRAS40**); regulatory-associated protein of mTOR (**Raptor**); mammalian lethal with Sec13 protein 8 (**mLST8**, aka GβL); and DEP-domain-containing mTOR-interacting protein (**Deptor**) (Peterson et al. 2009). mTOR, Raptor and mLST8 are indispensable for mTORC1 to mediate its cellular functions (Loewith et al. 2002), (Kim et al. 2002), (Kim et al. 2003). Unfortunately, the precise function(s) of most of the component proteins remains an unknown quantity. In 2007, the cryo-EM structure of yeast TOR in complex with KOG1, which is the yeast counterpart of Raptor was elucidated. The 25Å structure showed that TOR's N-terminal HEAT repeats form a curved tubular-shaped domain that interacts with KOG1's WD40 repeat domain in the C-terminus. In addition, KOG1's N-terminus is in the vicinity of TOR's kinase domain. It is thought that due to its propinquity to the catalytic region, KOG1's functions could be to recruit and present substrates to the kinase domain (Adami et al. 2007). A cryo-EM structure for mTORC1 has also been obtained. This model showed that mTORC1 exists as an obligate dimer that has a rhomboid shape and an aperture in its centre (Yip et al. 2010). See **Figs 1.6** and 1.**7**.

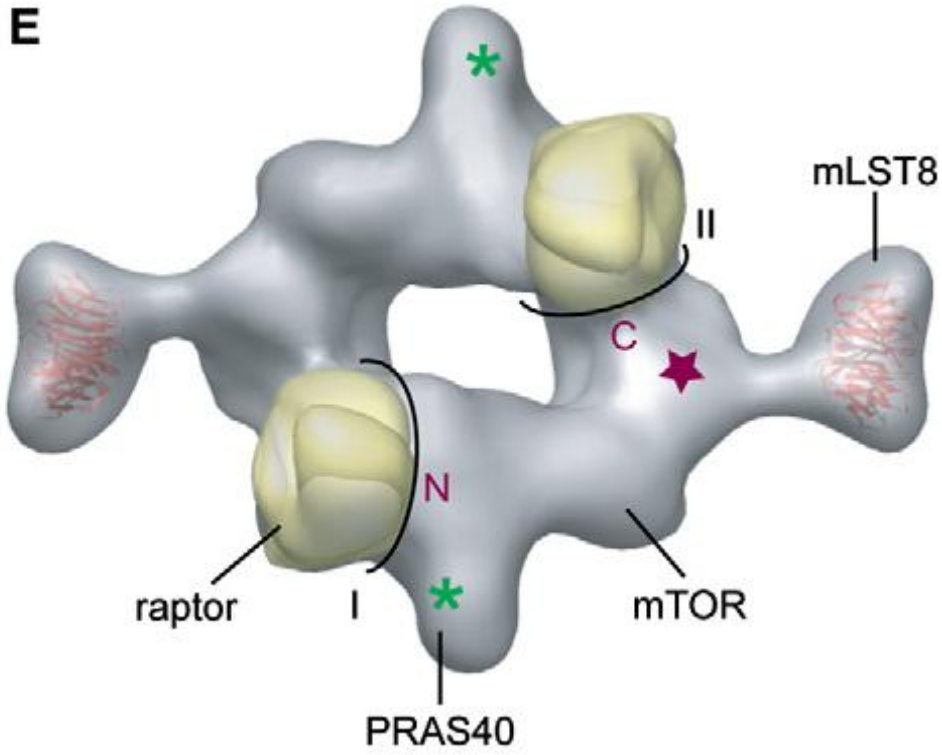

Fig. 1.6, Cryo-EM structure of mTORC1. The proposed locations of the N- and C-termini of mTOR have been marked and the purple star is the expected location of the kinase domain. The black lines I and II demarcate the two interaction faces formed by each mTOR molecule with the two raptor subunits. Antibody labelling was used to determine the positions of mLST8 and PRAS40 (green asterisk). (Yip et al. 2010)

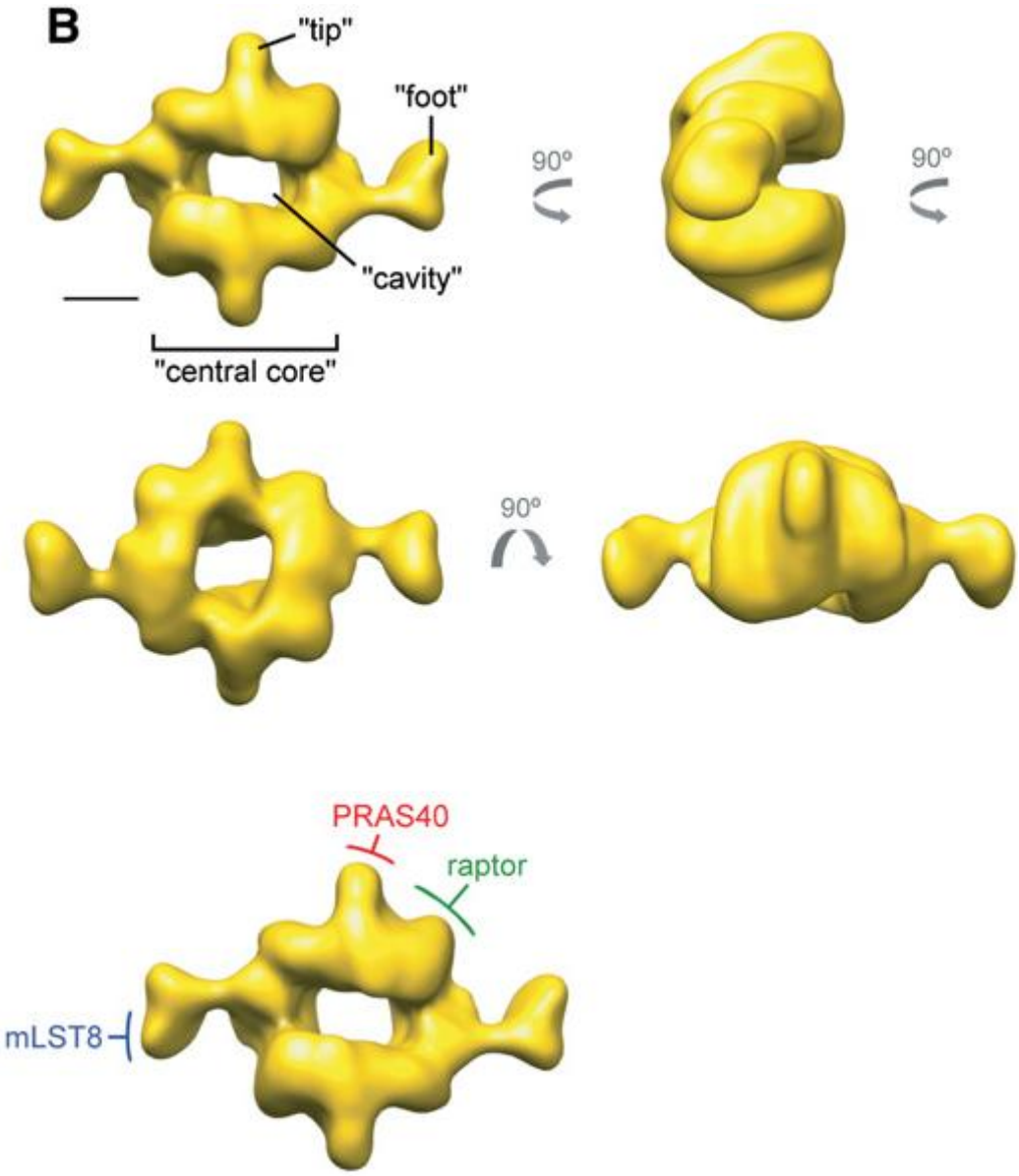

Fig. 1.7, Cryo-EM Reconstruction of mTORC1 filtered to 26Å, with the main structural features denoted. The protein has been shown from different angles and the locations of PRAS40, mLST8 and raptor have been marked. The scale bar represents 5nm. (Yip et al. 2010)

Raptor

Raptor behaves as an adaptor protein in mTORC1 by firstly binding and then presenting substrates to mTOR (Hara et al. 2002), (Kim et al. 2002). It has a MW of ~150kDa and its structural composition consists of an N-terminal RNC (raptor N-terminal conserved) domain adjacent to a set of three HEAT repeats and seven WD-40 repeats in the protein's C-terminus (Kim et al. 2002), (Kim et al. 2003).

mLST8

mLST8 has been shown to form an association with mTOR's kinase domain and to promote the kinase activity of mTOR (Kim et al. 2003). Nonetheless, it does not appear to be essential for the association of Raptor with mTOR (Guertin et al. 2006). The protein has a MW of 36-kDa and consists of seven WD40 repeats.

PRAS40 and Deptor

Both Deptor and PRAS40 have been defined as negative modulators of mTORC1 (Peterson et al. 2009), (Sancak et al. 2007), (Vander et al. 2007). Recruitment of PRAS40 and Deptor to mTORC1 stimulates mTORC1's inhibition. It is thought that PRAS40 modulates mTORC1 kinase activity by directly preventing the binding of substrates (Wang et al. 2007). Activation of mTORC1 results in it phosphorylating PRAS40 and Deptor. The physical interaction between mTORC1, PRAS40 and Deptor is then weakened, which serves to augment mTORC1 signalling to an even higher degree (Peterson et al. 2009), (Wang et al. 2007).

The Structure of mTORC2

In addition to mTOR, Deptor and mLST8 which are also possessed by mTORC1, mTORC2 also contains rapamycin-insensitive companion of mTOR (**Rictor**); protein observed with Rictor-1 (**Protor-1**) and mammalian stress-activated protein kinase interacting protein (**mSIN1**). A body of results supports the hypothesis that Rictor and mSIN1 exert a stabilising influence on one another, thereby creating the basis for mTORC2's structural foundation (Frias et al. 2006), (Jacinto et al. 2006). Protor-1 and Rictor also interact, but the significance of this association in unclear (Thedieck et al. 2007),. Mirroring its role in mTORC1, Deptor also regulates mTORC2 by exerting an inhibitory affect on its activity (Peterson et al. 2009). To date, Deptor is the only endogenous mTORC2 inhibitor that is known to exist. mLST8 is critical for the viability of mTORC2, since knockout of the protein gravely reduced the activity and stability of the complex (Guertin et al. 2006). A diagram showing the various proteins contained in mTORC1 and mTORC2 is shown in **Fig. 1.8**. A schematic showing the different mTOR complex components is displayed in **Fig. 1.9**.

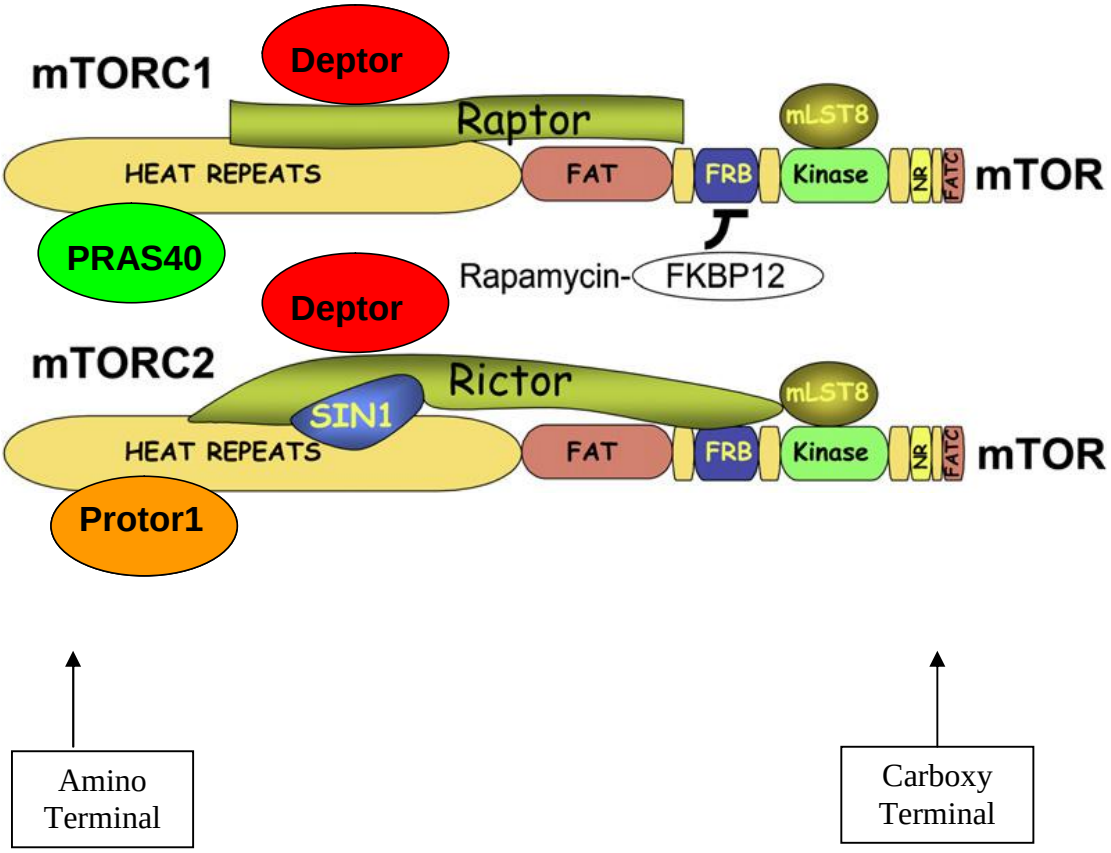

Fig. 1.8, The core components of the mTOR Complexes: The two distinct mTOR complexes are depicted. mTORC1 and mTORC2 both contain mTOR, Deptor and mLST8. The other proteins are unique to one of the complexes. mTORC1 possesses Raptor and PRAS40 exclusively, whereas Rictor, SIN1 and Protor1 are exclusive to mTORC2. Deptor is an inhibitor for both of the complexes. mLST8 binds to the kinase domain of both complexes, and appears to have an critical role in their assembly. Raptor functions as a scaffolding protein that links mTOR's kinase domain to mTORC1 substrates, which stimulates mTORC1 signalling. PRAS40 has been characterised as both a competitive mTORC1 substrate and a mTORC1 inhibitor. The function of Protor1 remains uncertain, but it has been shown that Rictor and mSIN1 promote the assembly and signalling of mTORC2. Rapamycin binds to its intracellular receptor FKBP12 and the complex formed interacts with the FRB domain in mTOR. The activity of mTORC1 is inhibited by rapamycin, whereas mTORC2 is only inhibited by prolonged treatment with high concentrations of rapamycin. (Modified from Bhaskar & Hay 2007)

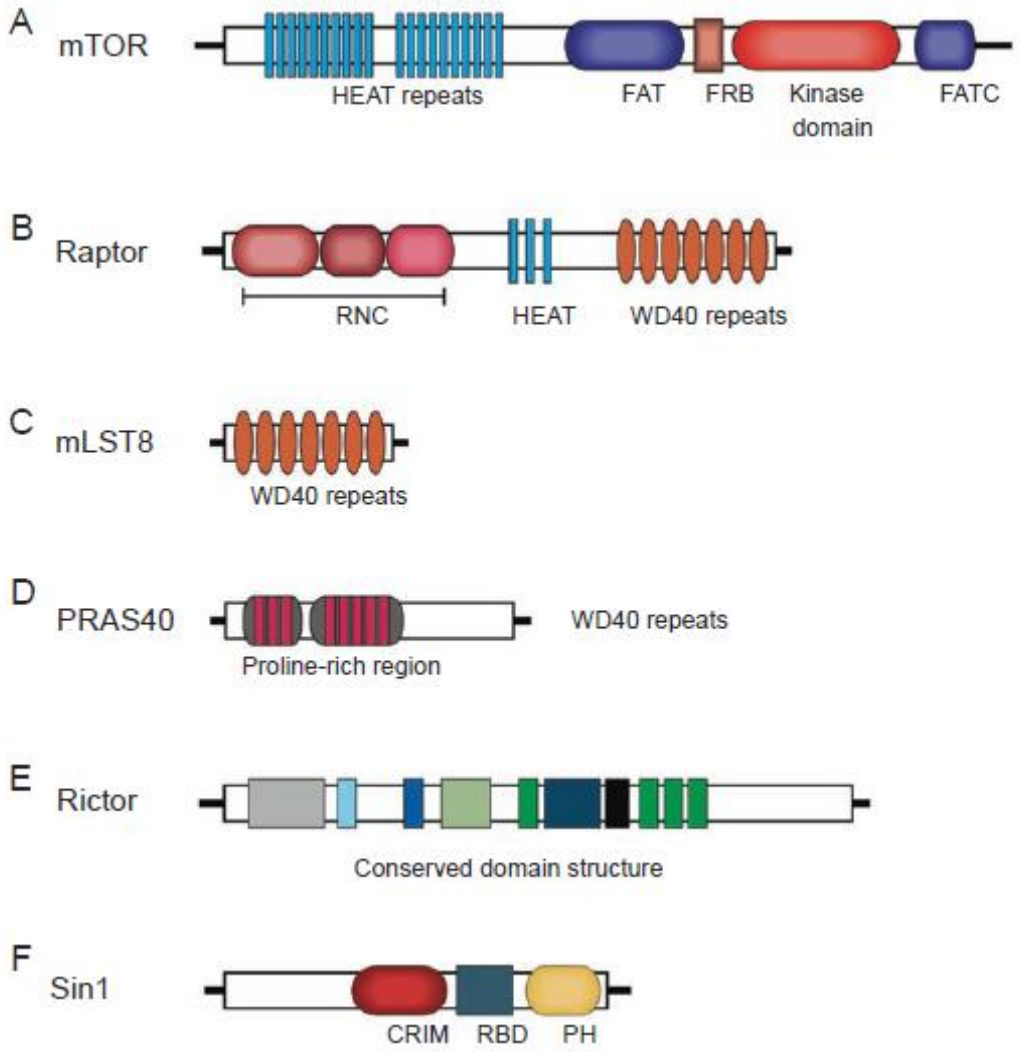

Fig. 1.9, Schematic of mTOR complex components. HEAT: a protein-protein interaction structure of two tandem anti-parallel α-helices found in *h*untingtin, *e*longation factor 3, PR65/*A* and *T*OR;; FAT: a domain structure shared by *F*RAP, *A*TM, and *T*RRAP, all of which are PIKK family members; FRB: *F*KBP12/*r*apamycin *b*inding domain; FATC: *FAT C*-terminus; RNC: *R*aptor *N*-terminal *c*onserved domain; WD40: about *40* amino acids with conserved *W* and *D* forming four anti-parallel beta strands; CRIM: *c*onserved *r*egion *i*n the *m*iddle; RBD: *R*as *b*inding *d*omain. (Yang & Guan 2007)

mTORC1 Signalling

Role in protein synthesis

Prior to division, a cell must double in size and mass. This process necessitates an augmentation in protein synthesis, which is dependent on a sufficient supply of nutrients and the presence of growth factors. G protein-coupled receptors and receptor Tyrosine kinases are activated by these extracellular signals. These in turn actuate key signal transduction pathways such as the Ras-ERK (extracellular signal-regulated kinase) pathway and the phosphoinositide 3-kinase (PI3K)-AKT pathway. mTORC1 signalling is then promoted by these upstream signal transduction networks. The contribution that mTORC1 makes to the increase in protein synthesis is two-fold. In the short-term (minutes) it activates translation, and on a longer time scale (hours) it augments the cell's overall translational capacity by augmenting the levels of certain translational components and ribosomes.

mRNA translation is traditionally divided into the three stages of initiation, elongation and termination. mTORC1 is currently known to regulate the initiation and elongation phases of protein synthesis. Of critical importance is the control of initiation since it is the rate-limiting step in the creation of new proteins. Initiation is modulated by mTORC1 via its two downstream substrates 4E-BP1 and S6K1 (Hay & Sonenberg 2004a), (Tee & Blenis 2005). Both S6K1 and 4E-BP1 contain TOS (TOR-signalling) motifs which bind to raptor, resulting in their recruitment to mTORC1 (Nojima et al. 2003;Schalm et al. 2003). In 4E-BP1 the TOS motif is located in the extreme C-terminus and consists of the sequence FEMDI (Phe-Glu-Met-Asp-Ile). The TOS sequence in S6K1 is situated in its N-terminus and is composed of the residues FDIDL (Phe-Asp-Ile-Asp-Leu) (Schalm et al. 2002). In vivo, this motif has been

shown to be required for the phosphorylation of these proteins by mTORC1 (Schalm & Blenis 2002).

When the cell is in a quiescent state, 4E-BP1 competes with the translation initiation factor eIF4G for an overlapping binding site on eIF4E. The association of 4E-BP1 with eIF4E prevents it from interacting with eIF4G and forming the eIF4F initiation complex. Contained within the initiation complex are eIF4E, eIF4G and crucially, the RNA helicase eIF4A. It is thought that eIF4A unravels secondary structure in 5'-UTRs (5'-untranslated regions) of mRNAs in order to permit the ribosome's 40S subunit and other accessory proteins to scan the mRNA and to find the start codon. This unravelling action is critically important for the translation of mRNAs that possess considerable secondary structure in their 5'-UTR regions. In essence, hypophosphorylated 4EBP-1 binds to eIF4E preventing it from forming the initiation complex, which inhibits translation. However, activated mTORC1 phosphorylates 4E-BP1 in a hierarchical manner on at least four of its numerous phosphorylation sites. In human 4E-BP1, the residues of interest are Thr37, Thr46, Thr70 and Ser65. Thr37 and Thr46 must be phosphorylated prior to the phosphorylation of Thr70 and Ser65 (Proud 2006a). Please see **Fig. 1.10** below for an illustration. The addition of phosphate groups to Thr37/Thr46 is totally independent of the TOS motif, but requires the 4E-BP1's N-terminal RAIP motif (Arg-Ala-Ile-Pro) (Wang et al. 2005), (Tee and Proud 2002). Phosphorylation of Thr70 and Ser65 leads to the dissociation of 4E-BP1 from eIF4E. This results in the binding of eIF4G to eIF4E and the creation of functional initiation complexes, thereby priming translation (**Fig. 1.11**).

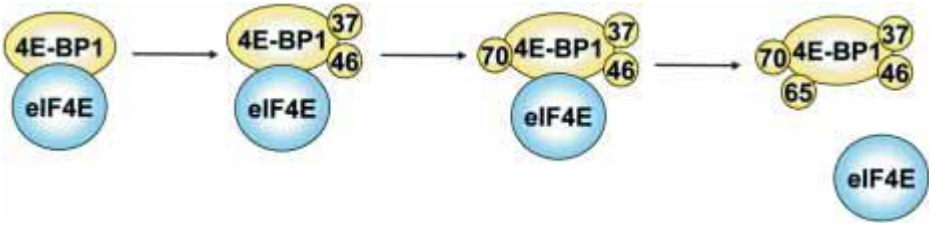

Fig. 1.10, Hierarchical phosphorylation of 4E-BP1 by mTORC1 results in release from eIF4E. Phosphorylation at four sites on 4E-BP1 occurs sequentially. mTORC1 directly phosphorylates the 'priming' sites Thr 37 and Thr 46, and then phosphorylates THr70 and Ser65. (Hay & Sonenberg 2004b)

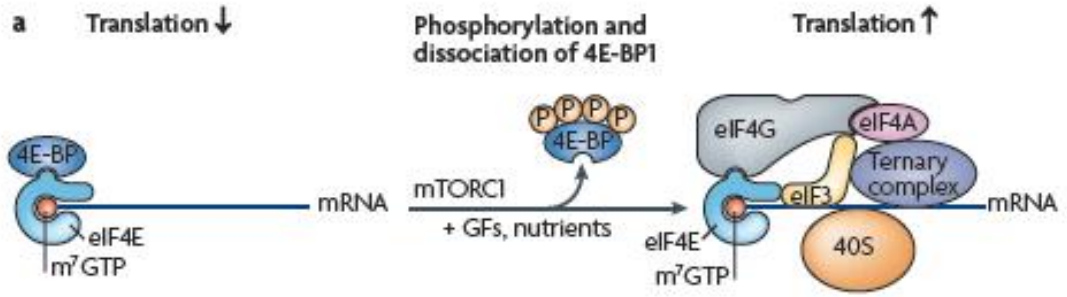

Fig. 1.11, Regulation of cap-dependent translation initiation by mTORC1 via 4E-BP. Hypophosphorylated 4E-binding proteins bind tightly to eIF4E, preventing it from interacting with eIF4G and thus inhibiting translation. When nutrients are abundant, mTORC1 phosphorylates 4E-BPs in a hierarchical manner, releasing the 4E-BP from eIF4E. This results in the recruitment of eIF4G to the 5' cap and allows translation initiation to proceed. (Ma & Blenis 2009)

S6K1 is a member of the AGC family of protein kinases and must be phoshporylated at two sites in order to be fully activated. These include Thr229 in the kinase domain's activation loop and Thr389 in the C-terminal's hydrophobic motif. mTORC1 firstly phosphorylates S6K1 on Thr389, which produces a docking site for phosphoinositide-dependent kinase 1 (PDK1). PDK1 then phosphorylates Thr229 which activates S6K1. This allows S6K1 to phosphorylate eIF4B on Ser422, resulting in its recruitment to the translation pre-initiation complex (Holz et al. 2005). eIF4B is a cofactor that significantly enhances the helicase activity of eIF4A when phosphorylated on its Ser422 residue (Hershey 1991). This has the consequence of greatly improving the efficiency and rapidity of translation initiation (**Fig. 1.12**). Furthermore, the protein Programmed cell death 4 (PDCD4) binds to eIF4A and is postulated to suppress eIF4A's helicase action (Yang et al. 2003). Upon stimulation with growth factors, S6K1 is able to phosphorylate PDCD4 on Ser67, resulting in its degradation through the ubiquitin ligase β-TrCP (Dorrello et al. 2006). As such, the phosphorylation of PDCD4 by S6K1 prevents PDCD4 from inhibiting eIF4A's helicase function. Moreover, the scaffold protein SKAR has been shown to associate with the activated form of S6K1, and recruits active S6K1 to newly formed mRNAs, where it augments the translational yield (Ma et al. 2008). In addition, Ribosomal protein S6 (rpS6 or just S6) is a component of the small (40S) ribosomal subunit and is phosphorylated by S6K1 when the environmental conditions favour cell growth and proliferation. Nevertheless, the phosphorylation of S6 is markedly disrupted by rapamycin, which insinuates that this could involve mTOR.

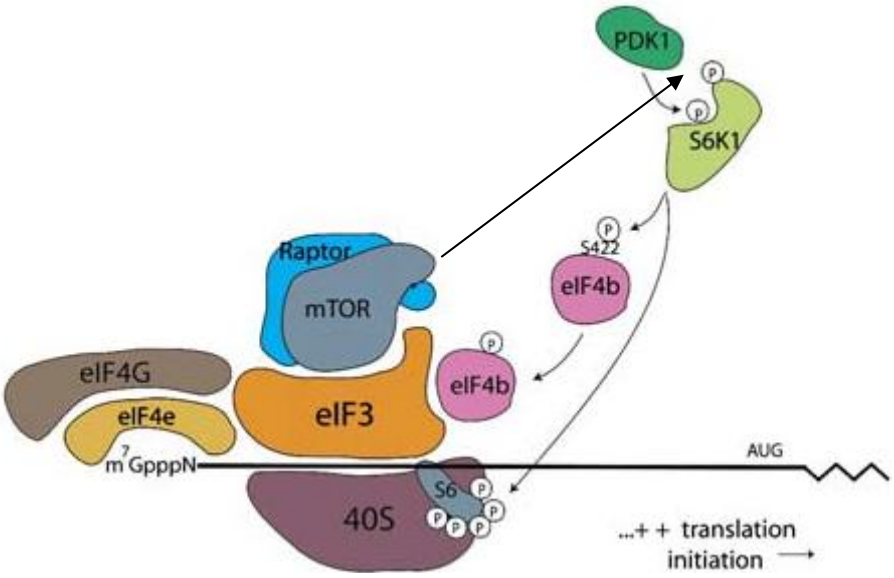

Fig. 1.12, Phosphorylation of S6K1 by mTORC1 augments the efficiency and rapidity of translation initiation. Growth factors and nutrients activate mTORC1 which then phosphorylates S6K1 on Thr389. This allows PDK1 to phosphorylate S6K1 on Thr229, which fully activates the protein. S6K1 then phosphorylates eIF4B on Ser422. eIF4B then associates with the eIF3 complex to facilitate cap-dependent translation initiation. (Peterson & Sabatini 2005)

Translation elongation is also regulated by mTORC1 via modulation of the phosphorylation status of eEF2 (eukaryotic elongation factor 2). The customary function of eEF2 is to assist in the translocation stage of elongation when it is dephosphorylated and active. However, eEF2 is inactivated by the addition of a phosphate group at its Thr56 residue by eEF2 kinase. eEF2 kinase is itself subject to regulation by phoshporylation on at least three in inhibitory sites (Ser76, Ser359 and Ser366 in human eEF2 kinase) by mTORC1 (Proud 2006b). Ser366 is phosphorylated by S6K but the precise mechanism whereby mTORC1 mediates phosphorylation of the other two residues is currently unknown. Consequently, mTORC1 signalling dephosphorylates and activates eEF2 in part by inhibiting eEF2 kinase by phosphorylation. Unphosphorylated and active eEF2 is then able to actuate the elongation apparatus.

Ribosomes are composed of approximately 85-90 distinct proteins (r proteins) and ribosomal RNAs (rRNAs). Translation of the r proteins is subject to regulation by mTOR. Furthermore, rDNA transcription which takes places in the nucleolus, and is primarily catalysed by RNA polymerase I (PolI), is also regulated by mTOR. It has been shown that mTOR is requisite for rDNA transcription activation (Hannan et al. 2003). The phosphorylation and function of UBF (upstream binding factor), which is an rDNA transcription factor is also positively modulated by mTOR. In the set of experiments conducted by Hannan et al. it was observed that S6K1 plays a key role in mediating the interaction between mTOR and its regulation of UBF an rDNA transcription. PolI transcription is also controlled by mTOR via its modulation of TIF-1A activity (Mayer et al. 2004). TIF-1A is a regulatory factor that is sensitive to the availability of growth factors and nutrients. When rapamycin is administered to cells,

TIF-1A is translocated into the cytoplasm, which has the consequence of inhibiting the formation of the transcription initiation complex.

Control of Autophagy

When cells are subjected to environmental stressors such as starvation and hypoxia, intracellular organelles are sequestered within autophagosomes and delivered to the lysosome (vacuole) for degradation. The subsequent release of biological material in the form of amino acids and other nutrients provides the raw material to sustain anabolic cellular functions such as energy production and protein synthesis, which are required for cell survival. It has been demonstrated that inhibition of mTORC1 augments autophagy, but activation of mTORC1 diminishes this process (Codogno & Meijer 2005). The regulation of autophagy by mTORC1 has been shown to be insensitive to treatment with rapamycin (Mayer, Zhao, Yuan, & Grummt 2004;Thoreen et al. 2009). Moreover, work conducted in the past couple of years by three different groups has shown that mTORC1 modulates autophagy via control of a protein complex comprising focal adhesion kinase family-interacting protein of 200kDa (FIP200), autophagy-related gene 13 (ATG13) and unc-51 like kinase 1 (ULK1) (Ganley et al. 2009;Hosokawa et al. 2009;Jung et al. 2009). These experiments demonstrated that mTORC1 suppresses autophagy by the phosphorylation and repression of ATG13 and ULK1. Furthermore, mTORC1 also regulates the movement of nutrient transporters, which stimulates the uptake of nutrients including amino acids, iron, lipoprotein and glucose (Edinger and Thompson 2002).

Regulation of Lipid Synthesis

The biosynthesis of lipids is of paramount importance for the preservation of cellular homeostasis. The lipids that cells produce (sphingolipids, glycerolipids, fatty acids, phospholipids and cholesterol) are utilised for various purposes. These include acting as an energy reserve and playing the role of signalling molecules. Additional functions include serving as the building blocks for the biosynthesis of membranes and providing the precursor molecules for the creation of numerous cellular products. When errors occur in the processing or synthesis of lipids, several diseases can arise such as type 2 diabetes and cancer.

Growth factors activate Rsk, Erk and Akt which leads to the phosphorylation and inactivation of TSC1/2, the upstream negative regulator of mTORC1. The subsequent activation of mTORC1, not only by the inhibition of TSC1/2, but also by the phosphorylation of PRAS40 by Akt, leads to the cleavage of SREBP-1. SREPBP-1 is a simple helix-loop-helix transcription factor that modulates lipid production by regulating the expression of genes necessary for the generation of phosholipid, fatty acid, triglyceride and cholesterol. mTORC1 mediated cleavage of SREBP-1 results in the protein's translocation from the ER where it is synthesised, to the nucleus where it is able to act as a transcription factor. Once in the nucleus, SREBP-1 is able to induce the expression of several genes that are required for lipogenesis. Fatty acid synthase (FASN), glucokinase (GK) and acetyl-CoA carboxylase represent an eclectic selection of these genes.

The biological process of adipogenesis consists of the creation of mature adipocytes from adipose precursor cells. The adipogenic cascade involves CCAAT/enhancer binding protein-β (C/EBP-β) and C/EBP-δ, which stimulate the expression of C/EBP-α. C/EBP-α then engenders the expression of peroxisome

proliferator-activated receptor-γ (PPAR-γ). PPAR-γ is a nuclear receptor. Stimulation of PPAR-γ activity results in dramatic alterations in gene expression, which causes the promotion of fatty acid uptake, production, esterification and deposition in the newly formed adipocyte. There is a strong body of evidence suggesting that mTORC1 regulates adipogenesis by the activation of PPAR-γ. It is thought that mTORC1 mediates control of PPAR-γ via several mechanisms. When mTORC1 is active, it triggers the phosphorylation of the 4E-BP proteins, which causes the release of eIF4E. This results in the translation of C/EBP-α and –δ, which are key players in the adipogenic signalling pathway. The expression of C/EBP-α and PPAR-γ is driven by C/EBP-δ, which also initiates the activation of a feed-forward loop in which the expression of the transcription factors PPAR-γ and C/EBP-α is induced in a reciprocal fashion. When sufficient quantities of PPAR-γ have been produced, it will instigate the expression of a plethora of lipogenic genes as aforementioned. Furthermore, the cleaving of SREBP-1 by mTORC1 not only results in the synthesis of triglycerides, but also promotes the generation of PPAR-γ's endogenous ligands. This represents an additional way by which mTORC1 may contribute to the stimulation of adipogenesis. In addition, Lipin-1, which is a phosphatidic phosphatase, has been demonstrated to possess an important function in adipogenesis. It serves as a coactivator for PPAR-γ and promotes the production of triglycerides. Rapamycin diminishes the phosphorylation of Lipin-1 (Huffman et al. 2002), but it is currently unknown whether it is a substrate for mTORC1 or mTORC2. A diagram illustrating the regulation of lipid synthesis by mTORC1 is shown in **Fig. 1.13**.

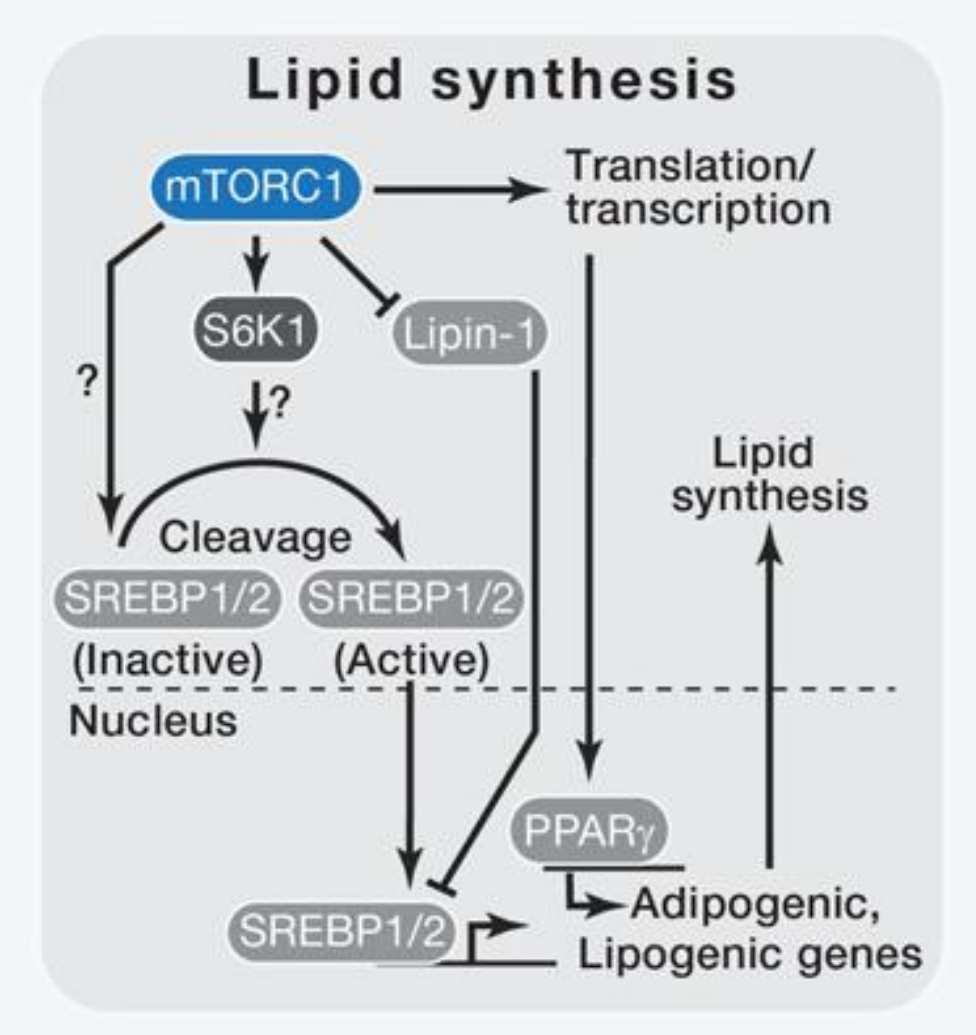

Fig. 1.13, Regulation of lipid synthesis by mTORC1. The presence of growth factors results in the inactivation of TSC1/2, and the activation of mTORC1. mTORC1 then mediates the cleavage of the transcription factor SREPBP-1, resulting in its translocation to the nucleus. Here, SREPBP-1 induces the expression of several genes that are required by lipogenesis. mTORC1 activates PPARγ via several mechanisms, which results in the expression of a plethora of lipogenic genes. (Laplante & Sabatini 2012)

Modulation of mitochondrial metabolism and biogenesis

mTORC1 regulates mitochondrial metabolism and biogenesis. When mTORC1 is inhibited with rapamycin, the cellular ATP levels, oxygen consumption and mitochondrial membrane potential are all diminished. Moreover, these changes induce a profound alteration in the mitochondrial phosphoproteome (Schieke et al. 2006). Work conducted in the past few years has demonstrated that mitochondrial DNA copy number and the expression of numerous genes that encode proteins involved in oxidative metabolism are reduced by rapamycin. Nevertheless, they are augmented by mutations that stimulate the mTORC1 pathway (Chen et al. 2008;Cunningham et al. 2007). Furthermore, when Raptor was conditionally deleted in mouse skeletal muscle, it was observed that there was a reduction in the expression of the genes that are involved in mitochondrial biogenesis (Bentzinger et al. 2008). It has also been noted that mTORC1 regulates the PPARγ coactivator 1's (PGC1-α) transcriptional activity. PGC1-α is a nuclear cofactor that plays a critical role in oxidative metabolism and mitochondrial metabolism by directly changing its physical association with yin-yang 1 (YY1), which is another transcription factor (Cunningham et al. 2007).

Regulation of mTORC1

Overview

mTORC1 regulates numerous cellular processes that stimulate cell growth by integrating four major signals. These are nutrients, energy status, growth factors and stress. The appropriate downstream response is then initiated by mTORC1 to preserve homeostasis within the cell. The tuberous sclerosis complex (TSC) is one of the principal sensors involved in the modulation of mTORC1 activity. TSC is a heterodimer that is composed of TSC1 (aka harmatin) and TSC2 (aka tuberin). TSC1/2 acts as a GTPase-activating protein (GAP) for the small Ras-related GTPase Rheb (Ras homologue enriched in brain). Rheb is activated by the addition of GTP, and interacts directly with mTORC1, promoting its activity (Long et al. 2005), (Sancak et al. 2007). TSC1/2's GTPase activity is specific for Rheb, and it inhibits mTORC1 signalling by converting Rheb into its inactive GDP-bound state (Inoki et al. 2003).

The effect of growth factors

Eukaryotes are reliant on long-range communication for the coordination of nutrient distribution and the concomitant growth of cells. When the organism is well fed, the concentrations of growth factors in the plasma will be sustained at a relatively high level. This leads to the promotion of anabolic processes such as nutrient storage, lipid biosynthesis and translation via stimulation of mTORC1 activity.

The quantities of growth factors circulating in the bloodstream are detected by mTORC1 through its connection to the PI3K pathway and the TSC1/2 complex. The binding of insulin or insulin-like growth factors to their cognate receptors results in the recruitment and phosphorylation of insulin receptor substrate 1 (IRS1). PI3K is

then recruited and binds to IRS1, where it converts phopsphatidylinositol-4,5-phosphate (PIP2) in the cell membrane to phosphatidylinositol-3,4,5-phosphate (PIP3). Akt and PDK1 are then both recruited to the membrane, where Akt is phosphorylated and activated by PDK1. Akt in conjunction with other kinases such as p90 RSK1 and MAPK that are downstream of growth factor signalling then phosphorylates TSC2 (Ballif et al. 2005), (Li et al. 2003), (Potter, Pedraza, & Xu 2002), (Roux et al. 2004), (Roux et al. 2004;Tee et al. 2003). The consequence is the inactivation of the TSC1/2 complex and the activation of mTORC1. Furthermore, two other pathways are currently known to regulate mTORC1 in response to growth factors. Extracellular signal-regulated kinase (ERK), which is part of the (MEK)-ERK axis inhibits TSC2 by phosphorylation (Ma et al. 2005). The Wnt pathway, which regulates cell growth and proliferation in adults, has also been shown to play a role in the modulation of mTORC1 activity (Castilho et al. 2009;Inoki et al. 2006), (Inoki et al. 2006). Glycogen synthase kinase 3β negatively regulates mTORC1 by phosphorylating TSC2. By its inhibition of GSK3β, Wnt mediates the activation of mTORC1.

Mechanisms also exist whereby mTORC1 is regulated by growth factors independently of TSC. For example, when Akt is activated by growth factors it phosphorylates PRAS40 at Ser247 leading to its inactivation. This results in the disruption of its inhibitory action on mTORC1 (Inoki et al. 2006;Oshiro et al. 2007), (Sancak et al. 2007), (Thedieck et al. 2007), (Vander et al. 2007), (Wang et al. 2007), (Wang et al. 2008).

Curiously enough, the activation of mTORC1 by growth factors also results in the attenuation of growth factor signalling by means of the ‘negative feedback loop’. Nevertheless, in stark contrast to conventional feedback loops where inhibition is only initiated upon attainment of a certain threshold, mTORC1 appears to repress growth

factor signalling pathways in an incremental and continuous manner. It is thought that more than one mechanism is involved in the actuation of the feedback loop. When S6K1 is active, it phosphorylates IRS1, which diminishes its expression and activity. This impairs its binding to the insulin receptor, which leads to the promotion of IRS1's degradation and a decline in the quantities of its mRNA (Harrington et al. 2004), (Sancak et al. 2007), (Shah and Hunter 2006), (Tremblay et al. 2007). Moreover, activated S6K1 is also capable of suppressing the function of other growth factor receptors that are not dependent on IRS1. An example is platelet-derived growth factor receptor (PDGFR), which demonstrates that IRS1 is not the sole target in feedback inhibition (Zhang et al. 2003). It has also been shown that mTORC1 can directly interact with IRS1 through Raptor. The result is the phosphorylation of IRS1 at residues that hinders its binding to PI3K (Tzatsos 2009).

The role of amino acids

Amino acids stimulate mTORC1 activity. Furthermore, it has been shown that arginine, and the branched chain amino acids leucine and isoleucine are particularly important in the promotion of mTORC1 function (Hara et al. 1998). Studies that were conducted more than ten years ago demonstrated that withdrawal of amino acids from cultured cells resulted in the inhibition of mTORC1 activity. No other known activating stimuli could force a resumption of mTORC1 signalling (Hara et al. 1998;Sancak et al. 2008;Wang et al. 1998). The level of amino acids can be detected within the cell instead of at the plasma membrane in mammals (Christie et al. 2002). As such, amino acid transporters, such as SLC7A5 have been shown to play an important role in the mTORC1 pathway. SLC7A5, which is a bidirectional transporter, imports Leucine into the cell via the concomitant efflux of glutamine (Nicklin et al. 2009).

However, the mechanisms by which amino acids activate mTORC1 signalling once inside the cell are only beginning to be revealed. Nonetheless, it is known that the stimulation of mTORC1 by amino acids is dependent on both Rag (Kim et al. 2008), (Sancak et al. 2008) and the Ras-like GTPase Rheb (Garami et al. 2003), (Inoki et al. 2003a), which both directly bind to mTORC1. In addition, Rag brings about the localisation of mTORC1 to the lysosomal membrane (Kim et al. 2008), (Sancak et al. 2008). There are four Rag GTPases; RagA, RagB, RagC and RagD. The heterodimeric Rag GTPase complex is formed by the binding of either RagA or RagB to either RagC or RagD, and appears to be constitutively located on lysosomal membranes. As individual components, the Rag GTPases are functionally redundant. Furthermore, lysosomal membranes possess a multi-subunit complex that is composed of p18, p14 and MP1, that is known as the Ragulator (Sancak et al. 2010).

This complex plays the part of a scaffold protein for Rag. When cells are starved of amino acids, RagC/D is bound to GTP, whereas RagA/B is bound to GDP. Nonetheless, amino acid stimulation of the cells results in the switching of the bound guanine nucleotides, via an unknown mechanism. RagA/B now binds GTP and RagC/D binds GDP, resulting in the activation of Rag. Activated Rag then interacts with Raptor and acts as a docking site for mTORC1 on the lysosome's surface (Sancak et al. 2008). Rheb-GTP, which exists in a lysosomal pool, then activates mTORC1 through an unknown mechanism. Moreover, since Rheb is required for the promotion of mTORC1 activity by all upstream inputs, it is speculated that the amino acid dependent targeting of mTORC1 to lysosomal membranes is a prerequisite for the stimulation of mTORC1 by all other signals (Sancak et al. 2008;Sancak et al. 2010). Other potential modulators of amino acid signalling to mTOR include the class III PI3K mVps34 (Byfield et al. 2005;Nobukuni et al. 2005) and the Ste20-related kinase MAP4K3 (Findlay et al. 2007). Unfortunately, the precise mechanisms by which these proteins regulate mTORC1 remain to be elucidated.

The importance of Energy Status

mTORC1 is sensitive to the energy level within the cell via AMP-activated protein kinase (AMPK) (Hardie 2007). Energy deficiency, as signified by a high AMP/ATP ratio activates AMPK, which then phosphorylates TSC2. This augments TSC2's GAP activity towards Rheb, which inhibits mTORC1 (Inoki, Zhu, & Guan 2003). Furthermore, AMPK can diminish mTORC1 signalling when energy is insufficient by directly phosphorylating Raptor (Gwinn et al. 2008). Furthermore, LKB1, which is a tumour suppressor, has been shown to be an upstream kinase for AMPK. This implies that LKB1 could form part of the TSC-mTORC1 signal transduction network. Moreover, it was demonstrated that LKB1 mutant cells possessed vastly increased mTORC1 signalling (Corradetti et al. 2004;Shaw et al. 2004).

The impact of stress and miscellaneous cellular signals

Hypoxia inhibits mTORC1 signalling via several mechanisms (Wouters & Koritzinsky 2008). Oxygen deprivation results in a decline in the level of cellular ATP by causing the inhibition of metabolic processes such as oxidative phosphorylation. The subsequent elevation of the AMP:ATP ratio activates AMPK, which dampens mTORC1 signalling through the promotion of TSC2 activation and the phosphorylation of raptor (Arsham et al. 2003), (Liu et al. 2006). TSC1/2 can also be activated by hypoxia via transcriptional regulation of the protein DNA damage response 1 (REDD1) (Brugarolas et al. 2004), (Reiling & Hafen 2004). REDD1 is a cytoplasmic protein that is 232 amino acids long. In addition it is thought to belong to a signal transduction pathway that is parallel to PI3K and AMPK (Sofer et al. 2005). Furthermore, it was observed that REDD1 inhibited mTORC1 signalling by liberating TSC2 from its growth-factor induced binding to 14-3-3 proteins and stabilising the

association of TSC1 and TSC2 (DeYoung et al. 2008), (Vega-Rubin-de-Celis et al. 2010). A variety of other cellular stressors such as cigarette smoke, oxidising agents and DNA damage also induce REDD1 (Ellisen et al. 2002; Wang et al. 2003;Yoshida et al. 2010). Moreover, signalling in the mTORC1 pathway is diminished during hypoxia by another two proteins; BCL2/adenovirus E1B 19 kDa protein-interacting protein 3 (BNIP3) and promyelocytic leukemia (PML) tumour suppressor. These proteins mediate mTORC1 inhibition by preventing mTORC1 from interacting with Rheb (Bernardi et al. 2006;Ellisen et al. 2002;Li et al. 2007).

When a cell's DNA is damaged, one of two paths can be taken. If the DNA damage is reversible, then cellular repair processes will be initiated. However, if the situation is irrevocable, then apoptosis will be activated (Ciccia & Elledge 2010). Furthermore, there is increasing realisation of the role that mTORC1 inhibition plays in DNA repair (Ellisen et al. 2002;Ghosh et al. 2006). The tumour suppressor protein p53 is a keystone in the regulation of DNA damage responses (Riley et al. 2008); (Vousden & Ryan 2009). When p53 is activated by DNA damage, it negatively modulates mTORC1 signalling by augmenting the transcription of TSC2, phosphatase and tensin homologue deleted on chromosome 10 (PTEN) and REDD1, which have all been implicated in the inhibition of mTORC1 activity (Ellisen et al. 2002; Feng et al. 2005; Stambolic et al. 2001). In addition, p53 also augments the expression of the genes for Sestrin1 and Sestrin2. These proteins are able to suppress mTORC1 through AMPK-dependent modulation of TSC1/2 (Budanov & Karin 2008); Feng et al. 2005). There is also limited evidence which insinuates that p53 induces a rapid decline in the initiation of translation, in part by controlling the phosphorylation of 4E-BP1 and S6K (Horton et al. 2002). Taken together, these findings suggest that p53 activation due to

genotoxic stress suppresses mTORC1 function in a multi-faceted manner (Ellisen, et al. 2002; Feng et al. 2005; Stambolic et al. 2001).

IκB kinase β (IKKβ) is one of the foremost activators of the proinflammatory NF-κB signal transduction network. When stimulated by inflammatory cytokines such as TNFα, IKKβ phosphorylates TSC1 causing its destabilisation (Lee et al. 2007). This results in mTORC1 activation. The link between inflammation and the promotion of mTORC1 function is speculated to be significant in insulin resistance (Lee et al. 2008) and tumour angiogenesis (Lee et al. 2007).

Finally, numerous labs have demonstrated that overexpression of PA-producing enzymes (i.e. PLD1 and PLD2), or exogenous PA markedly amplifies mTORC1 signalling (Foster 2007). It is thought that PA achieves this by either stabilising mTORC1 complexes, or by facilitating their assembly (Toschi et al. 2009).

mTORC2 Signalling-Overview

When compared with mTORC1, very little is known about the regulation and functions of mTORC2. This is largely due to the present lack of mTORC2 inhibitors. Nevertheless, it has been shown that mTORC2 plays a pivotal role in several cellular processes such as cell survival, metabolism, proliferation and the organisation of the cytoskeleton.

mTORC2's involvement in cell survival, metabolism and proliferation

Activation of AKT is of crucial importance in the positive modulation of cellular survival, metabolism and proliferation via the phosphorylation of numerous effector proteins (Manning & Cantley 2007). AKT is fully activated when it is phosphorylated at two sites, namely Ser308 by the action of phosphoinositide-dependent kinase 1 (PDK1), and Ser473 by mTORC2 (Sarbassov et al. 2005). When mTORC2 is depleted, AKT is inhibited. This leads to a diminution in the phosphorylation of forkhead box protein O1 (FoxO1) and FoxO3a, which are both transcription factors that regulate the expression of genes concerned with metabolism, stress resistance, cell-cycle arrest and apoptosis (Calnan & Brunet 2008). Diminished phosphorylation of these proteins inactivates them. Work done in the past few years has also shown that serum- and glucocorticoid-induced protein kinase 1 (SGK1) is modulated by mTORC2 (Garcia-Martinez & Alessi 2008). Unlike AKT, which still functions at a minimal level when mTORC2 is deactivated, the activity of SGK1 is completely abolished. Moreover, AKT and SGK1 phosphorylate FoxO1 and FoxO3a on common residues. Therefore, it is plausible that the absence of SGK1 activity in cells that lack mTORC2 leads to the inhibition of FoxO1 and FoxO3a phosphorylation.

Control of Cytoskeletal Organisation

Recent work has shown that mTORC2 regulates the organisation of the actin cytoskeleton by various means. These include enhancing the phosphorylation of protein kinase Cα (PKCα) as well as phosphorylating paxillin and relocating it to focal adhesions. The addition of GTP to RhoA and Rac1 has also shown to be important in the control of the actin cytoskeleton by mTORC2 (Jacinto et al. 2004), (Sarbassov et al. 2004), but the precise mechanisms by which mTORC2 controls these processes is still unknown.

Signalling upstream of mTORC2

Unfortunately, the upstream molecular events that lead to the activation of mTORC2 are not fully defined. However, upon growth factor stimulation, mTORC2 kinase activity is elevated, and it phosphorylates AKT in its C-terminal hydrophobic motif at residue Ser473 (Guertin & Sabatini 2007). In addition, in vitro tests have demonstrated that in order for AKT to be fully activated, it must be phosphorylated at both Ser473 and at Thr308. However, the phosphorylation of the Thr308 residue by PDK1 is not dependent on Ser473 phosphorylation (Biondi et al. 2001), (Collins et al. 2003). In addition, the mTORC2 component mSIN1 possesses a pleckstrin homology domain at its C-terminus. As such, it is speculated that mSIN1 may mediate the shuttling of mTORC2 to the membrane. Here, it would be able to interact with AKT via its PH domain and phosphorylate it at Ser473 (Schroder et al. 2007). In **Fig. 1.14**, a diagram showing a simplified version of the mTOR signalling network has been provided.

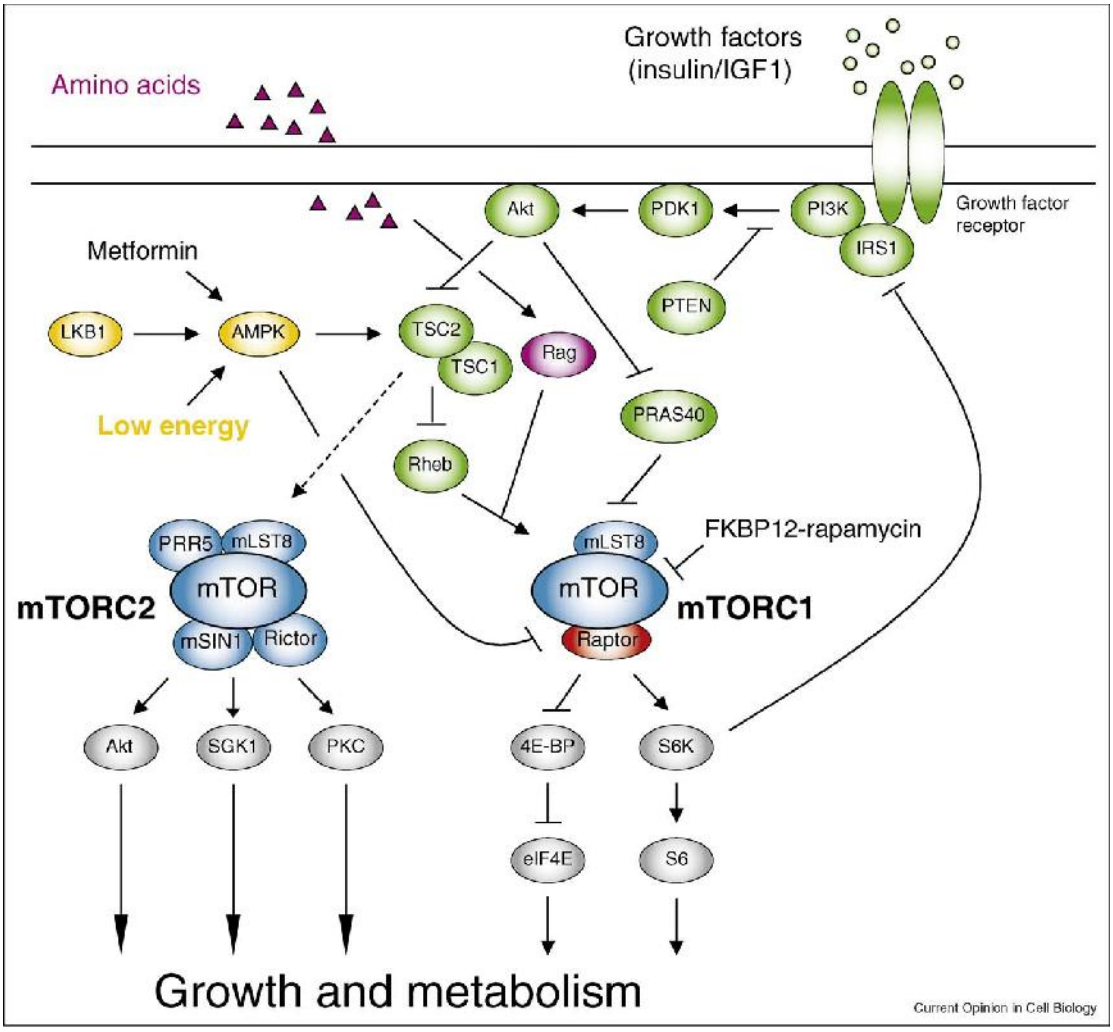

Figure 1.14: The mTOR signaling network. This is a simplified representation of the mTOR signalling pathway that demonstrates how the mTORC1 and mTORC2 complexes regulate growth and metabolism in the cell. Amino acids (purple) positively modulate the rapamycin-sensitive mTORC1 through the Rag GTPases. Growth factors (green) regulate mTORC1 activity in a positive manner via the Akt-PI3K pathway. Growth factors also stimulate mTORC2 function via an unknown pathway that involves the TSC complex. Low energy status (yellow) inhibits mTORC1 through AMPK. The mTORC substrates have been coloured grey. (Polak & Hall 2009)

mTOR as a Therapeutic Target

Due to the key role mTOR plays in the regulation of cellular growth and proliferation, mTOR is under intense investigation as a therapeutic target primarily for cancer. The earliest clinical trials involved the use of the classical mTOR inhibitor rapamycin. However, the results were disappointing because rapamycin proved to be of limited efficacy in the treatment of certain types of cancer. Research has shown that some of the key problems stem from its inability to directly inhibit mTORC2, the inhibition of the negative feedback loop upon mTORC1 inactivation and its poor solubility in water (Napoli & Taylor 2001). In order to remedy the problem of insolubility, rapalogues such as Temsirolimus and Everolimus were developed. Despite their modifications, these drugs are still capable of mimicking the inhibitory action of the FKBP12-rapamycin complex on mTOR. Their potency is currently being assessed in ongoing clinical tests.

The indifference that mTORC2 displayed towards rapamycin treatment also spurred the development of ATP-competitive inhibitors. These target mTOR's catalytic site and inhibit all mTORC1 and mTORC2 functions. Examples include Torin (Thoreen et al. 2009), P30 (Feldman et al. 2009), WAY-600 (Yu et al. 2009)and Ku-0063794 (Garcia-Martinez et al. 2009). The effect of inhibiting all mTOR functions on cell viability requires further investigation.

Attempts have been made to circumvent the issue of feedback inhibition by using dual PI3K-mTOR inhibitor strategies. So far inhibitors such as NVP-BEZ235 have been proven to possess superior anti-proliferative abilities when compared with rapalogues such as Everolimus in 21 different cancer cell lines (Serra et al. 2008). However, although inhibition of both mTOR and PI3K proved to be an effective treatment in tumours that displayed hyperactive PI3K signalling (Brachmann et al.

2009), it was ineffective when faced with hyperactivation of K-Ras. It appears that in the case of Ras-driven tumorigenesis, the simultaneous inhibition of mTOR, PI3K and Ras's downstream mediators is necessary (Engelman et al. 2008), (Ihle et al. 2009;Torbett et al. 2008). However, the potential toxicity of this approach has not yet been critically evaluated (Adami et al. 2007).

Mutations in mTOR

In 2010, Sato et al mined the COSMIC library (Catalogue of Somatic Mutations in Cancer) provided by the Sanger Institute. This database contains a huge quantity of information pertaining to somatic mutations in human cancers. The results of the search showed that 10 mutations in the *mTOR* gene have currently been identified from 750 cancer samples. Two of these mutations were silent mutations that did not alter the amino acid sequence. Another generated a stop codon that resulted in the production of a truncated mTOR protein that lacked a kinase domain. The mutation M135T was identified twice. The 6 different mutations that resulted in a change in amino acid are shown in **Fig. 1.15**. Of particular interest were the mutations that were located in the kinase domain or its vicinity. These were S2215Y, P2476L and R2505P respectively.

Mutation	Tissue (Cancer type)	COSMIC ID
A8S	lung (large cell carcinoma)	753390
M135T	skin (malignant melanoma)	753546
M2011V	ovary (mucinous carcinoma)	753344
S2215Y	large intestine (adenocarcinoma)	753426
P2476L	brain (glioma)	753417
R2505P	kidney (clear cell renal cell carcinoma)	948155

Fig 1.15, The locations of the 6 mutations identified in mTOR. Each of these 6 mutations results in a change in amino acid. The tissue type in which each of the mutations was found has also been indicated. (Sato et al. 2010)

Aims of this Study

Several years ago, an isoform of mTOR was discovered in the Gout lab, which was called mTORβ. The initial set of experiments performed revealed some key findings; the protein was able to form the mTORC1 and mTORC2 complexes and was a proto-oncogene. However, in order to further our understanding of the function and regulation of this novel protein, it was decided to gain insight into its structure. Therefore, the first part of my PhD studies involved comparative modelling of mTORβ's kinase domain. The effect of mutations on the kinase activity of mTORβ towards several mTOR substrates was then assessed in mammalian cells. Finally, a mTOR/TAP-tag fusion protein was generated. Had time permitted, this would have been used to search for novel mTORβ binding partners.

Chapter 2

Materials and Methods

Chapter 2: Materials and Methods

2.1) Materials

2.1.1 Common Chemicals and Reagents

All the general purpose chemicals were acquired from Sigma-Aldrich, Thermo Fisher Scientific UK limited, BDH Biosciences unless otherwise specified. General cell culture reagents were purchased from PAA Laboratories GmbH. Pre-stained protein molecular weight markers, restriction enzymes and DNA markers were obtained from Fermentas.

2.1.2 Antibodies

Horseradish peroxidase-linked (HRP) secondary antibodies (anti-rabbit and anti-mouse) were purchased from Promega. Antibodies against actin, myc and EE were generated in the lab by former students for other purposes. Anti-Akt (#9272), anti Phospho-Akt (#4051), anti 4E-BP1 (#9452) and anti Phospho-4E-BP1 (#2855) were obtained from Cell Signalling. Anti-S6K1 (ab32359) and anti-S6K1 (phosphpoT389) (ab2571) were acquired from Abcam. Anti-Phospho-mTOR (Ser2448) (09-213) and anti-mTOR (07-231) antibodies were obtained from Millipore.

2.1.3 Mammalian cells

HEK293 cells were obtained from the American Type Culture Collection (ATCC).

2.1.4 Plasmids and Primers

The pCeMM-NTAP(GS) plasmid was obtained courtesy of Dr Tilmann Burckstummer from the Research Centre for Molecular Medicine of the Austrian Academy of Sciences. All other plasmids were obtained from Invitrogen. Primers were ordered from MWG Operon.

2.2 Experimental Methods

2.2.1 Nucleic Acid Manipulation

2.2.1.1 Digestion of DNA with specific restriction enzymes

All restriction endonucleases were acquired from Fermentas and digests were carried out in the manufacturer's recommended digestion buffer. 5 units of restriction enzyme were used to digest 1µg of DNA in a total volume of 20µL. The reaction mixtures were placed in an incubator at 37°C for 1hr.

2.2.1.2 Electrophoresis of DNA and purification from an agarose gel

DNA fragments were visualised by separation on an agarose based gel. 0.75% w/v agarose gels were used throughout this thesis for DNA purification and analysis. The required weight of agarose was added to TAE buffer (1mM EDTA, 40mM Tris-Acetate, pH 7.0) and heated in order to dissolve the agarose. After cooling the solution to approximately 50°C, Gel-Red dye supplied by Biotium was added in a 10,000x dilution. The liquid agarose solution was then poured into a mould containing a well-forming comb and left at room temperature so that it could solidify. 6 x DNA loading buffer supplied by Fermentas was mixed with the DNA samples and they were loaded into the wells in the gel. The samples were then electrophoresed at 100V in TAE buffer to achieve separation. 1kb Gene Ruler standard molecular weight markers from Fermentas were utilised on the gel to ascertain the sizes of the various fragments. After electrophoresis, the DNA was observed by exposing the gel to long-wave UV light. Purification of the requisite DNA fragments from the gel was performed by excising the bands of interest and using manufacturer's gel extraction kits to obtain the DNA.

2.2.1.3 DNA Ligation

A rapid DNA ligation kit from Fermentas was used to ligate DNA fragments to linearised vector. In order to reduce the risk of self-ligation of the plasmids, at least a 1:3 molar ratio of vector:insert was utilised in the ligation reactions. The reactions were conducted at room temperature using 1μL of T4 DNA Ligase and 5μL of Rapid Ligation Buffer in a total reaction volume of 20μL. The reaction mixture was stored in the fridge until it was used for transformation.

2.2.1.4 Transformation and Growth of Bacteria

E.Coli XL-1 competent cells (obtained from Stratagene) that were stored at -80°C were thawed on ice and 50μL of bacterial suspension was mixed with 5μL of ligated plasmid reaction mix in 14mL BD Falcon polypropylene round-bottomed tubes. The mixture was then incubated on ice for 30 minutes. The cells were then subjected to heat-shock in a water bath at 42°C for 45 seconds, and then placed on ice for 2 minutes. 1mL of preheated LB media (42°C) was then added to the bacterial suspension and the tubes were incubated at 37°C for 1 hour with shaking at 225rpm. 50μL of this cellular suspension was then added to 200μL of LB media and spread on a selective agar plate. The plate was then placed overnight in an incubator at 37°C. Amplification of positively transformed bacteria was achieved by inoculating a bacterial colony from a selective agar plate into the requisite volume of LB media with antibiotic. The tubes were then placed in a shaker at 37°C overnight with shaking at 225rpm.

2.2.1.5 Purification of Plasmid DNA

Plasmid DNA was purified from bacterial suspension using the Promega PureYield Plasmid Miniprep System. In essence, cells in 3mL of bacterial culture were lysed by the addition of lysis buffer. The mixture was then neutralised with neutralisation solution. The bacterial cultures were then centrifuged at 13,000rpm for 3 minutes and the supernatant was transferred to a Minicolumn which would bind the plasmid DNA. The minicolumns were then washed and centrifuged to remove contaminants, and the DNA was eluted with water. The purity and concentration of the purified plasmid DNA was analysed by loading onto an agarose gel alongside a MW marker (1kb GeneRuler, Fermentas).

2.2.1.6 PCR Site-Directed Mutagenesis

Unfortunately, mTORβWT was not cloned into the pcDNA3.1(+) vector using the XhoI and NotI restriction enzymes. Therefore, it was not possible to excise it from its original vector and directly clone it into the TAP-tag plasmid pCeMM-NTAP(GS). As a result, primers were designed that would allow the XhoI and NotI restriction sequences to be artificially introduced at the N and C termini of mTORβ respectively by PCR. PCR reactions were carried out under different experimental conditions in order to find the set of conditions that would generate the most PCR product. The variables involved performing reactions either with or without DMSO. Furthermore, for the PCR reactions that were performed with DMSO, three different annealing temperatures were utilised. The PCR product would then be cloned into the pCeMM-NTAP(GS) TAP tag vector.

PCR site-directed mutagenesis was also used to introduce the S2215Y and 12del mutations into mTORβ DNA. Forward and reverse oligonucleotide primers

were designed for the S2215Y mutation and for the 12del mutation. Stratagene's QuikChange Site-Directed Mutagenesis Kit was used to create the required mutations in the mTORα and mTORβ plasmids. The manufacturer's manual can be viewed via the following link:

http://www.genomics.agilent.com/files/Manual/200516.pdf

However, some modifications were made to the PCR reaction mixture on p10 of the protocol. These included using 50ng of the mTORβ/pCDNA3.1(+) dsDNA template, and an oligonucleotide primer concentration of 50ng/μL.

For the PCR reactions with 5% DMSO the following reaction volumes and conditions were used:

Reaction Mixture (For 5% DMSO rxns):

Component	Amount per reaction
dH_2O	31μL
10x PfuUltra2 Reaction Buffer	5μL
50% DMSO	5μL
dNTP mix (2mM each dNTP)	5μL
DNA template (mTORB/pcDNA3.1(+)) (25ng/μL)	1μL
Primer #1 (10μM)	1μL
Primer #2 (10μM)	1μL
PfuUltra 2 fusion HS DNA Polymerase	1μL
Total Rxn Volume	50μL

PCR Cycling Parameters (For 5% DMSO rxns):

Segment	No. of Cycles	Temperature (°C)	Duration
1	1	98°C	2mins
2	30 cycles	98°C	20s
		60/62/64°C	20s
		72°C	1min
3	1	72°C	3mins

For the PCR reactions without DMSO the following reaction volumes and conditions were used:

Reaction Mixture (No DMSO):

Component	Amount per reaction
dH_2O	36µL
10x PfuUltra2 Reaction Buffer	5µL
dNTP mix (2mM each dNTP)	5µL
DNA template (mTORB/pcDNA3.1(+)) (25ng/µL)	1µL
Primer #1 (10µM)	1µL
Primer #2 (10µM)	1µL
PfuUltra 2 fusion HS DNA Polymerase	1µL
Total Rxn Volume	50µL

PCR Cycling Parameters (No DMSO):

Segment	No. of Cycles	Temperature (°C)	Duration
1	1	95°C	2mins
2	30 cycles	95°C	20s
		62°C	20s
		72°C	60s (15s per kb for targets > 1kb)
3	1	72°C	3mins

2.2.1.7 Purification of PCR product using Ethanol Precipitation

1/10 volume of 3M sodium acetate and 2 volumes of 100% ice-cold ethanol were added to the PCR product sample tubes. The tubes were then cooled on dry ice for 20mins. The tubes were then centrifuged at max speed for 10mins. The supernatant was decanted and the pellet was carefully washed with 100µL of 75% ice-cold ethanol. The pellet was then dried by aspiration and the DNA was dissolved in 20µL of ddH_2O.

2.2.2 Mammalian Cell Culture and Methodology

2.2.2.1 Maintenance of Cell Lines

HEK293 cells were maintained in Dulbecco's Modified Eagle's medium (DMEM from PAA) supplemented with 10% v/v foetal bovine serum (FBS from Hyclone) and 1% penicillin/streptomycin v/v antibiotics. Cells were grown in 37°C humidified incubators at 10% CO_2. When cells had reached 60-80% confluency, they were passaged. The medium was aspirated and the cells were washed with 1 x Dulbecco's phosphate buffered saline (PBS from PAA). The cells were then detached from the plates by the addition of trypsin-EDTA (supplied by PAA). The plates were then placed in the incubators at 37°C for 1-2 minutes in order to fully detach the cells. Fresh medium was then added to neutralise the trypsin and the cellular suspension was pipetted up and down continuously to break up any clumps of cells. The volume of cellular suspension required to achieve a desired ratio was then added into new plates containing fresh medium. Subculturing was conducted in a laminar flow hood, which was totally sterile with media and reagents that had been previously pre-warmed to 37°C.

2.2.2.2 Transient Transfection of HEK293 with plasmid DNA

When a 10cm plate had reached 80% confluency it was split (1/3) into three new 10cm plates with 8mL of fresh DMEM complete medium. 24hrs later, the media was aspirated and 10mL of new DMEM complete medium was added to each plate. 10µg of plasmid DNA was then mixed with 200µL of sterile 150mM NaCl. The DNA and NaCl were mixed very well by pipette action. 35µL of Exgen500 transfection reagent supplied by Fermentas was then added and the solution was immediately mixed by pipette action for 10secs. The tubes were then incubated at room temperature for

10mins before being added drop wise to the previously prepared plates of HEK293 cells with refreshed medium. The transfected cells were then placed in an incubator at 37℃ for 48 hours before being they were frozen at -80℃ or used for analysis.

2.2.2.3 Serum and Nutrient Starvation of cells and subsequent Stimulation

24hrs after transient transfection, the complete DMEM medium was aspirated and was replaced with serum-free DMEM medium. The cells were then incubated at 37°C overnight in this medium. The next morning, the serum-free media was removed and the PBS was introduced into the plates. The cells were then incubated at 37°C for 1hr to achieve nutrient starvation. At this point, the cells were either frozen at -80°C or used for analysis.

In the latter set of experiments involving starvation followed by stimulation, the conditions were altered slightly, but the methods employed were identical. Firstly, the duration of serum starvation was extended to 24 hours. In addition, the cells were subjected to nutrient deprivation for 3 hours rather than one. Stimulation was effected by removing the PBS and incubating the cells in DMEM complete medium for 1hr at 37°C. The cells were then utilised for analysis for frozen at -80°C.

2.2.3 Isolation and analysis of proteins from HEK293 cells

2.2.3.1 Isolation of protein in total cell lysate from cultured HEK239 cells

The plates were removed from the incubator and the medium was aspirated. The cells were washed with ice-cold PBS and placed on ice. The PBS was then aspirated and the cells were lysed on ice with ice-cold lysis buffer (150mM NaCl, 1% Triton X-100, 50mM NaF, 20mM Tris-HCl pH 7.5 and Roche Protease inhibitor cocktail) for 20 minutes. The cell lysates were scraped from the plates and were placed in

microcentrifuge tubes. The tubes were then centrifuged at maximum speed (14,000rpm at 4°C) for 20mins in order to pellet the insoluble fraction. The supernatants were then transferred to new tubes and the protein concentration of each sample was ascertained by the Bradford assay.

2.2.3.2 Measuring Protein Concentration

The Bradford Assay was utilised to measure the protein concentration in each sample's soluble fraction. Bio-Rad Protein Assay Reagent was diluted 5x with ddH_2O to generate the working solution. Samples were made up by adding 1µL of each sample to 1mL of diluted reagent solution. Measurements were made with a Bio-photometer (supplied by Eppendorf) at an absorbance of 595nm utilising lcm plastic cuvettes. The photometer generates results in the form of a curve on a graph of concentration against absorbance. In addition, all measurements are calculated based on standards provided in the preset.

2.2.3.3 Affinity Purification

Affinity purification was utilised to purify mTORβ/pCeMM-NTAP(GS) from the soluble fraction of transiently transfected HEK293 cells. For each sample, 50µL of Millipore PureProteome Protein G magnetic bead suspension was pipetted into a new microcentrifuge tube. The tube was then placed in a magnetic rack and the storage buffer was carefully removed with a pipette. 500µL of PBS containing 0.1% Tween 20 was then added to the beads and the tubes were vortexed vigorously for 20secs. The tubes were then replaced in the magnetic stand and the PBS was removed with a pipette. The soluble fractions of the HEK293 total cell lysates were then added to the tubes. The tubes were then placed on a loop at 4°C for 2hrs. At the end of this time

the tubes were placed in the magnetic rack and the beads were washed 3x with 500µL PBS containing 0.1% Tween 20 per wash. 50µL Laemmli sample buffer was then added to each sample tube, and the samples were mixed by vortexing. The tubes were then boiled in a heat block at 100°C for 8mins and then centrifuged at 13,300rpm in a desktop microcentrifuge for 10secs to collect any condensation. The samples were then loaded onto a SDS-PAGE gel and electrophoresed, or frozen at -20°C for later use.

2.2.3.4 Immunoprecipitation

Immunoprecipitation of particular proteins was achieved by using antibodies that were specific for the protein of interest. Antibody was added to Protein A sepharose beads followed by the total cell lysate in a microcentrifuge tube. The sample tubes were then placed on a rotating wheel for 2hrs at 4°C. Following incubation on the wheel, the tubes were washed 3x with extraction buffer containing protease inhibitors. 15µL of 2xSDS loading buffer was then added to the beads, and the mixture was boiled for 8mins. The tubes were then centrifuged at max speed for 10secs in a desktop centrifuge to collect condensation. The liquid component was then loaded onto a SDS-PAGE gel.

2.2.3.5 SDS-PAGE

When one boils a protein sample with Laemmlli sample buffer, the SDS detergent present in the buffer binds to the proteins. This results in the linearisation of the protein as well as the formation of a uniform negative charge across the length of the protein. Consequently, the protein samples can be separated by an electric current on the basis of size. During electrophoresis, movement of the larger proteins is physically

retarded by the matrix, whilst smaller proteins meet with less opposition and move further more quickly. This has the effect of separation by size.

5x Laemmlli sample buffer (10%SDS, 250mM Tris pH6.8, 50% glycerol, 0.5% bromophenol blue, 50mM DTT) was added to protein samples in order to obtain a final concentration of 1x. The samples were then boiled for 8 minutes in a heat block at 100°C and centrifuged briefly at 3,000rpm before they were loaded onto the polyacrylamide gel. 1mm thick NuPAGE 10% Bis-Tris gel with 10 wells were used in conjunction with Invitrogen's XCell SureLock Mini-Cell system. 20µL of sample was loaded into each well as required. The gel was run with 1x MOPS SDS running buffer (50mM MOPS, 50mM Tris Base, 0.1% SDS, 1mM EDTA, pH7.7) for 50mins at a constant voltage of 200V.

2.2.3.6 Western Blotting

After separation of the proteins by size on a SDS-PAGE gel using electrophoresis, the proteins were transferred from the gels using semi-dry transfer. The Trans-BlotTM system (Biorad) was utilised to perform the semi-dry transfer. Once the gel cassette was opened, superfluous parts of the gel were cut off and the gel was placed on a sheet of PVDF membrane. The membrane and gel were sandwiched between four sheets of pre-soaked 3MM filter paper and air bubbles were removed. Transfer was then conducted at a constant current of 0.3mA for 1 hour.

Following transfer, membranes were washed with TBST (10mM Tris-HCl pH7.5, 150mM NaCl, 0.1% Tween 20) before they were blocked for 1 hour in TBST containing 5% (w/v) non-fat dried milk powder. Blocking seeks to minimise non-specific binding of the antibodies to the membrane. Primary antibodies were diluted according to the manufacturer's guidelines in TBST containing 2% BSA and 0.02%

sodium azide. The membranes were then incubated with the primary antibody solutions overnight at 4°C. The following morning, the membranes were washed 3 times for 10mins per wash in fresh TBST buffer. The membranes were then incubated for 1 hour at room temperature with the relevant HRP-linked secondary antibody, which was diluted in TBST with 5% milk powder. TBST was then used to wash the membranes 3 times, 10mins per wash prior to development by enhanced chemiluminescence (ECL).

Equal volumes of ECL solution 1 (coumaric acid, luminol, 50mM Tris-HCl) and ECL solution 2 (0.02% H_2O_2, 50mM Tris-HCl) were mixed and incubated with the membrane for 1 and a half minutes at room temperature. The membrane was then encased in Saran wrap and excess ECL solution was removed by blotting. The bands were then visualised by exposing the membrane to an X-ray film in a dark room for different durations.

2.2.3.7 Table of all antibodies used

Antibody	Product Code	Manufacturer/Source	Dilution used
Anti-Actin	-	Produced by former student	1 to 1000
Anti-Myc	-	Produced by former student	1 to 1000
Anti-EE	-	Produced by former student	1 to 1000
Anti-Akt	#9272	Cell Signalling	1 to 1000
Anti-PAkt	#4051	Cell Signalling	1 to 1000
Anti-4E-BP1	#9452	Cell Signalling	1 to 1000
Anti-P4E-BP1	#2855	Cell Signalling	1 to 1000
Anti-S6K1	ab32359	Abcam	1 to 1000
Anti-S6K1 (Phospho T389)	ab2571	Abcam	1 to 1000
Anti-PmTOR (Ser2448)	09-213	Millipore	1 to 1000
Anti-mTOR	07-231	Millipore	1 to 1000
Anti-Rabbit Secondary AB	W4011	Promega	1 to 5000
Anti-Mouse Secondary AB	W4021	Promega	1 to 5000

2.3 Bioinformatics methods

2.3.1 Comparative Modelling

The basis of comparative modelling rests on the principle that the crystal or NMR structure of a protein can be used as a template to model another homologous protein. The Protein Data Bank was searched using BLAST (Altschul et al. 1997) with the amino acid sequence of mTOR's kinase domain. The search produced a list of proteins that shared a significant degree of sequence similarity with mTOR's kinase domain. From the list, the protein that had the best combination of percentage sequence identity, e-value and query coverage was selected to be the template protein. This was the crystal structure of PI3Kδ (PDB Cod e: 2X38) (Berndt et al. 2010) .

The alignment produced by BLAST between mTOR's kinase domain and PI3Kδ was then annotated with PI3Kδ's secondary structure. This was obtained from DSSP (Kabsch & Sander 1983) on the EBI website. The initial BLAST alignment was then manually amended to produce a more likely structural alignment; for example moving indels in the middle of secondary structure elements into adjacent loop regions. The individual amendments are described in detail in results chapter 1.

BLAST did not align the entire length of mTOR's kinase domain with PI3Kδ. The alignment was therefore extended to include the C-terminal and N-terminal regions that had initially been omitted. This was done by firstly converting the mTOR sequence into PIR format. Then, PI3Kδ's kinase domain was edited out of the PDB file (2X38) and the sequence was extracted in PIR format. The two sequences were then aligned in their entirety using Andrew Martin's Needleman and Wunsch (Needleman & Wunsch 1970) alignment program (nw). The terminal regions not present in the initial BLAST alignment were extracted from this new alignment and appended to the amended BLAST alignment.

A linker region joins the FRB and Kinase domains in mTORβ. The alignment between mTOR's linker and PI3Kγ in (Sturgill & Hall 2009) was copied. This was then annotated with PI3Kγ's secondary structure, which was obtained from DSSP at the EBI website. The position of one indel in the sequence alignment was altered in order to improve the alignment in structural terms.

Dr Andrew Martin's ProFit programme (Martin and Porter, http://www.bioinf.org.uk/software/profit/) was used to superimpose PI3Kδ onto PI3Kγ using the McLachlan algorithm, (McLachlan, 1982). This provided a reference point from which one could later position mTORβ's FRB, Kinase and linker domains relative to each other in a multiple alignment. Using the text editor Emacs, the PDB files for PI3Kδ (2X38), (Berndt et al. 2010) and PI3Kγ (1E8X), (Walker et al. 2000) were both trimmed down to their kinase domains. Starting from a sequence alignment, ProFit was used in iterative mode to align the two structures allowing Cα pairs to be considered if they were up to 10Å apart. This created a structural alignment, superimposing the structure for PI3Kδ onto the structure for PI3Kγ.

A multiple alignment was then generated between mTOR, FRB and PI3Kγ and PI3Kδ in PIR format (see **Fig. 11** in results chapter 1). A MODELLER control file was created to read the sequence alignment file and use PDB files for PI3Kδ (2X38_A), PI3Kγ (1E8X_A) and FRB (2GAQ_A) in standard homology modelling mode. MODELLER (Sali & Overington 1994) was then run to produce a 3D model of mTOR's kinase domain and the structure was viewed using RASMOL (Sayle & Milner-White 1995).

Chapter 3: Results

Comparative Modelling of mTORβ's kinase domain

Chapter 3: Comparative Modelling of mTORβ's kinase domain

3.0) Introduction

To date no 3D structures of mTOR or its kinase domain have been generated by either X-ray crystallography or NMR. However, cryo-EM structures of mTORC1 (Yip et al. 2010) as well as TOR and its complex with KOG1 (Adami et al. 2007) have been elucidated. Although models produced utilising these methods can be more accurate, the time and expense that are required by these techniques has led to the use of in silico techniques. A model for the catalytic region of TOR has already been generated by the comparative modelling approach using PI3Kγ as the homologue (Sturgill & Hall 2009). The principle of homology modelling is based on the idea that a protein of known structure can be used as the template to produce a model for a homologous protein. The accuracy of the resultant 3D structure generated increases with the higher degree of sequence similarity between the two proteins. Comparative modelling was used to generate a model of mTOR's kinase domain using PI3Kδ as the template. A BLAST search of the PDB showed that PI3Kδ's kinase domain possessed 28% sequence identity with the kinase domain of mTOR, whereas PI3Kγ only shared 21%. Therefore, using PI3Kδ (2X38) as the template should result in a more accurate model. A NMR structure of mTOR's FRB domain already exists (Leone et al. 2006). Rapamycin and rapalogues, which mimic its inhibitory action, bind to mTOR via the FRB domain when in complex with FKBP12. The goal was to produce a model of mTOR's kinase domain and then to link this with the NMR model of the FRB domain. The model produced would potentially help us to understand possible mechanisms by which rapamycin and ATP-competitive inhibitors act on mTOR. Aside from gaining experience and knowledge of molecular modelling using bioinformatics, it was also

hoped that the model would provide useful insights into the mechanisms of mTOR regulation and would help mTOR inhibitor studies in the group.

Results

3.1) Protein BLAST of PDB and annotation of alignment with secondary structure

A protein BLAST search of the PDB was performed using the amino acid sequence of mTORβ's kinase domain as the query sequence. From the list of proteins generated, it was observed that PI3Kδ (2X38), (Berndt et al. 2010) was the best homologue for mTOR's kinase domain. This was due to the fact that it possessed the highest percentage sequence identity (28%). PI3Kδ also had an E-value of $3x10^{-12}$, and an e-value ≤ 0.02 implies that the sequences are probably homologous. Therefore it is very likely that PI3Kδ is a homologue for mTOR's kinase domain. The alignment between PI3Kδ and mTOR Kinase produced by BLAST was annotated with PI3Kδ's secondary structure. The secondary structure data for PI3Kδ were obtained from DSSP (Kabsch & Sander 1983) on the EBI website. This can be seen in **Fig. 3.1**.

```
mTORβ  23   GSNGHEFVFLLKGHEDLRQDERVMQLFGLVNTLLANDPTSLRKNLSIQRYAVIPLSTNSG  82
            GS G+  + + K  +DLRQD   +Q+  L++ L   +   LR    +  Y  +P    +G
PI3Kδ  769  GSAGNVGI-IFKNGDDLRQDMLTLQMIQLMDVLWKQEGLDLR----MTPYGCLPTGDRTG  823
2° Struc    ####.EEE-EEEE##..HHHHHHHHHHHHHHHHHHH##.....----.....EEEEE..EE


mTORβ  83   LIGWVPHCDTLHALIRDYREKKKILLNIEHRIMLRMAPDYDHLTLMQKVEVFEHAVNNTA  142
            LI  V H DT+            I LN  +     MA                     A
PI3Kδ  824  LIEVVLHSDTI----------ANIQLNKSN-----MAA------------------TAA  849
2° Struc    EEE...#EEEH----------HHHH#..##-----###------------------..#


mTORβ  143  GDDLAKLLWLKSPSSEVWFDRR-TNYTRSLAVMSMVGYILGLGDRHPSNLMLDRLSGKIL  201
             +  A L WLKS +     DR    +T S A   +  Y+LG+GDRH  N+M+ R SG++
PI3Kδ  850  FNKDALLNWLKSKNPGEALDRAIEEFTLSCAGYCVATYVLGIGDRHSDNIMI-RESGQLF  908
2° Struc    ####HHHHHHHHH#.##HHHHHHHHHHHHHHHHHHHHHHH#.....###EEE-E###.EE


mTORβ  202  HIDFGDCFEVAMTREKFP---EKIPFRLTRMLTNAMEVTGLDGN-----YRITCHTVMEV  253
            HIDFG    +   + KF    E++PF LT    + ++    + +     +R  C     +
PI3Kδ  909  HIDFGHF--LGNFKTKFGINRERVPFILTYDFVHVIQQGKTNNSEKFERFRGYCERAYTI  966
2° Struc    E.......-##..!!!!!!!!!.......HHHHHHH###.#..HHHHHHHHHHHHHHHHHH


mTORβ  254  LREH  257
            LR H
PI3Kδ  967  LRRH  970

2° Struc    HHH#
```

Legend (The same legend has been used in all the following figures)

E = extended strand, participates in β-ladder

H = 4-helix (α-helix)

- = insertion in mTORβ with respect to PI3Kδ

. = no secondary structure has been defined at this location (i.e. coil)

= secondary structure other than an alpha-helix or extended strand (i.e. 3-helix (G), bend (S) or residue in isolated β-bridge (B))

! = region of unknown amino acid sequence

+ = conservative substitution

2° Struc = Protein secondary structure annotation

Fig. 3.1, BLAST alignment between mTORβ Kinase and PI3Kδ. PI3Kδ has been annotated with its secondary structure, which was obtained from the DSSP in the EBI website.

3.2) Amending the BLAST alignment between mTORβ Kinase and PI3Kδ to produce a structural alignment

The sequence alignment produced by BLAST between mTORβ kinase and PI3Kδ was manually amended. This sought to achieve a far more plausible structural alignment between the two proteins which would ultimately result in a more accurate model. The reason(s) behind each of the changes are described below:

(a) The presence of an indel in the middle of the beta strand that stretched from residues 774-780 in the PI3Kδ line was not structurally viable, so it was moved to the start of the N-terminus. It was not moved into the loop region in the C-terminal direction because it would have been undesirable to disrupt the relatively higher sequence identity between the two proteins in that region. See **Fig. 3.2A and 3.2B**.

(b) The position of the insertion was checked in Ramsol, and it was decided that the 4 indels (b) should be shifted one position to the right by moving M810 in PI3Kδ's sequence one place to the left. This sought to minimise structural clashes (i.e. insertion clashing with other secondary structure elements). See **Fig. 3.3A and 3.3B**.

(c) The BLAST alignment positioned loop regions of 5 and 19 residues in length either side of the undefined, small piece of secondary structure defined by the 3 residues MAA (PI3Kδ line, residues 844-846). It was thought to be far more logical to coalesce these loop regions since they will be poorly modelled anyway. See **Fig. 3.4A and 3.4B**.

(d) The indel in the middle of the beta strand at position 901 in PI3Kδ's sequence was moved one position to the right into the adjacent loop region, where indels are usually found. See **Fig. 3.5A and 3.5B**.

(e) The deleted residues (238-242) in the mTORβ line (951-955 in PI3Kδ line) were moved 7 residue positions to the left. This was prudent in terms of a structural alignment because it was far better to have a deletion in a loop region rather than in an α-helix. The N242 amino acid was connected to the Y243 residue, which is part of an α-helix. This was because it was structurally unfavourable to have a single residue long piece of α-helix existing in isolation. **See Fig. 3.6A and 3.6B**.

```
mTORβ  23   GSNGHEFVFLLKGHEDLRQDERVMQLFGLVNTLLANDPTSLRKNLSIQRYAVIPLSTNSG  82
            GS G+  + + K  +DLRQD   +Q+  L++ L   +   LR    +  Y  +P    +G
PI3Kδ  769  GSAGNVGI-IFKNGDDLRQDMLTLQMIQLMDVLWKQEGLDLR----MTPYGCLPTGDRTG  823
2° Struc    ####.EEE-EEEE##..HHHHHHHHHHHHHHHHHHH##.....-----.....EEEEE..EE
                   (a)

mTORβ  83   LIGWVPHCDTLHALIRDYREKKKILLNIEHRIMLRMAPDYDHLTLMQKVEVFEHAVNNTA  142
            LI  V H DT+            I LN  +     MA                    A
PI3Kδ  824  LIEVVLHSDTI----------ANIQLNKSN-----MAA------------------TAA  849
2° Struc    EEE...#EEEH----------HHHH#..##-----###------------------..#

mTORβ  143  GDDLAKLLWLKSPSSEVWFDRR-TNYTRSLAVMSMVGYILGLGDRHPSNLMLDRLSGKIL  201
             +  A L WLKS +     DR    +T S A   +  Y+LG+GDRH  N+M+ R SG++
PI3Kδ  850  FNKDALLNWLKSKNPGEALDRAIEEFTLSCAGYCVATYVLGIGDRHSDNIMI-RESGQLF  908
2° Struc    ####HHHHHHHHH#.##HHHHHHHHHHHHHHHHHHHHHHH#.....###EEE-E###.EE

mTORβ  202  HIDFGDCFEVAMTREKFP---EKIPFRLTRMLTNAMEVTGLDGN-----YRITCHTVMEV  253
            HIDFG    +   + KF    E++PF LT    + ++    + +     +R  C     +
PI3Kδ  909  HIDFGHF--LGNFKTKFGINRERVPFILTYDFVHVIQQGKTNNSEKFERFRGYCERAYTI  966
2° Struc    E.......--##..!!!!!!!!!.......HHHHHHH###.#..HHHHHHHHHHHHHHHHHH

mTORβ  254  LREH  257
            LR H
PI3Kδ  967  LRRH  970

2° Struc    HHH#
```

Fig. 3.2A, Location of first change to the initial BLAST alignment. The initial position of the indel (a) has been highlighted yellow.

```
mTORβ    23   GSNGHEFVFLLKGHEDLRQDERVMQLFGLVNTLLANDPTSLRKNLSIQRYAVIPLSTNSG  82
              ++ + + + K  +DLRQD   +Q+  L++ L   +   LR    +  Y  +P    +G
PI3Kδ    769  -GSAGNVGIIFKNGDDLRQDMLTLQMIQLMDVLWKQEGLDLRM----TPYGCLPTGDRTG  823
2°Struc  769  -####.EEEEEEE##..HHHHHHHHHHHHHHHHHHHH##....-----....EEEEE..EE  823
             (a)                                          (b)

mTORβ    83   LIGWVPHCDTLHALIRDYREKKKILLNIEHRIMLRMAPDYDHLTLMQKVEVFEHAVNNTA  142
              LI  V H DT              I LN  + ++                        A
PI3Kδ    824  LIEVVLHSDTI----------ANIQLNKSNMAA------------------------TAA  849
2°Struc  824  EEE...#EEEH----------HHHH#..#####--------------------------..#  849
                                     (c)

mTORβ    143  GDDLAKLLWLKSPSSEVWFDRR-TNYTRSLAVMSMVGYILGLGDRHPSNLMLDRLSGKIL  201
               +  A L WLKS +     DR    +T S A   +  Y+LG+GDRH  N+M+   SG++
PI3Kδ    850  FNKDALLNWLKSKNPGEALDRAIEEFTLSCAGYCVATYVLGIGDRHSDNIMIR-ESGQLF  908
2°Struc  850  ####HHHHHHHHH#.##HHHHHHHHHHHHHHHHHHHHHHH#.....###EEEE-###.EE  908
                                                        (d)
                                                   (e)
mTORβ    202  HIDFGDCFEVAMTREKFP---EKIPFRLTRMLTNAME-----VTGLDGNYRITCHTVMEV  253
              HIDFG    +   + KF    E++PF LT    + ++      +     +R  C     +
PI3Kδ    909  HIDFGHF--LGNFKTKFGINRERVPFILTYDFVHVIQQGKTNNSEKFERFRGYCERAYTI  966
2°Struc  909  E.......--##..!!!!!!!!!.......HHHHHHH###.#..HHHHHHHHHHHHHHHHHH  966

mTORβ    254  LREH  257
              LR H
PI3Kδ    967  LRRH  970
2°Struc  967  HHH#  970
```

Fig. 3.2B, Amended BLAST alignment between mTORβ Kinase and PI3Kδ. The indel that has been shifted from its original position has been highlighted blue in PI3Kδ and red in the secondary structure annotation line. The change of interest has been marked (a).

```
mTORβ  23   GSNGHEFVFLLKGHEDLRQDERVMQLFGLVNTLLANDPTSLRKNLSIQRYAVIPLSTNSG  82
            GS G+  + + K  +DLRQD   +Q+  L++ L   +   LR    +  Y  +P    +G
PI3Kδ  769  GSAGNVGI-IFKNGDDLRQDMLTLQMIQLMDVLWKQEGLDLR----MTPYGCLPTGDRTG  823
2° Struc    ####.EEE-EEEE##..HHHHHHHHHHHHHHHHHHH##....----.....EEEEE..EE
                                                      (b)

mTORβ  83   LIGWVPHCDTLHALIRDYREKKKILLNIEHRIMLRMAPDYDHLTLMQKVEVFEHAVNNTA  142
            LI  V H DT+            I LN  +     MA                    A
PI3Kδ  824  LIEVVLHSDTI----------ANIQLNKSN-----MAA------------------TAA  849
2° Struc    EEE...#EEEH----------HHHH#..##-----###------------------..#

mTORβ  143  GDDLAKLLWLKSPSSEVWFDRR-TNYTRSLAVMSMVGYILGLGDRHPSNLMLDRLSGKIL  201
             +  A L WLKS +     DR    +T S A   +  Y+LG+GDRH  N+M+ R SG++
PI3Kδ  850  FNKDALLNWLKSKNPGEALDRAIEEFTLSCAGYCVATYVLGIGDRHSDNIMI-RESGQLF  908
2° Struc    ####HHHHHHHHH#.##HHHHHHHHHHHHHHHHHHHHHHH#.....###EEE-E###.EE

mTORβ  202  HIDFGDCFEVAMTREKFP---EKIPFRLTRMLTNAMEVTGLDGN-----YRITCHTVMEV  253
            HIDFG    +   + KF    E++PF LT    + ++    + +     +R  C     +
PI3Kδ  909  HIDFGHF--LGNFKTKFGINRERVPFILTYDFVHVIQQGKTNNSEKFERFRGYCERAYTI  966
2° Struc    E.......--##..!!!!!!!!!.......HHHHHHH###.#..HHHHHHHHHHHHHHHHH

mTORβ  254  LREH  257
            LR H
PI3Kδ  967  LRRH  970

2° Struc    HHH#
```

Fig. 3.3A, Location of second change to the initial BLAST alignment. The initial positions of the indels and M810 residue (b) have been highlighted yellow.

```
mTORβ   23   GSNGHEFVFLLKGHEDLRQDERVMQLFGLVNTLLANDPTSLRKNLSIQRYAVIPLSTNSG  82
               ++ + + + K  +DLRQD   +Q+  L++ L   +   LR       Y  +P    +G
PI3Kδ   769  -GSAGNVGIIFKNGDDLRQDMLTLQMIQLMDVLWKQEGLDLRM----TPYGCLPTGDRTG  823
2°Struc 769  -####.EEEEEEE##..HHHHHHHHHHHHHHHHHHHH##....-----....EEEEE..EE  823
            (a)                                          (b)

mTORβ   83   LIGWVPHCDTLHALIRDYREKKKILLNIEHRIMLRMAPDYDHLTLMQKVEVFEHAVNNTA  142
             LI  V H DT              I LN  + ++                        A
PI3Kδ   824  LIEVVLHSDTI----------ANIQLNKSNMAA------------------------TAA  849
2°Struc 824  EEE...#EEEH----------HHHH#..#####--###------------------..#  849
                                     (c)

mTORβ   143  GDDLAKLLWLKSPSSEVWFDRR-TNYTRSLAVMSMVGYILGLGDRHPSNLMLDRLSGKIL  201
              +  A L WLKS +     DR    +T S A   +  Y+LG+GDRH  N+M+   SG++
PI3Kδ   850  FNKDALLNWLKSKNPGEALDRAIEEFTLSCAGYCVATYVLGIGDRHSDNIMIR-ESGQLF  908
2°Struc 850  ####HHHHHHHHH#.##HHHHHHHHHHHHHHHHHHHHHHH#.....###EEEE-###.EE  908
                                                      (d)
                                                   (e)
mTORβ   202  HIDFGDCFEVAMTREKFP---EKIPFRLTRMLTNAME-----VTGLDGNYRITCHTVMEV  253
             HIDFG    +   + KF    E++PF LT    + ++      +     +R  C     +
PI3Kδ   909  HIDFGHF--LGNFKTKFGINRERVPFILTYDFVHVIQQGKTNNSEKFERFRGYCERAYTI  966
2°Struc 909  E.......--##..!!!!!!!!!.......HHHHHHH###.#..HHHHHHHHHHHHHHHHH  966

mTORβ   254  LREH  257
             LR H
PI3Kδ   967  LRRH  970
2°Struc 967  HHH#  970
```

Fig. 3.3B, Amended BLAST alignment between mTORβ Kinase and PI3Kδ. The indels and residue that have been shifted from their original positions have been highlighted blue in PI3Kδ and red in the secondary structure annotation line. The change of interest has been marked (b).

```
mTORβ  23   GSNGHEFVFLLKGHEDLRQDERVMQLFGLVNTLLANDPTSLRKNLSIQRYAVIPLSTNSG  82
            GS G+  + + K  +DLRQD   +Q+  L++ L   +   LR    +  Y  +P    +G
PI3Kδ  769  GSAGNVGI-IFKNGDDLRQDMLTLQMIQLMDVLWKQEGLDLR----MTPYGCLPTGDRTG  823
2° Struc    ####.EEE-EEEE##..HHHHHHHHHHHHHHHHHHH##.....----.....EEEEE..EE


mTORβ  83   LIGWVPHCDTLHALIRDYREKKKILLNIEHRIMLRMAPDYDHLTLMQKVEVFEHAVNNTA  142
            LI  V H DT+            I LN  +     MA                    A
PI3Kδ  824  LIEVVLHSDTI----------ANIQLNKSN-----MAA-------------------TAA  849
2° Struc    EEE...#EEEH----------HHHH#..##-----###-------------------..#
                                           (c)

mTORβ  143  GDDLAKLLWLKSPSSEVWFDRR-TNYTRSLAVMSMVGYILGLGDRHPSNLMLDRLSGKIL  201
             +  A L WLKS +     DR    +T S A   +  Y+LG+GDRH  N+M+ R SG++
PI3Kδ  850  FNKDALLNWLKSKNPGEALDRAIEEFTLSCAGYCVATYVLGIGDRHSDNIMI-RESGQLF  908
2° Struc    ####HHHHHHHHH#.##HHHHHHHHHHHHHHHHHHHHHHH#.....###EEE-E###.EE


mTORβ  202  HIDFGDCFEVAMTREKFP---EKIPFRLTRMLTNAMEVTGLDGN-----YRITCHTVMEV  253
            HIDFG    +   + KF    E++PF LT    + ++    + +     +R  C     +
PI3Kδ  909  HIDFGHF--LGNFKTKFGINRERVPFILTYDFVHVIQQGKTNNSEKFERFRGYCERAYTI  966
2° Struc    E.......--##..!!!!!!!!!.......HHHHHHH###.#..HHHHHHHHHHHHHHHHHH


mTORβ  254  LREH  257
            LR H
PI3Kδ  967  LRRH  970

2° Struc    HHH#
```

Fig. 3.4A, Location of third change to the initial BLAST alignment. The initial position of the indels and MAA residues (c) have been highlighted yellow.

```
mTORβ    23   GSNGHEFVFLLKGHEDLRQDERVMQLFGLVNTLLANDPTSLRKNLSIQRYAVIPLSTNSG  82
              ++ + + + K  +DLRQD   +Q+  L++ L   +   LR    +  Y  +P    +G
PI3Kδ    769  -GSAGNVGIIFKNGDDLRQDMLTLQMIQLMDVLWKQEGLDLRM----TPYGCLPTGDRTG  823
2°Struc  769  -####.EEEEEEE##..HHHHHHHHHHHHHHHHHHHH##....-----....EEEEE..EE  823
             (a)                                          (b)

mTORβ    83   LIGWVPHCDTLHALIRDYREKKKILLNIEHRIMLRMAPDYDHLTLMQKVEVFEHAVNNTA  142
              LI  V H DT             I LN  + ++                        A
PI3Kδ    824  LIEVVLHSDTI----------ANIQLNKSNMAA-----------------------TAA  849
2°Struc  824  EEE...#EEEH----------HHHH#..#####-----------------------..#  849
                                      (c)

mTORβ    143  GDDLAKLLWLKSPSSEVWFDRR-TNYTRSLAVMSMVGYILGLGDRHPSNLMLDRLSGKIL  201
              +  A L WLKS +     DR    +T S A   +  Y+LG+GDRH  N+M+   SG++
PI3Kδ    850  FNKDALLNWLKSKNPGEALDRAIEEFTLSCAGYCVATYVLGIGDRHSDNIMIR-ESGQLF  908
2°Struc  850  ####HHHHHHHHH#.##HHHHHHHHHHHHHHHHHHHHHHH#.....###EEEE-###.EE  908
                                                        (d)
                                                  (e)
mTORβ    202  HIDFGDCFEVAMTREKFP---EKIPFRLTRMLTNAME-----VTGLDGNYRITCHTVMEV  253
              HIDFG    +   + KF    E++PF LT    + ++      +     +R  C     +
PI3Kδ    909  HIDFGHF--LGNFKTKFGINRERVPFILTYDFVHVIQQGKTNNSEKFERFRGYCERAYTI  966
2°Struc  909  E.......--##..!!!!!!!!!.......HHHHHHH###.#..HHHHHHHHHHHHHHHHHH  966


mTORβ    254  LREH  257
              LR H
PI3Kδ    967  LRRH  970
2°Struc  967  HHH#  970
```

Fig. 3.4B, Amended BLAST alignment between mTORβ Kinase and PI3Kδ. The indels and residues that have been shifted from their original positions have been highlighted blue in PI3Kδ and red in the secondary structure annotation line. The change of interest has been marked (c).

```
mTORβ  23   GSNGHEFVFLLKGHEDLRQDERVMQLFGLVNTLLANDPTSLRKNLSIQRYAVIPLSTNSG  82
            GS G+  + + K  +DLRQD   +Q+  L++ L   +   LR    +  Y  +P    +G
PI3Kδ  769  GSAGNVGI-IFKNGDDLRQDMLTLQMIQLMDVLWKQEGLDLR----MTPYGCLPTGDRTG  823
2° Struc    ####.EEE-EEEE##..HHHHHHHHHHHHHHHHHHH##.....-----.....EEEEE..EE

mTORβ  83   LIGWVPHCDTLHALIRDYREKKKILLNIEHRIMLRMAPDYDHLTLMQKVEVFEHAVNNTA  142
            LI  V H DT+            I LN  +     MA                     A
PI3Kδ  824  LIEVVLHSDTI----------ANIQLNKSN-----MAA-------------------TAA  849
2° Struc    EEE...#EEEH----------HHHH#..##-----###-------------------..#


mTORβ  143  GDDLAKLLWLKSPSSEVWFDRR-TNYTRSLAVMSMVGYILGLGDRHPSNLMLDRLSGKIL  201
             +  A L WLKS +     DR    +T S A   +  Y+LG+GDRH  N+M+ R SG++
PI3Kδ  850  FNKDALLNWLKSKNPGEALDRAIEEFTLSCAGYCVATYVLGIGDRHSDNIMI-RESGQLF  908
2° Struc    ####HHHHHHHHH#.##HHHHHHHHHHHHHHHHHHHHHHH#.....###EEE-E###.EE
                                                        (d)

mTORβ  202  HIDFGDCFEVAMTREKFP---EKIPFRLTRMLTNAMEVTGLDGN-----YRITCHTVMEV  253
            HIDFG    +   + KF    E++PF LT    + ++    + +     +R  C     +
PI3Kδ  909  HIDFGHF--LGNFKTKFGINRERVPFILTYDFVHVIQQGKTNNSEKFERFRGYCERAYTI  966
2° Struc    E.......--##..!!!!!!!!!.......HHHHHHH###.#..HHHHHHHHHHHHHHHHH


mTORβ  254  LREH  257
            LR H
PI3Kδ  967  LRRH  970

2° Struc    HHH#
```

Fig. 3.5A, Location of fourth change to the initial BLAST alignment. The initial position of the indel at position 901 in PI3Kδ's sequence (d) has been highlighted yellow.

```
mTORβ   23   GSNGHEFVFLLKGHEDLRQDERVMQLFGLVNTLLANDPTSLRKNLSIQRYAVIPLSTNSG  82
               ++ + + + K  +DLRQD   +Q+  L++ L   +   LR    +  Y  +P    +G
PI3Kδ   769  -GSAGNVGIIFKNGDDLRQDMLTLQMIQLMDVLWKQEGLDLRM----TPYGCLPTGDRTG  823
2°Struc 769  -####.EEEEEEE##..HHHHHHHHHHHHHHHHHHH##....-----....EEEEE..EE  823
            (a)                                          (b)

mTORβ   83   LIGWVPHCDTLHALIRDYREKKKILLNIEHRIMLRMAPDYDHLTLMQKVEVFEHAVNNTA  142
             LI  V H DT             I LN  + ++                          A
PI3Kδ   824  LIEVVLHSDTI----------ANIQLNKSNMAA-------------------------TAA  849
2°Struc 824  EEE...#EEEH----------HHHH#..#####--------------------------..#  849
                                    (c)

mTORβ   143  GDDLAKLLWLKSPSSEVWFDRR-TNYTRSLAVMSMVGYILGLGDRHPSNLMLDRLSGKIL  201
              +  A L WLKS +     DR    +T S A   +  Y+LG+GDRH  N+M+   SG++
PI3Kδ   850  FNKDALLNWLKSKNPGEALDRAIEEFTLSCAGYCVATYVLGIGDRHSDNIMIR-ESGQLF  908
2°Struc 850  ####HHHHHHHHH#.##HHHHHHHHHHHHHHHHHHHHHHH#.....###EEEE-###.EE  908
                                                        (d)
                                                    (e)
mTORβ   202  HIDFGDCFEVAMTREKFP---EKIPFRLTRMLTNAME-----VTGLDGNYRITCHTVMEV  253
             HIDFG    +   + KF    E++PF LT    + ++      +     +R  C     +
PI3Kδ   909  HIDFGHF--LGNFKTKFGINRERVPFILTYDFVHVIQQGKTNNSEKFERFRGYCERAYTI  966
2°Struc 909  E.......--##--!!!!!!!!!.......HHHHHHH###.#..HHHHHHHHHHHHHHHHH  966


mTORβ   254  LREH  257
             LR H
PI3Kδ   967  LRRH  970
2°Struc 967  HHH#  970
```

Fig. 3.5B, Amended BLAST alignment between mTORβ Kinase and PI3Kδ. The indels that was shifted from its original positions has been highlighted blue in PI3Kδ and red in the secondary structure annotation line. The change of interest has been marked (d).

```
mTORβ  23   GSNGHEFVFLLKGHEDLRQDERVMQLFGLVNTLLANDPTSLRKNLSIQRYAVIPLSTNSG  82
            GS G+  + + K  +DLRQD   +Q+  L++ L   +   LR    +  Y  +P    +G
PI3Kδ  769  GSAGNVGI-IFKNGDDLRQDMLTLQMIQLMDVLWKQEGLDLR----MTPYGCLPTGDRTG  823
2° Struc    ####.EEE-EEEE##..HHHHHHHHHHHHHHHHHHH##.....----.....EEEEE..EE


mTORβ  83   LIGWVPHCDTLHALIRDYREKKKILLNIEHRIMLRMAPDYDHLTLMQKVEVFEHAVNNTA  142
            LI  V H DT+            I LN  +     MA                     A
PI3Kδ  824  LIEVVLHSDTI----------ANIQLNKSN-----MAA-------------------TAA  849
2° Struc    EEE...#EEEH----------HHHH#..##-----###-------------------..#


mTORβ  143  GDDLAKLLWLKSPSSEVWFDRR-TNYTRSLAVMSMVGYILGLGDRHPSNLMLDRLSGKIL  201
             +  A L WLKS +     DR    +T S A   +  Y+LG+GDRH  N+M+ R SG++
PI3Kδ  850  FNKDALLNWLKSKNPGEALDRAIEEFTLSCAGYCVATYVLGIGDRHSDNIMI-RESGQLF  908
2° Struc    ####HHHHHHHHH#.##HHHHHHHHHHHHHHHHHHHHHHH#.....###EEE-E###.EE


                                                        (e)
mTORβ  202  HIDFGDCFEVAMTREKFP---EKIPFRLTRMLTNAMEVTGLDGN-----YRITCHTVMEV  253
            HIDFG    +   + KF    E++PF LT    + ++    + +     +R  C     +
PI3Kδ  909  HIDFGHF--LGNFKTKFGINRERVPFILTYDFVHVIQQGKTNNSEKFERFRGYCERAYTI  966
2° Struc    E.......--##..!!!!!!!!!.......HHHHHHH###.#..HHHHHHHHHHHHHHHHHH


mTORβ  254  LREH  257
            LR H
PI3Kδ  967  LRRH  970

2° Struc    HHH#
```

Fig. 3.6A, Location of fifth change to the initial BLAST alignment. The initial positions of the deletions and N amino acid residues have been highlighted yellow (e).

```
mTORβ    23   GSNGHEFVFLLKGHEDLRQDERVMQLFGLVNTLLANDPTSLRKNLSIQRYAVIPLSTNSG  82
              ++ + + + K  +DLRQD   +Q+  L++ L   +   LR    +  Y  +P    +G
PI3Kδ    769  -GSAGNVGIIFKNGDDLRQDMLTLQMIQLMDVLWKQEGLDLRM----TPYGCLPTGDRTG  823
2°Struc  769  -####.EEEEEEE##..HHHHHHHHHHHHHHHHHHHH##....-----....EEEEE..EE  823
             (a)                                          (b)

mTORβ    83   LIGWVPHCDTLHALIRDYREKKKILLNIEHRIMLRMAPDYDHLTLMQKVEVFEHAVNNTA  142
              LI  V H DT             I LN  + ++                         A
PI3Kδ    824  LIEVVLHSDTI----------ANIQLNKSNMAA------------------------TAA  849
2°Struc  824  EEE...#EEEH----------HHHH#..#####-----------------------..#  849
                                      (c)

mTORβ    143  GDDLAKLLWLKSPSSEVWFDRR-TNYTRSLAVMSMVGYILGLGDRHPSNLMLDRLSGKIL  201
              +  A L WLKS +     DR    +T S A   +  Y+LG+GDRH  N+M+   SG++
PI3Kδ    850  FNKDALLNWLKSKNPGEALDRAIEEFTLSCAGYCVATYVLGIGDRHSDNIMIR-ESGQLF  908
2°Struc  850  ####HHHHHHHHH#.##HHHHHHHHHHHHHHHHHHHHHHH#.....###EEEE-###.EE  908
                                                        (d)
                                                    (e)
mTORβ    202  HIDFGDCFEVAMTREKFP---EKIPFRLTRMLTNAME-----VTGLDGNYRITCHTVMEV  253
              HIDFG    +   + KF    E++PF LT    + ++      +     +R  C     +
PI3Kδ    909  HIDFGHF--LGNFKTKFGINRERVPFILTYDFVHVIQQGKTNNSEKFERFRGYCERAYTI  966
2°Struc  909  E.......--##--!!!!!!!!!.......HHHHHHH###.#..HHHHHHHHHHHHHHHHHH  966


mTORβ    254  LREH  257
              LR H
PI3Kδ    967  LRRH  970
2°Struc  967  HHH#  970
```

Fig. 3.6B, Amended BLAST alignment between mTORβ Kinase and PI3Kδ. The deletions and N residue that were shifted from their original positions have been coloured red in the mTORβ line. The change of interest has been marked (e).

Change	Identity	Similarity
WT	28%	14%
a	27%	16%
b	27%	15%
c	27%	15%
d	26%	16%
e	26%	16%

Fig. 3.7, A table showing changes in percentage identity and similarity between the amino acids in the alignment between mTORβ and PI3Kδ after each alteration in the alignment was made.

3.3) Extending the alignment produced by BLAST between mTORβ Kinase and PI3Kδ

The alignment produced between PI3Kδ and mTORβ Kinase produced by BLAST did not cover the whole length of the mTORβ Kinase domain. Residues were omitted and were not aligned at both the C-terminus and the N-terminus. Therefore, it was necessary to extend this alignment to encompass the full length of mTORβ's kinase domain. To do this, the mTOR sequence was firstly converted into PIR format. Then, PI3Kδ's kinase domain was edited out of the PDB file (2X38) and the sequence was extracted in PIR format. The two sequences were then aligned in their entirety using Andrew Martin's Needleman and Wunsch (Needleman & Wunsch 1970) (nw) align program. The terminal regions not present in the alignment shown in **Fig. 3.2B** were extracted from this new alignment and appended to the original alignment shown in **Fig. 3.2B**. The full, extended alignment is shown in **Fig. 3.8A**, and the additional N-terminal and C-terminal alignments that were appended to the BLAST alignment in **Fig. 3.2B** are shown in **Fig. 3.8B**.

PI3Kδ Kinase is sequence in top line (blue), and mTORβ Kinase is sequence in second line (pink)

```
STHHMKVLMKQGEALSKLKALNDFVKVSSQKTTKPQTKEMMHMCMRQETYMEALSHLQSPLDPSTLLEEVCVEQCTFMDS
------------------------------------------------------------------------------IQS

KMKPLWIMYSSEEA------ GSAGN-VGIIFKNGDDLRQDMLTLQMIQLMDVLWKQEGLDLR----MTPYGCLPTGDRTG
IAPSLQVITSKQRPRKLTLM GSNGHEFVFLLKGHEDLRQDERVMQLFGLVNTLLANDPTSLRKNLSIQRYAVIPLSTNSG

LIEVVLHSDTIA----------NIQLNKSN---MAATAAFNKDALLN--------------------WLKSKNPGEALD
LIGWVPHCDTLHALIRDYREKKKILLNIEHRIMLRMAPDYDHLTLMQKVEVFEHAVNNTAGDDLAKLLWLKSPSSEVWFD

RAIEEFTLSCAGYCVATYVLGIGDRHSDNIMI-RESGQLFHIDFGH-F-LGNFRVPFI--LTYDFVHVIQQGKTNNSEKF
RRTN-YTRSLAVMSMVGYILGLGDRHPSNLMLDRLSGKILHIDFGDCFEVAMTREKFPEKIPFRLTRMLTNAMEVTGLD-

ERFRGYCERAYTILRRH GLLFLHLFALMRAAGLPELSCSKDIQYLKDSLALGKTEEEALKHFRVKFNEALRESW
GNYRITCHTVMEVLREH KDSVMAVLEAFVYDPLLNWRL-----------------------------------
```

Fig. 3.8A, Full alignment between mTOR Kinase and PI3Kδ. This was generated using Dr Andrew Martin's Needleman and Wunsch program. The alignment upstream of the first solid dark blue line represents the extended N-terminal region that was manually appended to the initial alignment produced by BLAST between PI3Kδ and mTOR's Kinase domain. The alignment downstream of the second solid dark blue line adds the C-terminal portion of mTOR's kinase domain that was omitted by the BLAST programme. The alignment in between the two dark blue lines shows the amended BLAST alignment shown in **Fig. 3.2B**.

Additional N-terminal alignment between PI3Kδ Kinase and mTORβ Kinase

```
mTORβ       ------------------------------------------------------------

PI3Kδ   675 STHHMKVLMKQGEALSKLKALNDFVKVSSQKTTKPQTKEMMHMCMRQETYMEALSHLQSP  734
2°Struc 675 .HHHHHHHHHHHHHHHHHHHHHHHHHHHHHH..HHHHHHHHHHHH..HHHHHHH..EEE.  675

mTORβ   1   -----------------IQSIAPSLQVITSKQRPRKLTLM                      23
                              ++S +++L ++ S++
PI3Kδ   735 LDPSTLLEEVCVEQCTFMDSKMKPLWIMYSSEEA------                      768
2°Struc 735 .EEEEEE.EE.....EE.......EEEEEE..........                      768
```

Additional C-terminal alignment betweeen PI3Kδ Kinase and mTORβ Kinase

```
mTORβ   259 KDSVMAVLEAFVYDPLLNWRL-----------------------------------   279
                + +  +     L + +
PI3Kδ   971 GLLFLHLFALMRAAGLPELSCSKDIQYLKDSLALGKTEEEALKHFRVKFNEALRESW  1027
2°Struc 971 HHHHHHHHHHH..........HHHHHHHHHH......HHHHHHHHHHHHHHHHHH..
```

Fig. 3.8B, The additional alignments that were generated between mTOR's kinase domain and PI3Kδ by Andrew Martin's Needleman and Wunsch align program. For the sake of clarity, the extended alignments at the N and C termini have been shown below separately.

3.4) Aligning the linker between mTOR's Kinase and FRB domains with PI3Kγ

A linker region joins the FRB and Kinase domains in mTORβ. The alignment between mTOR's linker and PI3Kγ in Mike Hall's paper (Sturgill & Hall 2009) was copied. This was then annotated with PI3Kγ's secondary structure, which was obtained from DSSP at EBI's website. The position of one indel in the sequence alignment was altered in order to improve the alignment in structural terms. This can be seen in **Figs. 3.9 and 3.10**. PI3Kγ (Walker et al. 2000) was used as the homologue to model the linker.

Target Strand (mTORα)
(mTORα is sequence on top line and spans residues 2109-2159, i.e. 51 residues)

```
RRISKQLPQLTSLELQYVSPKLLMCRDLELAVPGTYD-PNQPIIRIQSIAP-S
 +   +   +    S ++      K   +++   +L +P ++   P +P++++   ++   +
IKSLSAEKYDVSSQVISQL-KQKLENLQNLNLPQSFRVPYDPGLKAGALVIEK
HHH.........HHHHHHH-HHHHHHHH.......EEE..EEEEEEEE....
```

Parent Strand (PI3Kγ)

(PI3Kγ is sequence on bottom line and spans residues 749-800, i.e. 52 residues)

Fig. 3.9, Initial alignment of mTOR's Linker with PI3Kγ. The red indel is its initial position prior to amendment.

Target Strand (mTORα)

(mTORα is the sequence on the top line and spans residues 2109-2159, i.e. 51 residues)

```
RRISKQLPQLTSLELQYVSPKLLMCRDLELAVPGTYD-PNQPIIRIQSIAP-S
 +   +   +    S +     + K   +++   +L +P ++   P +P++++   ++   +
IKSLSAEKYDVS-SQVISQLKQKLENLQNLNLPQSFRVPYDPGLKAGALVIEK
HHH.........-HHHHHHHHHHHHHHH.......EEE..EEEEEEEE....
```

Parent Strand (PI3Kγ)

(PI3Kγ is the sequence on the bottom line and spans residues 749-800, i.e. 52 residues)

Fig. 3.10, Amended alignment between mTOR's Linker and PI3Kγ. The indel that has been highlighted red was moved from the middle of the helix in Mike Hall's alignment to the N-terminal loop region.

3.5) Fitting PI3Kδ Kinase onto PI3Kγ

Dr Andrew Martin's ProFit programme (Martin, A.C.R. and Porter, C.T., http://www.bioinf.org.uk/software/profit/) was used to superimpose PI3Kδ onto PI3Kγ using the McLachlan algorithm, (McLachlan, A.D., 1982). This provided a reference point from which one could later position mTORβ's FRB, Kinase and linker domains relative to each other in a multiple alignment. Using the text editor Emacs, the PDB files for PI3Kδ (2X38), (Berndt et al. 2010) and PI3Kγ (1E8X), (Walker et al. 2000) were both trimmed down to their kinase domains. ProFit was then used to align the two structures so that no pair of aligned Cα atoms was more than 10Å apart. The program created a structural alignment, whereby the structure for PI3Kδ was super-imposed onto the structure for PI3Kγ.

3.6) Producing the multiple alignment between mTOR, FRB, PI3Kδ and PI3Kγ

The alignment between PI3Kγ and PI3Kδ was merged with the alignment between PI3Kδ and mTOR. The alignment between the Linker and PI3Kγ was also introduced into mTOR's alignment (See **Figs. 3.9 and 3.10** above). Since PI3Kγ does not have a FRB domain, it could not be used as a homologue to model the position of the FRB domain relative to the kinase domain. This problem was circumvented by retaining 6 residues from PI3Kγ's helical domain to the N-terminus of PI3Kγ's linker. The other 94 residues that were originally aligned with FRB in Hall and Sturgill's paper were then shifted in the C-terminal direction by 94 residue positions. 94 gaps were inserted in the place of the helical residues. The FRB domain would then be aligned with the start of this gap region. MODELLER would effectively see the 6-residues from PI3Kγ's helical domain as a structural anchor, and would join the FRB domain to the linker. This would avoid FRB being fitted onto PI3Kγ's helical domain. The 94 residue gap was maintained throughout the 4 sequences in the alignment. A simple

block diagram illustrating how the different domains and proteins were aligned can be seen in **Fig. 3.11**. The sequences were aligned in PIR format. The final alignment can be seen in **Fig. 3.12** and **Fig. 3.13**.

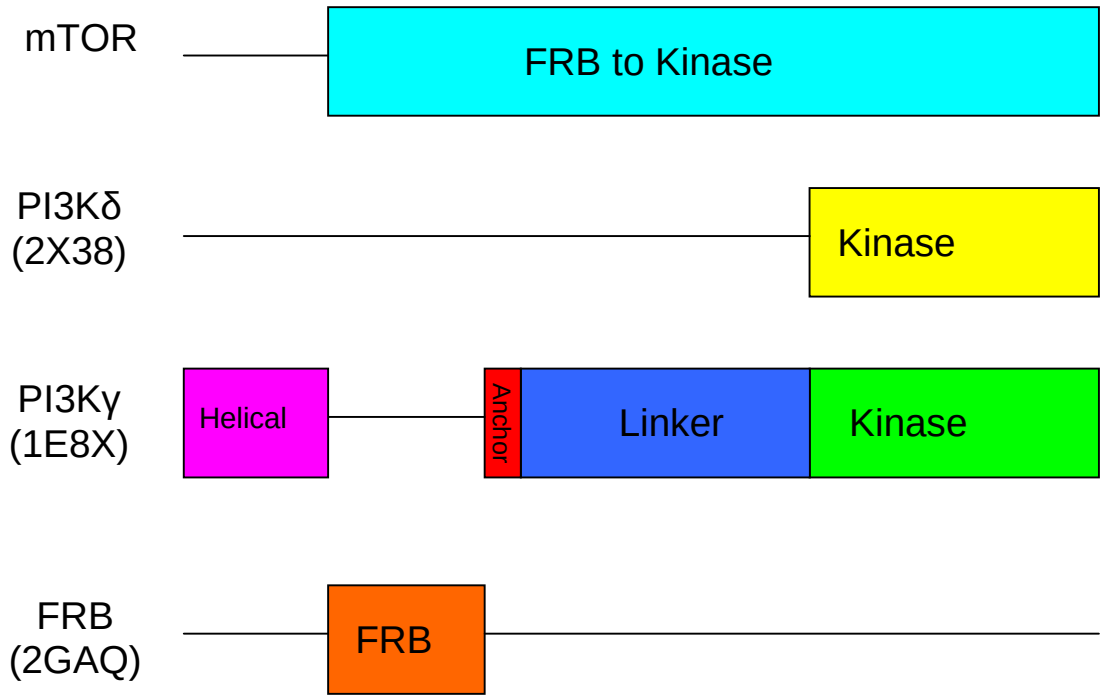

Fig. 3.11, Diagram showing the alignment of the different proteins in the final multiple alignment. mTOR's kinase domain was aligned and modelled on PI3Kδ's kinase domain. mTOR's linker was aligned and modelled using the corresponding sequence in PI3Kγ. A NMR structure for mTOR's FRB domain has already been elucidated. It was appended to the N-terminus of PI3Kγ's linker via the 6 residue long 'structural anchor'.

```
>P1;MTORBP
sequence::::::mTORBetaFRB_to_Kinase:HUMAN::
------------------------------------------------------------
---------------------------------ELIRVAILWHEMWHEGLEEASRLYFG
ERNVKGMFEVLEPLHAMMERGPQTLKETSFNQAYGRDLMEAQEWCRKYMKSGNVKDLTQA
WDLYYHVFRRISKQLPQLTSLELQYVSPKLLMCRDLELAVPGT-----------YD-PNQ
PIIRIQSIAPSLQVITSK--QRPRKLTLMGSNGHEFVFLLKGHEDLRQDERVMQLFGLVN
TLLANDPTSLRKNLSIQRYAVIPLSTNSGLIGWVPHCDTLHALIRDYREKKKILLNIEHR
IMLRMAPDYDHLTLMQKVEVFEHAVNNTAGDDLAKLLWLKSPSS-EVWFDRR-TNYTRSL
AVMSMVGYILGLGDRHPSNLMLDRLSGKILHIDFGDCFEVAMTREKFP---EKIPFRLTR
MLTNAME-----VTGLDGNYRITCHTVMEVLREHKDSVMAVLEAFVYDPLLNWRL*


>P1;2X38_A
structureX:2X38:742:A:991:A:PI3KDelta Kinase:MOUSE:2.20:0.240
------------------------------------------------------------
------------------------------------------------------------
------------------------------------------------------------
----------------------------------------------------EEVCVE
QCTFMDSKMKPLWIMYSS--EEA-------GSAGNVGIIFKNGDDLRQDMLTLQMIQLMD
VLWKQEGLDLRM----TPYGCLPTGDRTGLIEVVLHSDTI----------ANIQLNKSNM
AA-----------------------TAAFNKDALLNWLKSKNP-GEALDRAIEEFTLSC
AGYCVATYVLGIGDRHSDNIMIR-ESGQLFHIDFGHF--LGNF---------RVPFILTY
DFVHVIQQGKTNNSEKFERFRGYCERAYTILRRHGLLFLHLFALMRAAGLPELSC*


>P1;1E8X_A
structureX:1E8X:655:A:1044:A:PI3KGamma from FRB to
Kinase:WILDBOAR:2.20:0.255
DVLHYLLQLVQAVKFEPYHDSALARFLLKRGLRNKRIGHFLFWFLRSEIAQSRHYQQRFA
VILEAYLRGCGTAMLHDFTQQVQVIDMLQKVTID--------------------------
------------------------------------------------------------
--------IKSLSAEKYDVS-SQVISQLKQKLENLQNLNLPQSFRVPYDPGLKAGALVIE
KCKVMASKKKPLWLEFKCADP-------TALSNETIGIIFKHGDDLRQDMLILQILRIME
SIWETESLDLCL----LPYGCISTGDKIGMIEIVKDATTI----------AKIQ--QSTV
GN-----------------------TGAFKDEVLSHWLKEKCPIEEKFQAAVERFVYSC
AGYCVATFVLGIGDRHNDNIMIS-ETGNLFHIDFGH-----------------VPFVLTP
DFLFVMGTSGKKTSLHFQKFQDVCVKAYLALRHHTNLLIILFSMMLMTGMPQLTS*


>P1;2GAQ_A
structureN:2GAQ:1:A:100:A:NMR Structure of mTOR's FRB
domain:HUMAN:HUMAN:0.00:0.00
------------------------------------------------------------
---------------------------------ELIRVAILWHEMWHEGLEEASRLYFG
ERNVKGMFEVLEPLHAMMERGPQTLKETSFNQAYGRDLMEAQEWCRKYMKSGNVKDLTQA
WDLYYHVFRRISKQ----------------------------------------------
------------------------------------------------------------
------------------------------------------------------------
------------------------------------------------------------
------------------------------------------------------------
----------------------------------------------------------*
```

Fig. 3.12, Final Multiple Alignment between mTOR, FRB, PI3Kγ and PI3Kδ in PIR format.

```
------------------------------------------------------------ mTORBeta
------------------------------------------------------------ PI3KDelta
DVLHYLLQLVQAVKFEPYHDSALARFLLKRGLRNKRIGHFLFWFLRSEIAQSRHYQQRFA PI3KGamma
------------------------------------------------------------ FRB

----------------------------------ELIRVAILWHEMWHEGLEEASRLYFG mTORBeta
------------------------------------------------------------ PI3KDelta
VILEAYLRGCGTAMLHDFTQQVQVIDMLQKVTID---------------------------- PI3KGamma
----------------------------------ELIRVAILWHEMWHEGLEEASRLYFG FRB

ERNVKGMFEVLEPLHAMMERGPQTLKETSFNQAYGRDLMEAQEWCRKYMKSGNVKDLTQA mTORBeta
------------------------------------------------------------ PI3KDelta
------------------------------------------------------------ PI3KGamma
ERNVKGMFEVLEPLHAMMERGPQTLKETSFNQAYGRDLMEAQEWCRKYMKSGNVKDLTQA FRB

WDLYYHVFRRISKQLPQLTSLELQYVSPKLLMCRDLELAVPGT-----------YD-PNQ mTORBeta
-------------------------------------------------------EEVCVE PI3KDelta
--------IKSLSAEKYDVS-SQVISQLKQKLENLQNLNLPQSFRVPYDPGLKAGALVIE PI3KGamma
WDLYYHVFRRISKQ---------------------------------------------- FRB

PIIRIQSIAPSLQVITSK--QRPRKLTLMGSNGHEFVFLLKGHEDLRQDERVMQLFGLVN mTORBeta
QCTFMDSKMKPLWIMYSS--EEA-------GSAGNVGIIFKNGDDLRQDMLTLQMIQLMD PI3KDelta
KCKVMASKKKPLWLEFKCADP--------TALSNETIGIIFKHGDDLRQDMLILQILRIME PI3KGamma
------------------------------------------------------------ FRB

TLLANDPTSLRKNLSIQRYAVIPLSTNSGLIGWVPHCDTLHALIRDYREKKKILLNIEHR mTORBeta
VLWKQEGLDLRM----TPYGCLPTGDRTGLIEVVLHSDTI----------ANIQLNKSNM PI3KDelta
SIWETESLDLCL----LPYGCISTGDKIGMIEIVKDATTI----------AKIQ--QSTV PI3KGamma
------------------------------------------------------------ FRB

IMLRMAPDYDHLTLMQKVEVFEHAVNNTAGDDLAKLLWLKSPSS-EVWFDRR-TNYTRSL mTORBeta
AA-------------------------TAAFNKDALLNWLKSKNP-GEALDRAIEEFTLSC PI3KDelta
GN-------------------------TGAFKDEVLSHWLKEKCPIEEKFQAAVERFVYSC PI3KGamma
------------------------------------------------------------ FRB

AVMSMVGYILGLGDRHPSNLMLDRLSGKILHIDFGDCFEVAMTREKFP---EKIPFRLTR mTORBeta
AGYCVATYVLGIGDRHSDNIMIR-ESGQLFHIDFGHF--LGNF---------RVPFILTY PI3KDelta
AGYCVATFVLGIGDRHNDNIMIS-ETGNLFHIDFGH-----------------VPFVLTP PI3KGamma
------------------------------------------------------------ FRB

MLTNAME-----VTGLDGNYRITCHTVMEVLREHKDSVMAVLEAFVYDPLLNWRL*     mTORBeta
DFVHVIQQGKTNNSEKFERFRGYCERAYTILRRHGLLFLHLFALMRAAGLPELSC*     PI3KDelta
DFLFVMGTSGKKTSLHFQKFQDVCVKAYLALRHHTNLLIILFSMMLMTGMPQLTS*     PI3KGamma
------------------------------------------------------------*     FRB
```

Fig 3.13, Final Multiple Alignment between mTOR, FRB, PI3Kγ and PI3Kδ in block format.

3.7) Modelling the final alignment

The multiple alignment (**Fig. 3.12**) took into account the fit that had been made between PI3Kδ and PI3Kγ, as well ensuring that the alignment between PI3Kδ and mTOR Kinase was preserved. MODELLER (Sali et al. 1995) was then used to generate a model. The key residues in the ATP binding pocket of the kinase domain, and the rapamycin binding residues in the FRB domain were then highlighted in the models produced images of the models in Rasmol (Sayle & Milner-White 1995) can be seen in **Figs. 3.14-3.16**.

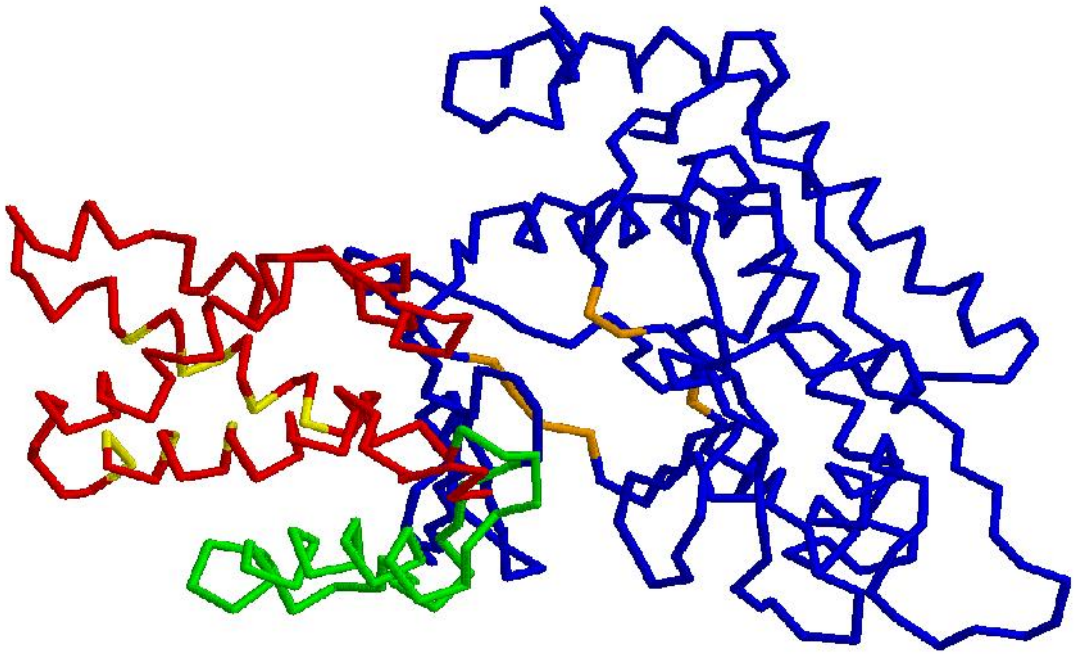

Red Backbone = FRB domain

Yellow Backbone = Rapamycin Binding residues

Green Backbone = Linker

Blue Backbone = Kinase domain

Orange Backbone = Key residues in ATP binding pocket

Fig. 3.14, Cα trace of the model with domains and key residues highlighted.

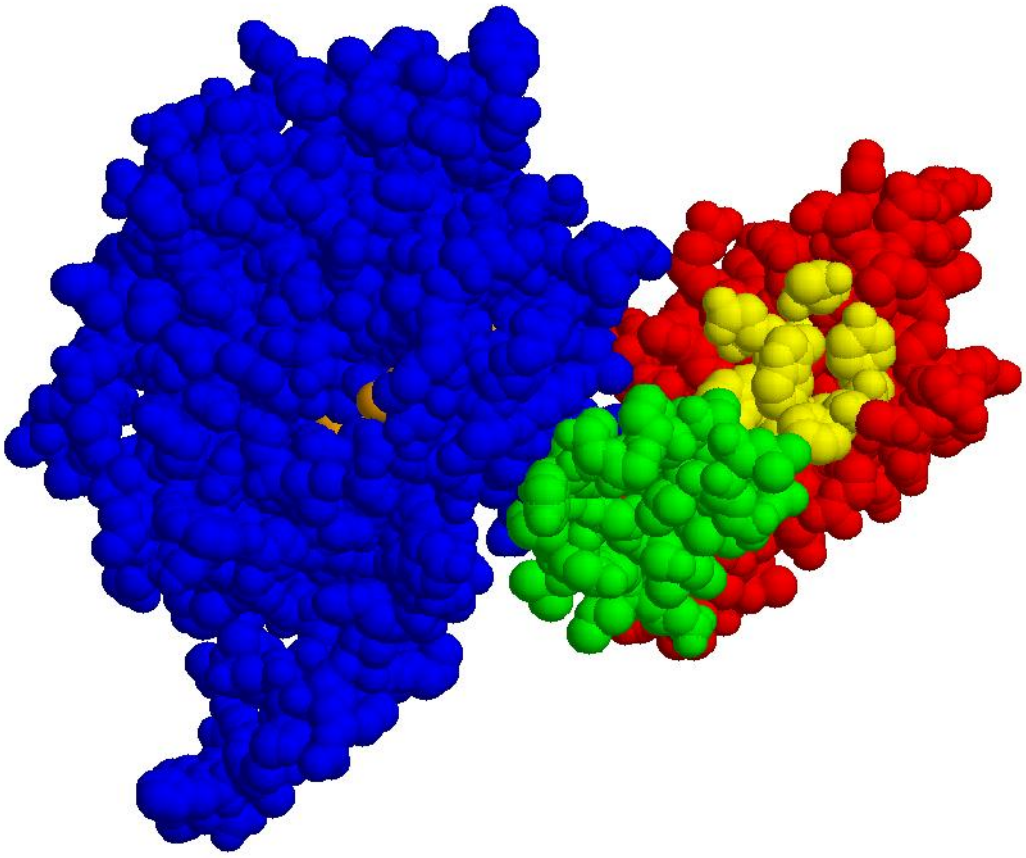

Red Spheres = FRB domain

Yellow Spheres = Rapamycin Binding residues

Green Spheres = Linker

Blue Spheres = Kinase domain

Orange Spheres = Key residues in ATP binding pocket

Fig. 3.15, Space-Filling view of the model centred on FRB's rapamycin binding residues.

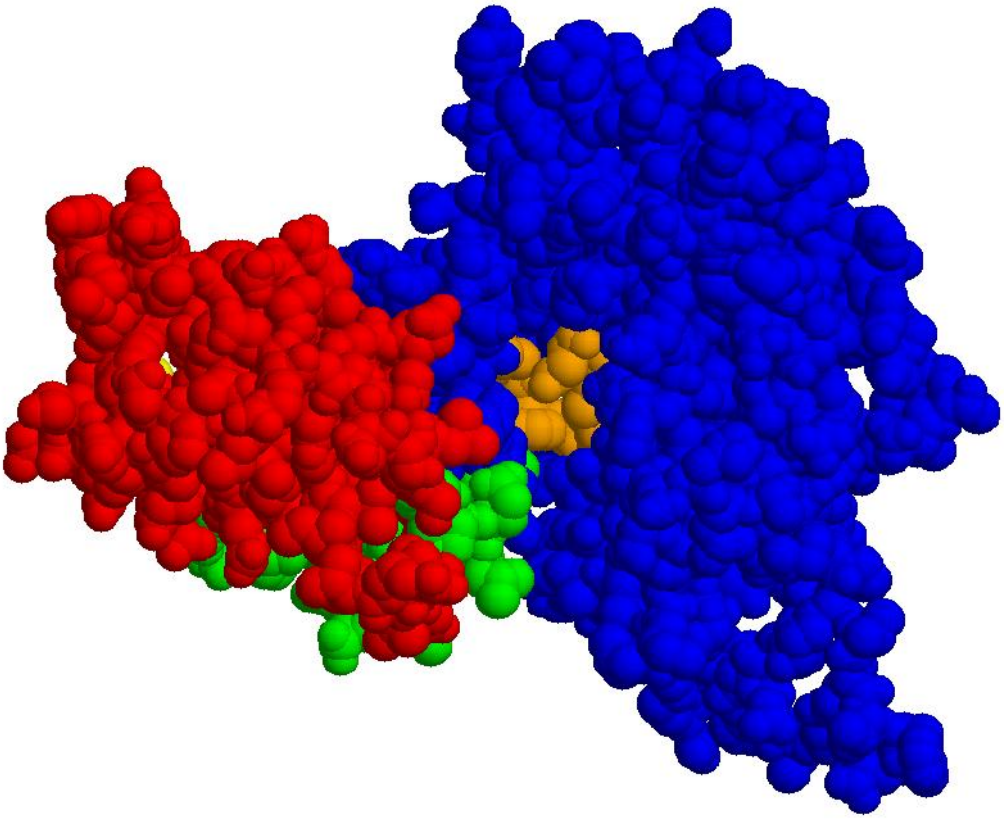

Red Spheres = FRB domain

Yellow Spheres = Rapamycin Binding residues

Green Spheres = Linker

Blue Spheres = Kinase domain

Orange Spheres = Key residues in ATP binding pocket

Fig. 3.16, Space-Filling view of the model centred on the key residues in the Kinase domain's ATP binding pocket.

3.8) Discussion

A 3D model of mTOR from the FRB domain to the end of the kinase domain was produced using comparative modelling. Key residues in the model were highlighted to facilitate easy visualisation of the regions to which ATP or inhibitors would bind. A major benefit that resulted from the project compared with Hall's model was that a model had been generated that would enable myself and other members of the group to gain insight into potential mechanisms for the inhibition of mTOR.

Chapter 4: Results

mTOR mutant studies

Chapter 4: mTOR mutant studies

4.0) Introduction

An alternatively spliced form of mTOR was recently discovered in the Gout lab by Alexander Zhyvoloup. This isoform was found in the cell lysate of HEK293 cells. Analysis of the protein revealed that in contrast to the full-length wild-type mTOR, 12 amino acids were absent in this isoform's kinase domain. This mutation removes the entire kbeta5 strand from the catalytic site, which includes the critical Lys2187 residue. This amino acid is thought to interact with the α-phosphate of ATP. Consequently, it is thought that the 12del mutation disrupts mTOR activity. Furthermore, a Japanese lab recently created a point mutation (S2215Y) in mTORα's kinase domain (Sato et al. 2010). **Figs. 4.1-4.3** illustrate the locations of these mutations. Experiments showed that this alteration conferred constitutive activation on mTORα, even under conditions of nutrient deprivation (Sato et al. 2010). We were interested to see what potential effects these mutations could have on mTORβ activity.

Therefore, site-directed mutagenesis was utilised to introduce these mutations into the DNA sequences of mTORβWT. This resulted in the creation of two different types of mutant for mTORβ. The S2215Y point mutant was named 'S2215Y', and the alternatively spliced form was denoted '12del' in all future work. Sequence analysis of the DNA was then performed in order to verify that the mutations were present. HEK293 cells were then transiently transfected with the appropriate plasmid DNA and Western blots were carried out to confirm expression of the proteins in the mammalian cells. Immunoprecipitation was also performed in order to purify the mTOR proteins from the HEK293 total cell lysates.

The effects of the mutations on mTORβ activity were then explored by assessing the phosphorylation status of 4E-BP1, S6K1 and Akt with Western blots.

4E-BP1 and S6K1 are known as substrates for mTORC1, whereas Akt has been shown to be a phosphorylation target for mTORC2. In order to assess whether the S2215Y point mutation also conferred constitutive activation on mTORβ, the HEK293 cells were subjected to serum and nutrient starvation as has been performed by Sato et al with mTORαS2215Y (Sato et al. 2010). Moreover, we also wished to observe whether stimulation of HEK293 cells that had been starved would restore phosphorylation of 4E-BP1, which would be indicative of mTORC1 activity.

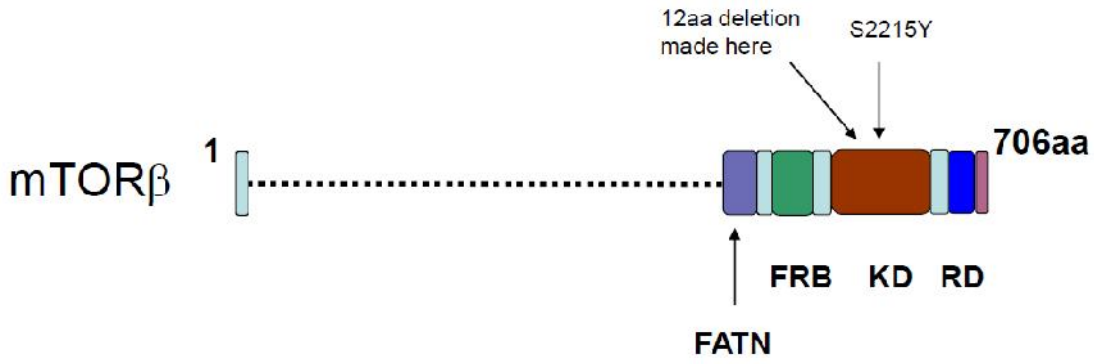

Fig. 4.1, Locations of the mutations in mTORβ. mTORα shares the same C-terminal region as mTORβ, so the position of the '12del' mutation will be at the same position in mTORα. The 12aa deletion is near the junction of the FRB and the Kinase domains. It is thought to be an alternatively spliced form of mTOR. The S2215Y point mutation was identified by searching the COSMIC database of somatic mutations. It has been shown to confer constitutive activation on mTOR even under conditions of nutrient deprivation.

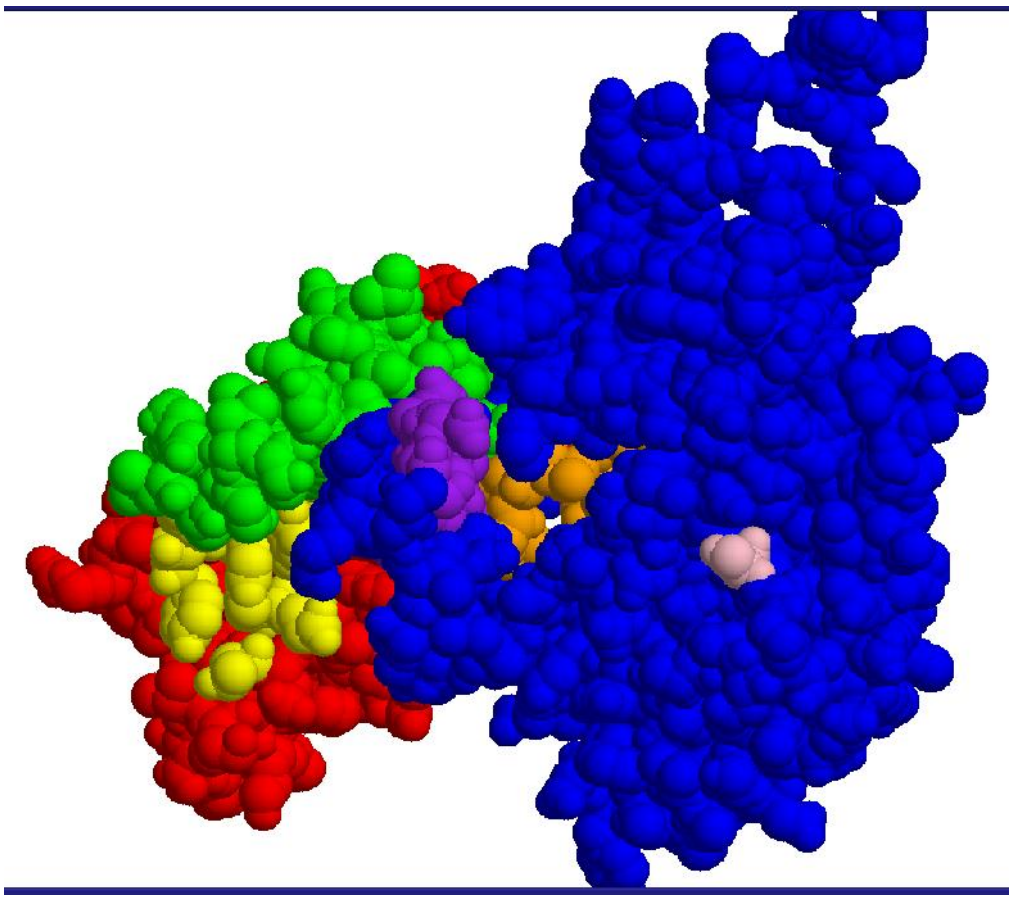

Red Spheres = FRB domain

Yellow Spheres = Rapamycin Binding residues

Green Spheres = Linker

Blue Spheres = Kinase domain

Orange Spheres = Key residues in ATP binding pocket

Purple Spheres = 12del mutation

Pink Spheres = S2215Y mutation

Fig. 4.2, Space-filled model of mTOR, from the N-terminus of the FRB domain to the C-terminus of the Kinase domain, showing the locations of the 12del and S2215Y mutations.

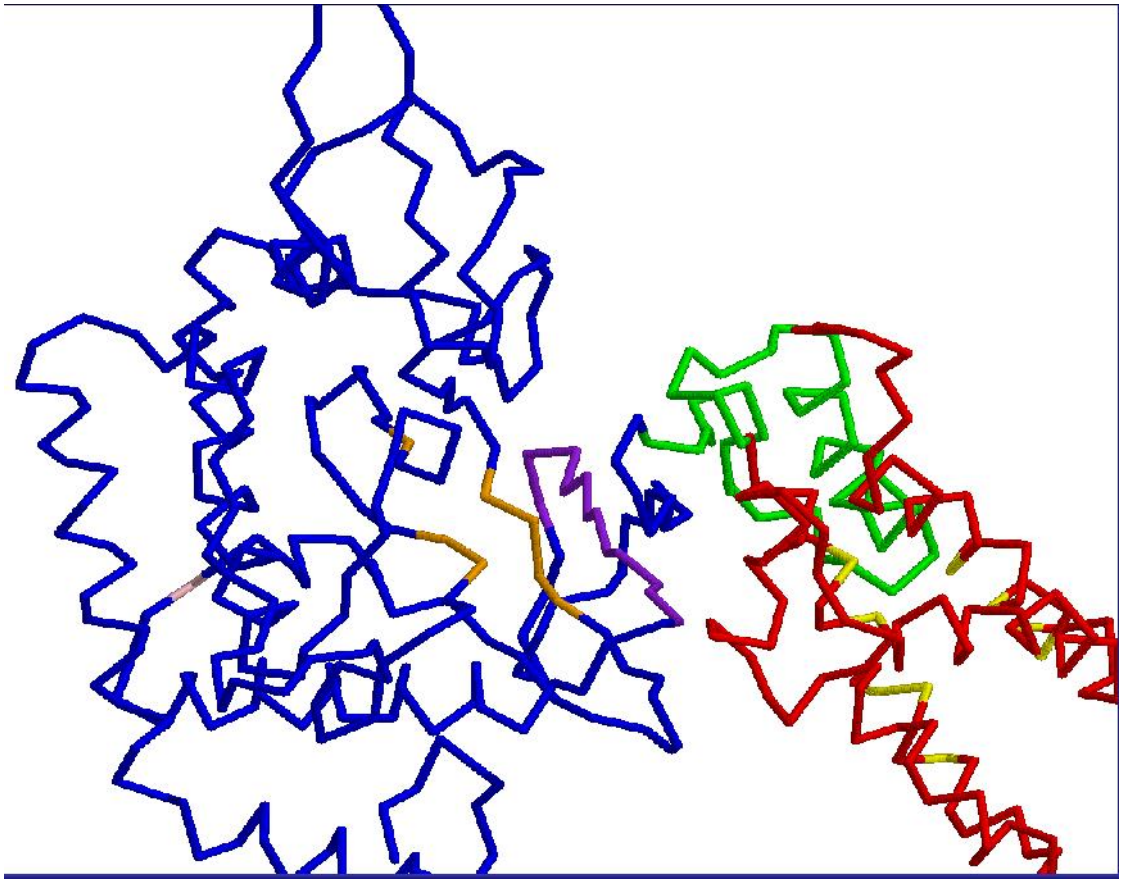

Red Backbone = FRB domain

Yellow Backbone = Rapamycin Binding residues

Green Backbone = Linker

Blue Backbone = Kinase domain

Orange Backbone = Key residues in ATP binding pocket

Purple Backbone = 12del mutation

Pink Backbone = S2215Y mutation

Fig. 4.3, Backbone model of mTOR, from the N-terminus of the FRB domain to the C-terminus of the Kinase domain showing the locations of the 12del and S2215Y mutations.

4.1) Agarose gel analysis of mutant mTORα and mTORβ mutant DNA

PCR site-directed mutagenesis was used to create the S2215Y and 12del mutations in the mTORα and mTORβ containing plasmids. The mutant DNA was then amplified and restriction analysis was performed on an agarose gel with Pvu2. This can be seen in **Fig. 4.4**.

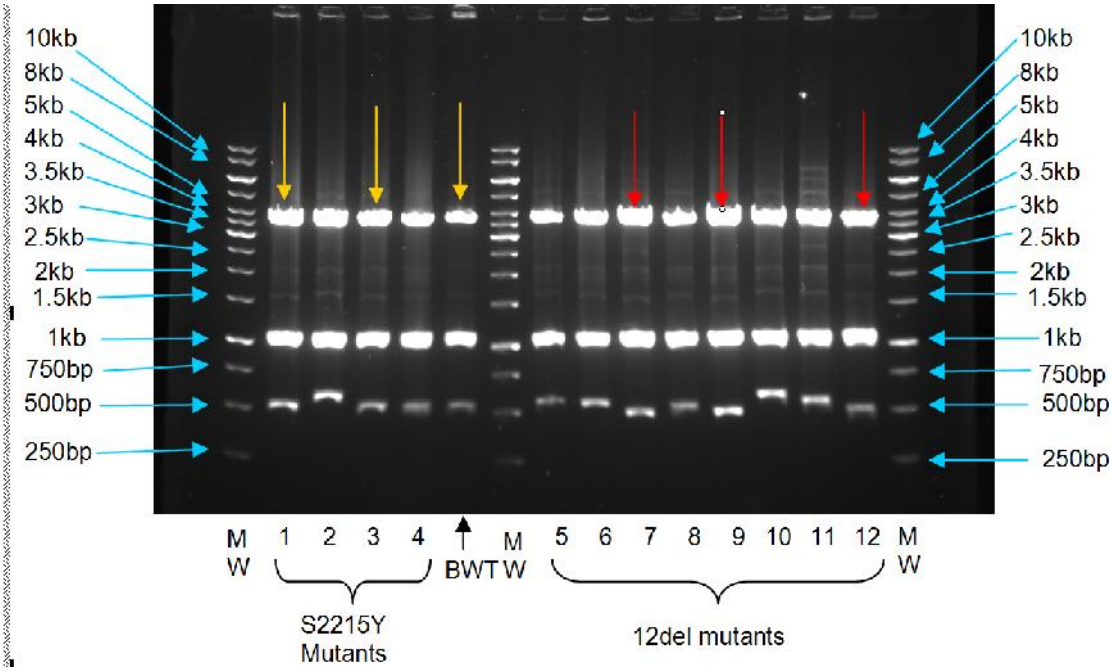

Fig. 4.4, Agarose gel of mTORβWT-myc/pcDNA3.1(+), mTORβS2215Y-myc/pcDNA3.1(+) and mTOR12del-myc/pcDNA3.1(+) plasmids digested with Pvu2. The plasmids were electrophoresed on a 0.75% agarose gel.

Digestion of the three plasmids with their respective inserts should result in an identical pattern of bands for the WT and S2215Y point mutant. However, restriction of the 12del mutant would produce the same set of fragments as the WT, with the exception of a 505bp band in lieu of the WT's 536bp band. Samples 1,3 and 4 of the S2215Y mutants all possessed the same fragments as the mTORβWT, so they were sent for sequence analysis. Similarly, the three 12del mutant samples that have been

marked with red arrows all contain the critical 505bp band, indicative of a 12aa deletion. These three samples were also dispatched for sequence analysis.

4.2) DNA sequence analysis of the mutant mTORβ DNA

Samples of the mTORβS2215Y, mTORβ12del and mTORα12del plasmids were sent to GATC Biotech for DNA sequence analysis. Chromatograms showing the locations of the S2215Y and 12del mutations are shown in **Fig. 4.5** and **Fig. 4.6**. In **Fig. 4.6**, a sequence alignment between mTORβWT and mTORβ12del in which the location of the 12del deletion has been highlighted has also been included.

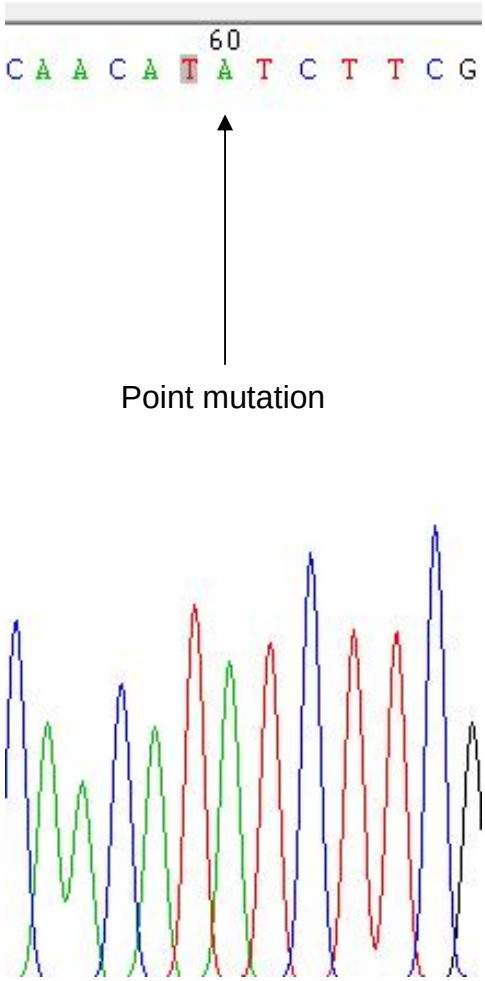

Fig. 4.5, Chromatogram showing mTORβS2215Y point mutation. Here one can clearly see that the S2215Y point mutation (TCT to TAT) has been successfully created in the mTORβWT-myc/pcDNA3.1(+) plasmid after mutagenesis.

A)

Clustalw alignment between mTORβWT and mTORβ12del mutant DNA after sequence analysis

```
mTORBΔ12        GCCCCGGAAATTGACACTTATGGGC---------------------------------- 656
mTORBWT         GCCCCGGAAATTGACACTTATGGGCAGCAACGGACATGAGTTTGTTTTCCTTCTAAAAGG 1980
                ************************

mTORBΔ12        -CATGAAGATCTGCGCCAGGATGAGCGTGTGATGCAGCTCTTCGGCCTGGTTAACACCCT 715
mTORBWT         CCATGAAGATCTGCGCCAGGATGAGCGTGTGATGCAGCTCTTCGGCCTGGTTAACACCCT 2040
                 ************************************************************
```

B)

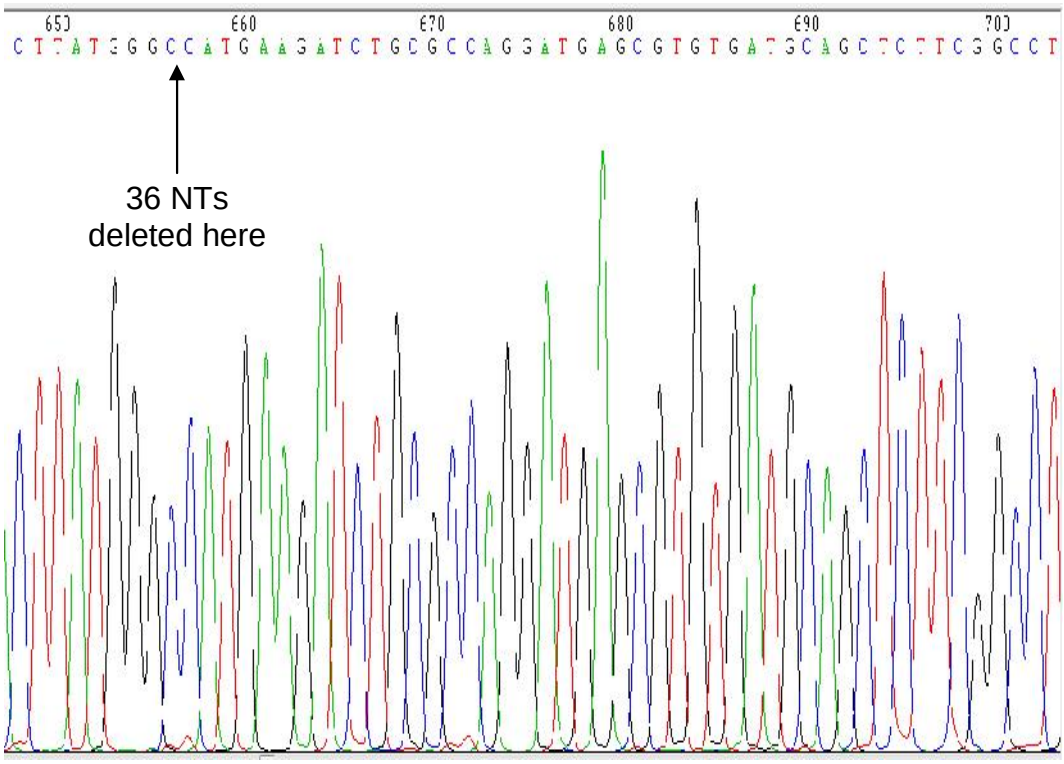

Fig. 4.6, Sequencing of the mTORβ12del mutation. (A) Sequence alignment highlighting the deletion. **(B)** Chromatogram and sequence indicating the site of the deletion.

4.3) Western Blot to confirm expression of the mTORβ proteins

HEK293 cells were defrosted and grown to a suitable confluency as described in the Materials and Methods chapter. The cells were then transiently transfected with either mTORβWTβ-myc/pcDNA3.1(+), mTORβS2215Y-myc/pcDNA3.1(+), mTORβ12del-myc/pcDNA3.1(+) or empty pcDNA3.1(+) vector respectively. After 24hrs the cells were lysed and the samples were loaded on a Bis-Tris gel. The proteins were then detected by Western Blot analysis (**Fig. 4.7**) using anti-myc tag antibodies.

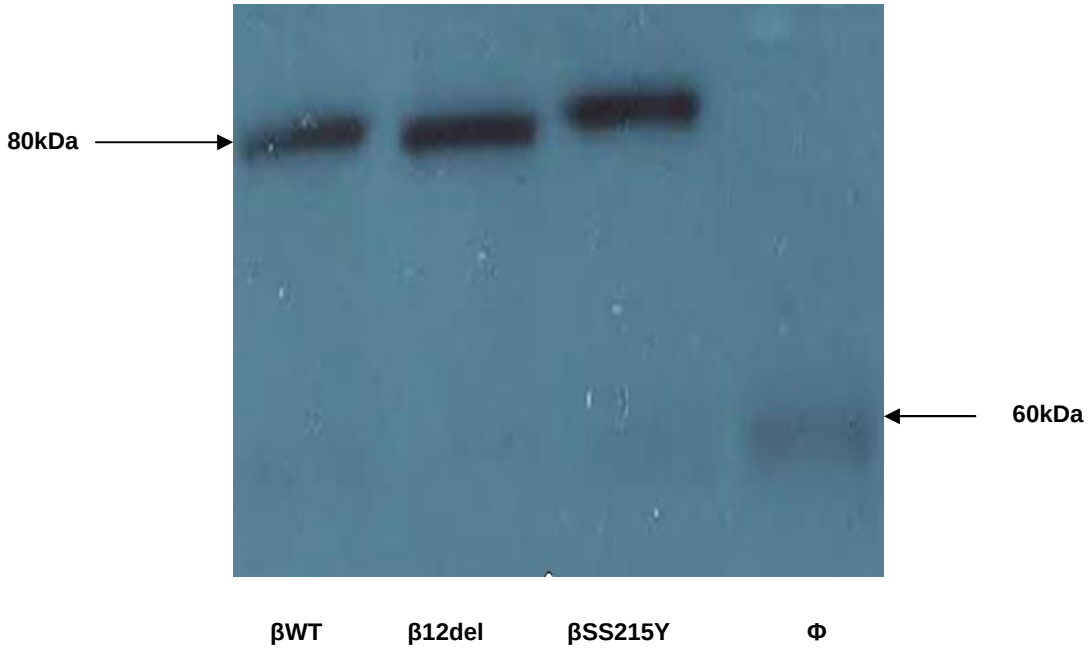

Fig. 4.7, Western Blot confirming expression of the mTORβWT and mutant proteins in transiently transfected HEK293 cells. Φ denotes HEK293 cells transiently transfected with empty pcDNA3.1(+) vector. The mTORβ proteins were detected and non-specific binding was detected in the negative control lane Φ.

4.4) Immunoprecipitation of the mTORβ proteins

HEK293 cells that had been transiently transfected in the same manner as outlined in section 2.3 above were also lysed, and the mTORβ proteins were purified by immunoprecipitation using an anti-myc tag antibody. The protein samples purified by immunoprecipitation were then detected by Western blotting using an anti-myc tag primary antibody (**Fig. 4.8**).

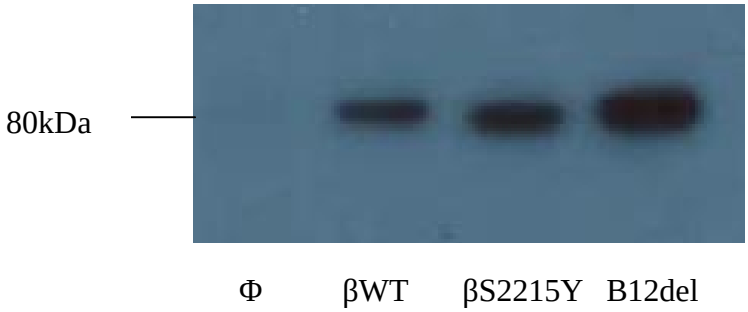

Fig. 4.8, mTORβ proteins purified by immunoprecipitation from transiently transfected HEK293 cell lysate and then detected by Western Blotting. Φ denotes HEK293 cells transiently transfected with empty pcDNA3.1(+) vector.

4.5) pAkt and Akt Western Blots

HEK293 cells were co-transfected with either empty pcDNA3.1(+) vector or with pcDNA3.1(+) containing a mTORβ insert and Akt-WT-EE/pCMV3. The cells were co-transfected with Akt-WT-EE/pCMV3 to increase the levels of Akt expressed in the cell. This would augment the level of substrate that would be available for mTORβ proteins to phosphorylate. Consequently, it would be easier to detect P-Akt and Akt via Western Blotting and to observe whether mTORC2 activity was present. Following serum and nutrient starvation, the cells were then lysed and Akt, PAkt and the mTORβ proteins were detected by Western blotting. See **Fig. 4.9**. As expected, no proteins were visible in the negative control lane and all mTOR proteins were detected in **Fig. 4.9A**. Proteins were detected with Anti-myc antibody. Contrary to expectation, PAkt was present in all the sample lanes in **Fig. 4.9B**. In the similar experiment conducted with mTORα proteins by Sato et al (Sato, Nakashima, Guo, Coffman, & Tamanoi 2010), the intensity of the PAkt bands for all samples were negligible. Significant levels of Akt proteins were visible in all sample lanes in **Fig. 4.9C**, which demonstrated that high levels of Akt protein were expressed by the HEK293 cells. In HEK293 cells which have been starved, little or no phosphorylation of Akt should have occurred, since mTORC2 activity would be inhibited. A possible explanation was that the cells were not starved for long enough to diminish mTORC2 activity.

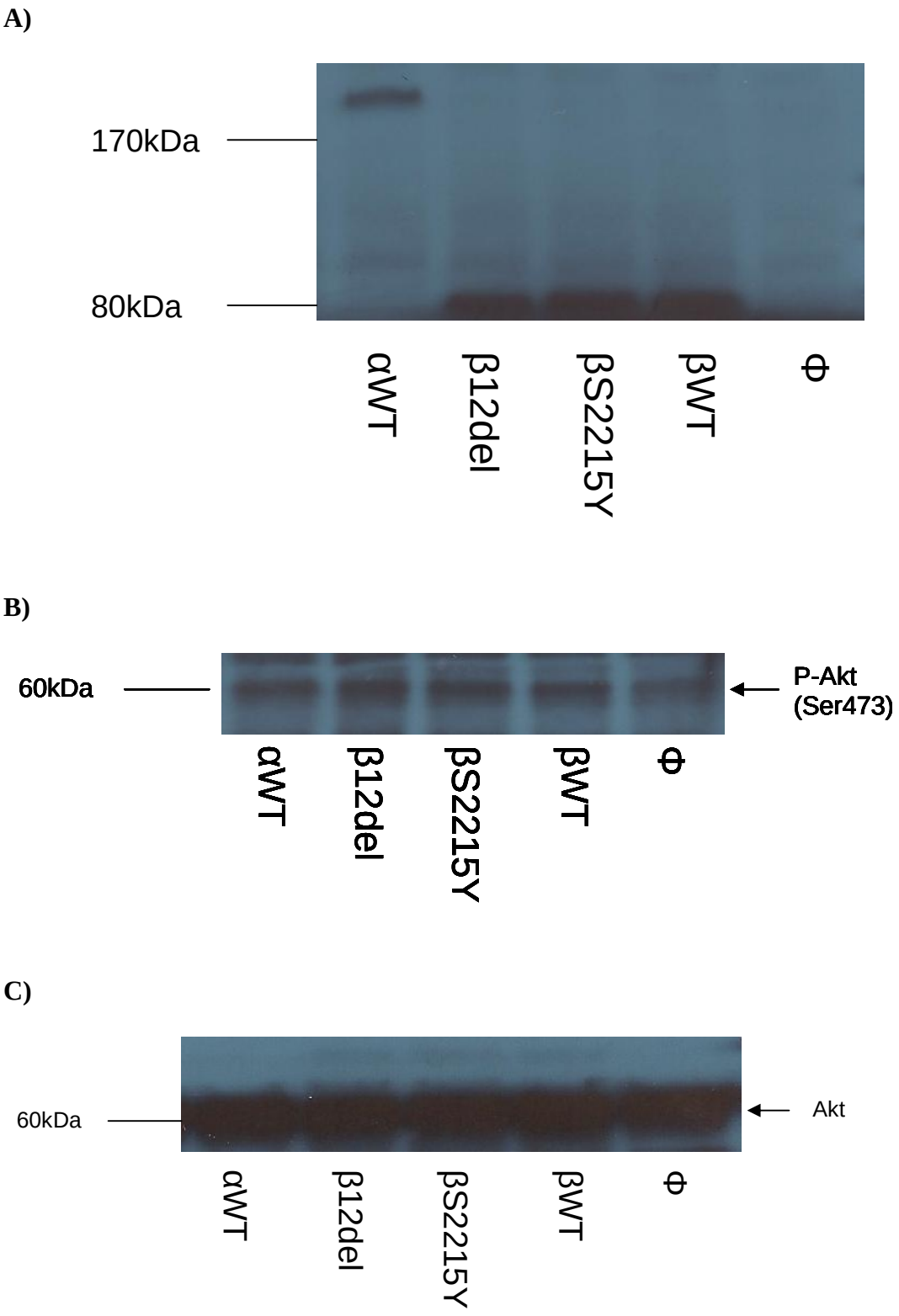

Fig. 4.9, Western Blots showing detection of mTORβ (A), P-Akt (B) and Akt (C) proteins respectively in HEK293 cells co-transfected with either empty pcDNA3.1(+) vector or with pcDNA3.1 containing a mTORβ insert and Akt-WT-EE/pCMV3. In all figures Φ denotes HEK293 cells transiently transfected with empty pcDNA3.1 (+) vector and was the negative control.

4.6) pS6K1 and S6K1 Western Blots

HEK293 cells were co-transfected with either empty pcDNA3.1(+) vector or with pcDNA3.1(+) containing a mTORβ insert and S6K1-EE/pcDNA3.1(+). Following serum and nutrient starvation, the cells were then lysed and P-S6K1 and the mTORβ proteins were detected by Western blotting. In order to ensure that equal quantities of sample had been loaded onto each gel a Western Blot to detect the levels of actin was also performed. The Western Blots to detect the various proteins can be seen in **Fig. 4.10**. In **Fig. 4.10A**, the mTOR proteins were all expressed, and no myc-tagged proteins were detected in the negative control lane as was expected. Proteins were detected with Anti-myc antibody. The level of actin visible was similar in each of the sample lanes in **Fig. 4.10B**. This was evidence that equal quantities of sample had been loaded into each well in the gel. Anti-Actin antibody was used to detect the proteins. Surprisingly, P-S6K1 was discernible with every sample in **Fig. 4.10C**. This was clear proof of the existence of mTORC1 activity in the starved HEK 293 cells. Nutrient deprivation has been shown to diminish phosphorylation of S6K1 by mTORC1, so this result was unanticipated. The PS6K1 present in the negative control lane (Φ) could only be attributed to endogenous mTORC1. A potential explanation was that the cells were not sufficiently starved to curtail protein synthesis, and as a result mTORC1 activity was not diminished. Almost no S6K1-EE tagged protein was detected in **Fig. 4.10D** with anti EE-tag antibody. A possible reason for these results was that mTORC1 was active and phosphorylated almost all the cellular S6K1 to P-S6K1, leaving little to be detected.

A)

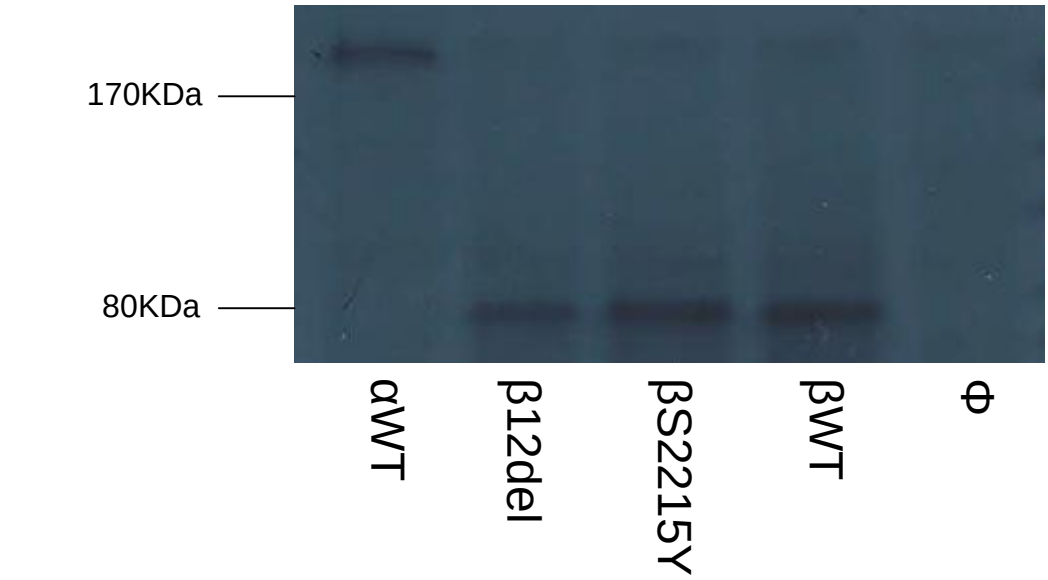
170KDa
80KDa
αWT
β12del
βS2215Y
βWT
Φ

B)


Actin
(42KDa)
αWT
β12del
βS2215Y
βWT
Φ

C)

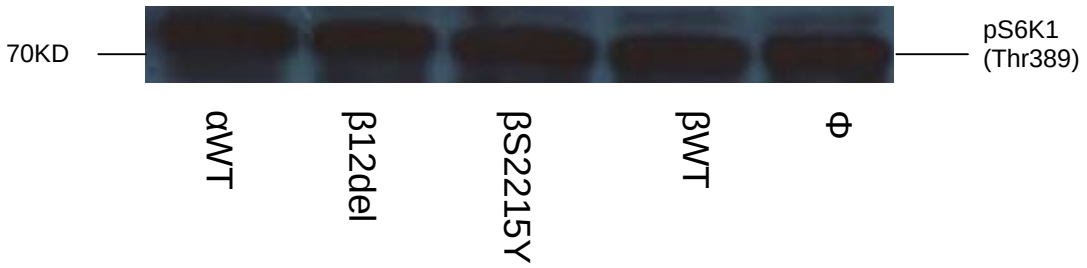
70KD
pS6K1
(Thr389)
αWT
β12del
βS2215Y
βWT
Φ

D)

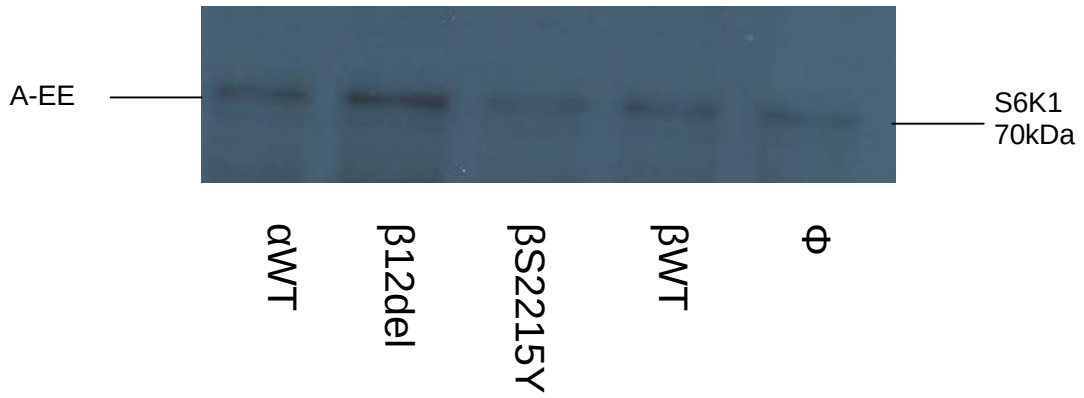

Fig. 4.10, Western Blots showing detection of the mTOR (A), actin (B), pS6K1 (C) and S6K1 (D) proteins in HEK293 cells co-transfected with either empty pcDNA3.1(+) vector or with pcDNA3.1 containing a mTORβ insert and S6K1-EE/pcDNA3.1(+). In all figures Φ denotes HEK293 cells transiently transfected with empty pcDNA3.1(+) vector and was the negative control.

4.7) p4E-BP1 and 4E-BP1 Western Blots (Starvation only)

HEK293 cells were transiently transfected with empty pcDNA3.1(+) vector and pcDNA3.1(+) vector containing a mTORβ insert. Following serum and nutrient starvation, the cells were lysed and Western blots were performed. The mTORβ proteins, p4E-BP1 and 4E-BP1 were probed for with the appropriate antibodies. The blots are shown in **Fig. 4.11**. As one can see in **Fig. 4.11A**, the mTORβ proteins were all well expressed, and no myc-tagged proteins was visible in the negative control lane as expected. The mTORβ proteins were detected using Anti-myc antibodies. In **Fig. 4.11B**, phosphorylated 4E-BP1 was present in significant quantities in every sample lane, demonstrating the existence of mTORC1 activity. This was totally contrary to expectations, since cells subjected to nutritional deprivation would not have the resources to continue protein synthesis. A potential explanation could be that the antibody that was used to detect P4E-BP1 was exceptionally efficient and was capable of detecting truly minute quantities of phosphorylated protein. p4E-BP1 was

detected using anti phospho-4E-BP1 (Thr37/46) antibody. Large quantities of 4E-BP1 were detected in every sample lane in **Fig. 4.11C** using anti 4E-BP1 antibody**.** In cells that had been starved one, would expect to see very low levels of mTORC1 activity, hence the level of P4E-BP1 protein should be low and the amount of 4E-BP1 protein should be high. Therefore, this result conformed to expectations.

A)

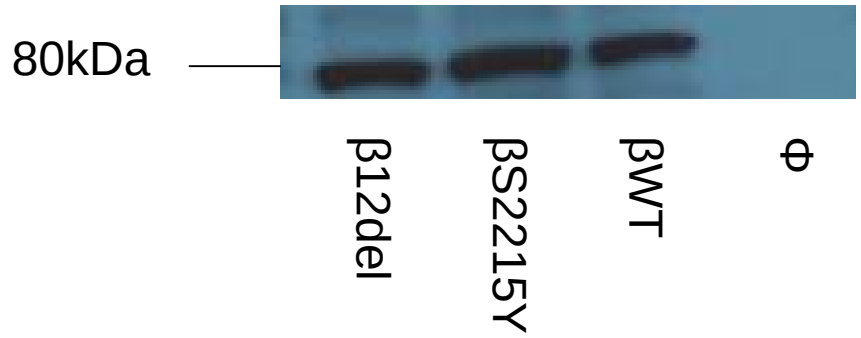

B)

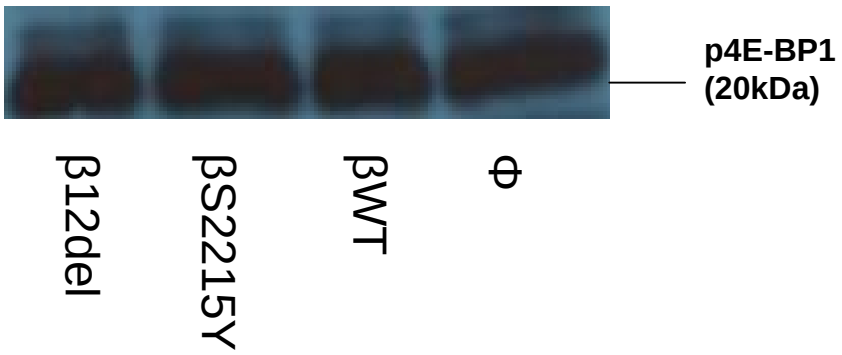

C)

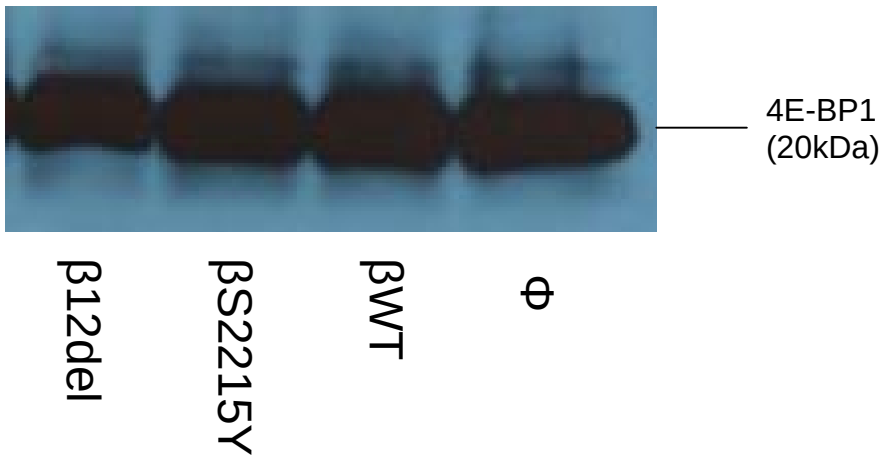

Fig. 4.11, Western Blots showing expression of the mTORβ (A), p4E-BP1 (Thr37/46) (B) and 4E-BP1 (C) proteins in HEK293 cells transiently transfected with pcDNA3.1(+) containing a mTORβ insert or empty pcDNA3.1(+) plasmid. In all figures Φ denotes HEK293 cells transiently transfected with empty pcDNA3.1 vector and was the negative control.

4.8) p4E-BP1 and 4E-BP1 Western Blots (Starvation followed by stimulation of negative control)

The Western Blots outlined in section 2.7 were repeated with the exception that HEK293 cells were serum starved for 24 hours rather than merely overnight. Furthermore, nutrient starvation was carried out for 3 hours instead of 1 hour as had been done with all previous experiments. HEK293 cells that had been transiently transfected with an empty pcDNA3.1(+) plasmid were also stimulated for 1 hour with complete media after being subjected to the same starvation conditions as the other cells. This additional stimulated negative control was then loaded on the gels alongside the standard negative control. There were two reasons for the variation in experimental conditions. Firstly, we wanted to observe the effects of increasing the duration of starvation upon mTORC1 activity, and secondly we wished to see whether stimulation of cells would restore the levels of P4E-BP1. Western Blots to detect the levels of mTORβ proteins, endogenous P4E-BP1 and 4E-BP1 were carried out and the results can be seen in **Fig. 4.12**. As can be seen in **Fig. 4.12A**, expression of all the mTORβ proteins was strong and no myc-tagged proteins were detected in any of the negative control lanes as expected. The mTORβ proteins were detected using anti-myc antibodies. In **Fig. 4.12B** above, starving the cells for a longer period resulted in a drastic reduction in the levels of P4E-BP1 in all samples apart from the stimulated negative control cells. These results suggested that prolonged starvation was necessary in order to inhibit mTORC1 activity. Another conclusion was the S2215Y point mutation did not confer constitutive activation on mTORβ. Stimulation of the cells dramatically elevated the levels of P4E-BP1, as can be seen in the Φ (stimulated) lane. In **Fig. 4.12C**, all of the cells that had been starved without subsequent stimulation, 4E-BP1 was present. However, in the case of the Φ (stimulated) sample,

almost no 4E-BP1 was visible. This demonstrated that stimulation after starvation rapidly restored mTORC1 activity, which phosphorylated large quantities of endogenous 4E-BP1.

A)

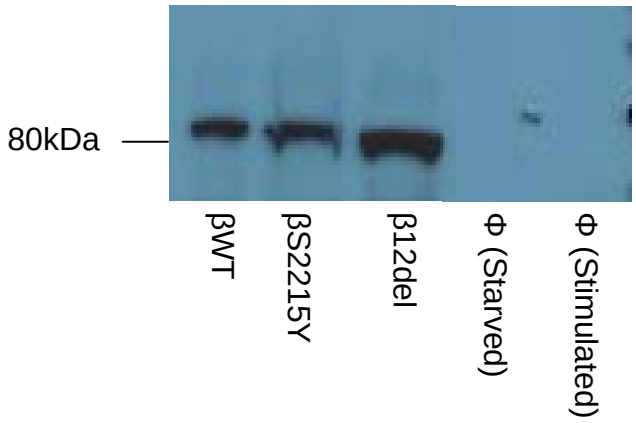

B)

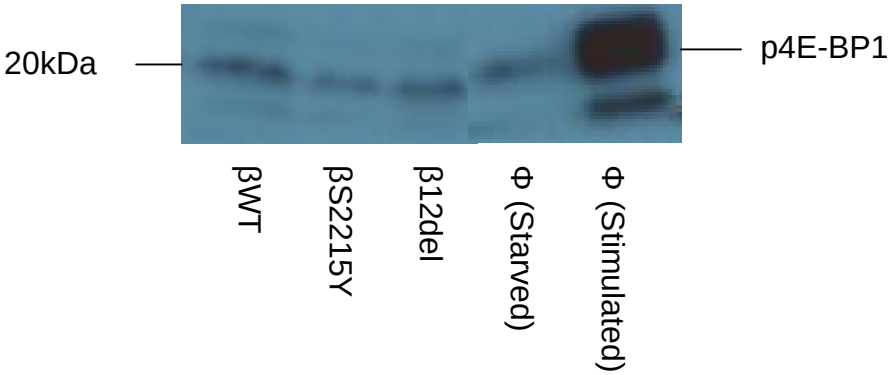

C)

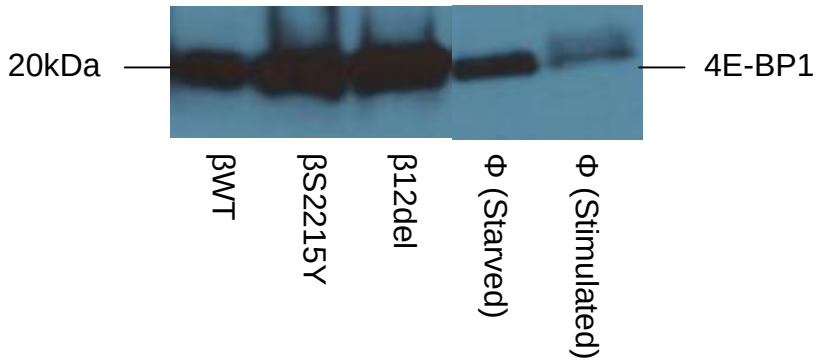

Fig. 4.12, Western Blots showing expression of the mTORβ proteins (A), detection of endogenous p4E-BP1 (B) and 4E-BP1 in HEK293 cells transiently transfected with pcDNA3.1(+) containing a mTORβ insert or empty pCDNA3.1(+) vector. In all figures Φ (starved) denotes HEK293 cells transfected with empty pcDNA3.1 vector that were starved and not stimulated. The Φ (stimulated) sample consisted of HEK293 cells that had been transfected with empty pcDNA3.1(+) vector, starved and then stimulated with complete media.

4.9) Discussion

It was clear that the S2215Y and 12del mutations did not confer constitutive activation on mTORβ. The most conclusive result that led to this conclusion is shown in **Fig 4.12**. Under conditions of extended starvation, the HEK293 cells that had been transiently transfected with the mTORβ mutant plasmids in **Fig 4.12A** did not display high levels of P4E-BP1, which would be indicative of mTORC1 activity. This led to the suggestion that they were not oncogenic mutations, since hyperactive mTOR signalling has been shown to be a hallmark of cancer. The 12del mutation results in the deletion of the critical Lys2187 residue, which is thought to contact the α-phosphate of ATP. Therefore, it was expected that the 12del mutation would inhibit mTOR activity.

The results in **Fig 4.12** also demonstrated that the extended starvation conditions employed were required to bring about inhibition of mTORC1 activity. It would be interesting to repeat the Western blots shown in **Figs 4.9** and **4.10** to assess the effect on Akt and S6K1 phosphorylation after prolonged starvation.

Chapter 5: Results

Creating a mTORβ-TapTag construct

Chapter 5: Creating a mTORβ-TapTag construct

5.0) Introduction

The tandem affinity purification (TAP) method allows one to purify protein complexes from endogenous sources. The system was developed by Rigaut et al. (Rigaut et al. 1999) and was initially utilised in yeast cells. Subsequently, it was discovered that the technique could also be used with mammalian tissues. The principle behind the TAP methodology involves the fusion of the TAP tag to the N or C terminus of the protein of interest. The construct is then introduced into the organism or host cell. Cellular extracts are then prepared and the fusion protein and any potential binding partners are purified in two specific purification/elution stages. If one desires to characterise protein complexes, then the proteins recovered must be concentrated and fractionated on a denaturing gel prior to elucidation by mass spectrometry. Furthermore, since the TAP technique is relatively gentle, damage to the proteins during purification is highly unlikely. Consequently, the purified proteins can be tested for their activities in various assays or utilised in structural studies (Puig et al. 2001). The high yield and simplicity of the TAP method makes it a very attractive tool to use for protein purification and elucidation of their functions. A diagram showing the classical TAP tag is shown in **Fig. 5.1**.

Over the years, numerous modifications and improvements to the first TAP tag have been made. These adaptations have principally been introduced in order to improve the recovery of protein complexes in mammalian systems. The TAP tag that I used was a GS-TAP tag (**Fig. 5.2**). This was fused to the N-terminus of the mTORβ protein. The advantages offered by the GS-TAP tag over the ProtA and CBP TAP tag combination include higher yield of bait protein (mTORβ) and fewer contaminants. An overview of the tandem affinity purification process using the GS-TAP tag is

shown in **Fig. 5.3**. Unfortunately, there was insufficient time to carry out purifications of the fusion protein from HEK293 cells, but the recombinant protein was created. This will allow future students to continue the work that I have started.

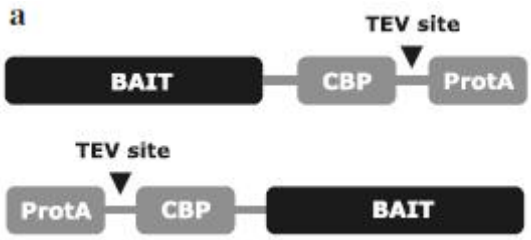

Fig. 5.1, Schematic showing the original TAP tag. The classical TAP tag consists of CBP and ProtA with a TEV protease cleavage site in the intervening region. As shown below, the TAP-tag construct can be fused either N or C terminally to the protein of interest. (Taken from (Li 2011))

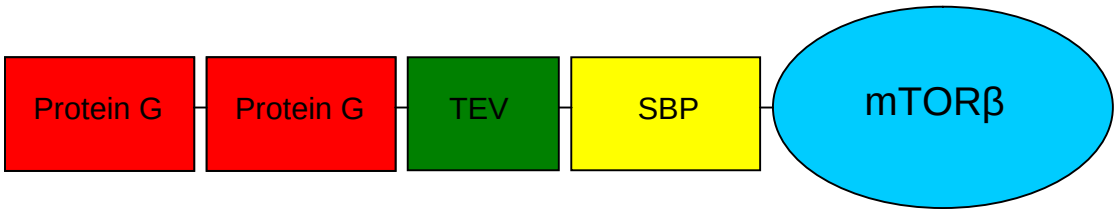

Fig. 5.2, Schematic of the GS-TAP tag fused to the N-terminus of mTOR. The protein A modules have been replaced with 2 protein G modules and the calmodulin binding peptide has been replaced by a streptavidin binding peptide. A TEV protease cleavage site is situated in between the protein G modules and the streptavidin binding peptide. The GS-TAP tag offers superior recovery of bait protein with fewer associated contaminants compared to the protein A/CBP TAP tag depicted in **Fig. 5.1**.

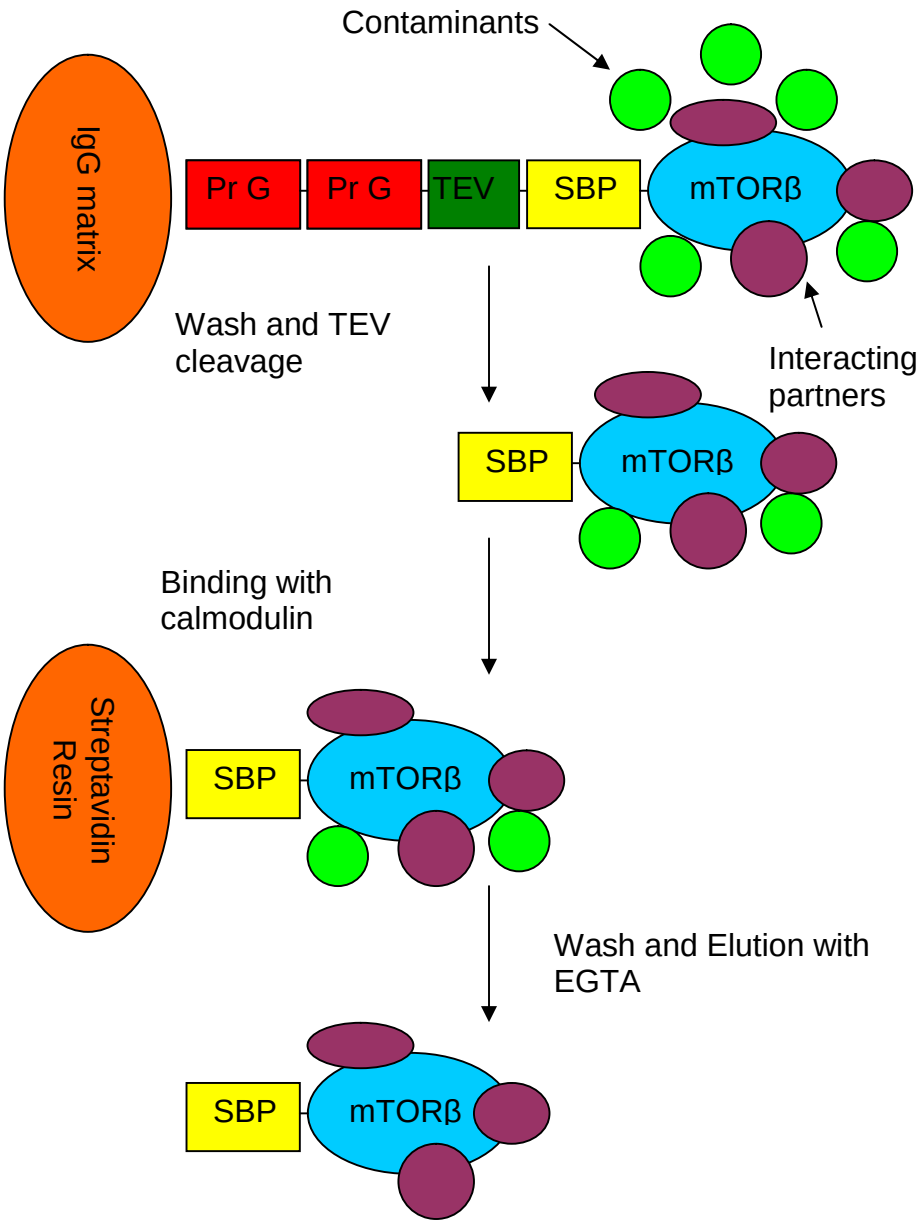

Fig. 5.3, Overview of the tandem affinity purification procedure using a GS-TAP tag. The tandem-affinity-purification (TAP) tag is composed of three components: a streptavidin-binding peptide, a tobacco etch virus (TEV) protease cleavage site and Protein G as immunoglobulin G (IgG)-binding domains. Cells or organisms are produced that contain TAP-tagged protein(s). Cells expressing the fusion protein are lysed and TAP is performed. The first column contains IgG beads. TEV protease cleavage releases SBP-mTORβWT. An additional round of binding is performed on a second column that consists of Streptavidin-binding peptide beads. The native complex is then eluted.

Results

5.1) Using PCR to introduce XhoI and NotI restrictions sites into mTORβWT/pcDNA3.1(+)

mTORβWT was not cloned into the pcDNA3.1(+) vector using the XhoI and NotI restriction enzymes. Therefore, it was not possible to excise it from its original vector and directly clone it into the TAP-tag plasmid pCeMM-NTAP(GS), which contained XhoI and NotI restriction sequences. As a result, primers were designed that would allow the XhoI and NotI restriction sequences to be artificially introduced at the N and C termini of mTORβ respectively by PCR. See the materials and methods chapter for details of the PCR reaction conditions utilised. After PCR amplification had been performed, the PCR reaction mixtures were analysed on an agarose gel. This can be seen in **Fig. 5.4**. The PCR product was successfully produced in all cases. Addition of DMSO appeared to increase the production of high MW impurities, but also diminished the presence of lower MW contaminants. DMSO also had the effect of decreasing the yield of PCR product. The samples in lanes 2 and 3 were purified using ethanol precipitation and the other PCR reaction mixtures were frozen.

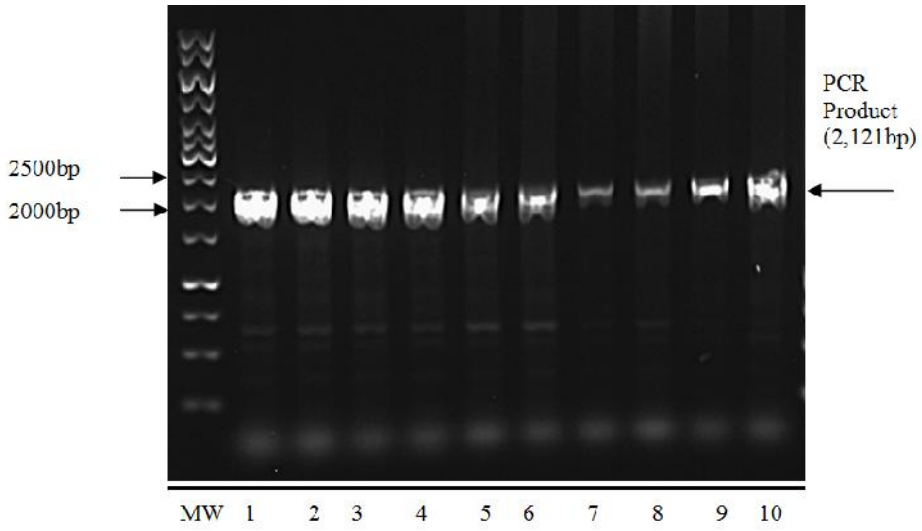

Fig. 5.4, The PCR reaction mixtures were analysed on a 0.75% agarose gel. A range of reaction conditions were used in order to ascertain those that would produce the most PCR product. MW was the Fermentas Generuler DNA ladder used to ascertain the size of the fragments. The samples in lane 1-4 were PCR reaction mixtures, where PCR was performed at 62°C. Samples 5-6 were PCR reaction mixtures containing DMSO, where reactions were carried out at 60°C. Samples 7-8 were PCR reaction mixtures with DMSO, and PCR was conducted at 62°C. Samples 9-10 were PCR reaction mixtures containing DMSO, and PCR was performed at 64°C.

5.2) Agarose gel analysis of XhoI and NotI restriction of pCeMM-NTAP(GS) and mTORB PCR product

The PCR products that had been purified by ethanol precipitation and the TAP tag plasmid (pCeMM-NTAP(GS)) were restricted with XhoI and NotI enzymes. This resulted in the linearisation of the plasmid and digestion of the ends of the linear PCR product. In order to confirm that the digested DNA was of the correct size and of good quality, the DNA was analysed on an agarose gel. The result is shown in **Fig. 5.5**. The vectors were linearised successfully as can be seen in the agarose gel and the DNA fragments were all of the expected size. The agarose gel was placed on a UV light box and the relevant bands were excised from the gel. Promega's Wizard SV gel and PCR clean-up system was utilised to purify the gel fragments. From the gel, it was estimated that the concentration of the PCR product in lane 2 was 20ng/μL and in lane 3 was 8ng/μL.

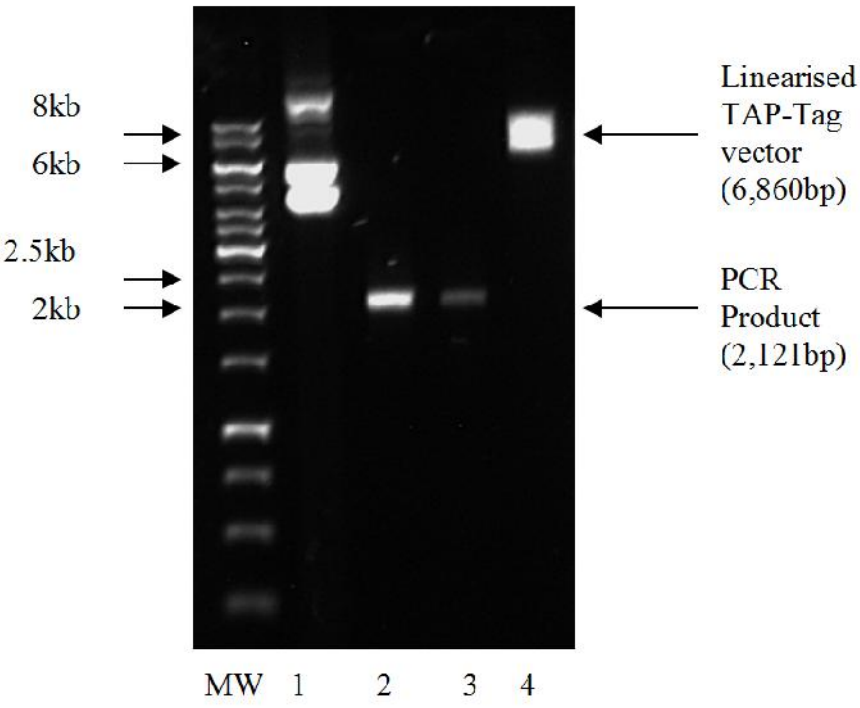

Fig. 5.5, pCeMM-NTAP(GS) and PCR product (mTORβ/pcDNA3.1(+) with XhoI and NotI restriction sequences) were linearised by restriction with XhoI and NotI. The digested DNA was run on a 0.75% agarose gel. MW was the Fermentas Generuler DNA ladder used to ascertain the size of the fragments. Lane 1 contained a DNA Quantity Marker (0.1µg/µL), which was used to deduce the DNA concentration of the other samples. Lanes 2 and 3 were linearsied mTORβPCR products Clones 1 and 2 respectively. The sample in lane 4 was the linearised pCeMM-NTAP(GS) vector.

5.3) Ligation of mTORβ to pCeMM-NTAP(GS), amplification and agarose gel analysis

After the DNA fragments had been purified from the agarose gel, the mTORβ PCR product was ligated to the pCeMM-NTAP(GS) vector. The ligated DNA was then transformed into E.coli XL-10 competent cells. After growth on selective agar plates, colonies were seeded into LB with selective antibiotics and then purified with a mini-prep kit. The DNA obtained was restricted with XhoI and NotI and analysed on an agarose gel, shown in **Fig. 5.6**.

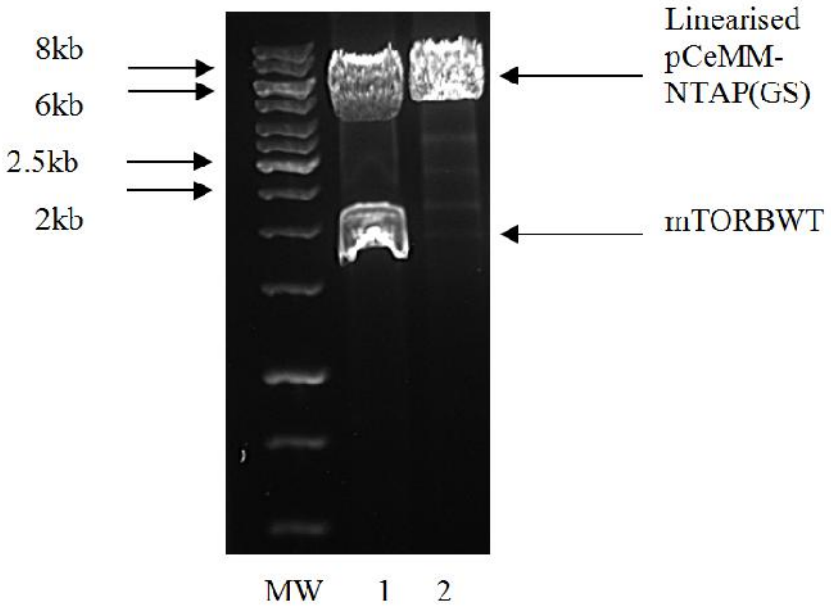

Fig. 5.6, 0.75% Agarose gel analysis of XhoI/NotI digestion of mTORB/pCeMM-NTAP(GS) Clone 1 and pCeMM-NTAP(GS). MW was the Fermentas Generuler DNA ladder used to ascertain the size of the fragments. Lane 1 contained linearised mTORβ/pCeMM-NTAP(GS) Clone 1. Lane 2 contained linearised pCeMM-NTAP(GS). Digestion of the recombinant DNA product produced by DNA ligation resulted in the generation of the linearised mTORβWT insert and pCeMM-NTAP(GS) vector. This was proof that the cloning had been successfully performed.

5.4) Expression of mTORβ/pCeMM-NTAP(GS) in HEK293 cells

HEK293 cells were then transiently transfected with mTORβ/pCeMM-NTAP(GS) Clones 1 and 2, pCeMM-NTAP(GS) and mTORβ/pcDNA3.1(+) when they had reached a suitable confluency. After 72 hours the cells were lysed and the total cell lysates were mixed with SDS and run on a protein polyacrylamide gel. mTORα, mTORβ and mTORβ/pCeMM-NTAP(GS) were then detected on a Western blot using an anti Phospho-mTOR S2448 antibody. This can be seen in **Fig. 5.7**. mTORα and mTORβ were detected in all sample lanes as expected since both proteins are endogenous and possess a S2448 phosphorylation site. The mTORβ/NTAP(GS) protein was also present in lanes 3 and 4, which were cell lysates from HEK293 cells transiently transfected with Clones 1 and 2 respectively. This proved that transfection had been successful and that the HEK293 cells were capable of expressing the fusion protein.

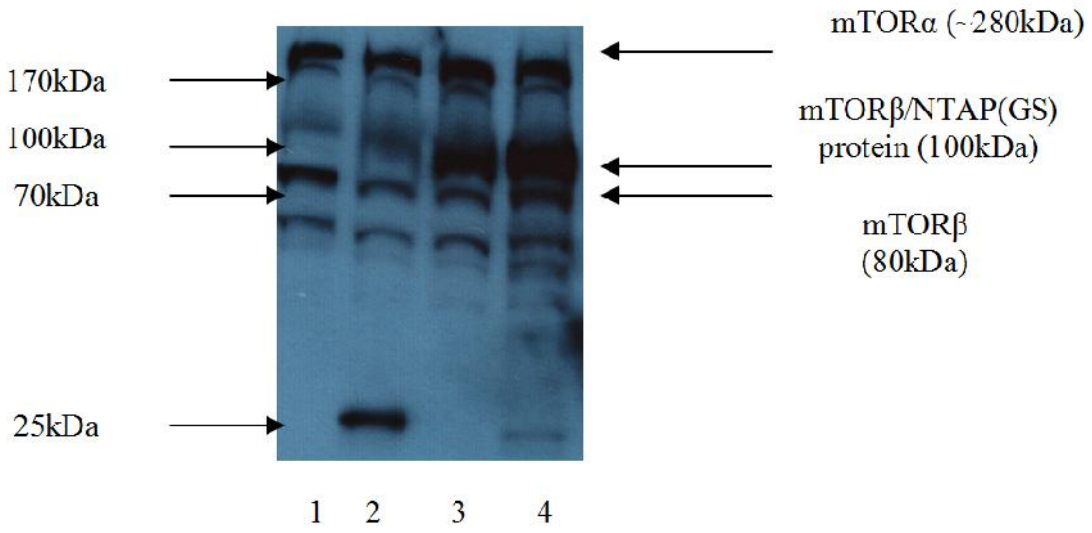

Fig. 5.7, Western blot of total cell lysate of HEK293 cells transiently transfected with mTORβ/pcDNA3.1(+), pCeMM-NTAP(GS) and mTORβ/pCeMM-NTAP(GS) clones 1 and 2. The primary AB used was anti Phospho-mTOR S2448. Akt phosphorylates mTORα and mTORβ at S2448. The sample in lane 1 was mTORβ/pcDNA3.1(+) and lane 2 contained pCeMM-NTAP(GS). Lanes 3 and 4 were mTORβ/pCeMM-NTAP(GS) Clones 1 and 2 respectively.

5.5) Affinity purification of mTORβ/NTAP(GS) with Protein G Sepharose beads and Western Blotting

Affinity purification with Protein G sepharose beads was performed with the soluble fractions of HEK293 total cell lysates. The HEK293 cells were transiently transfected in the same manner outlined in section 5.4. Proteins were detected with Western Blotting. For the first blot, an anti phospho-mTOR S2448 mTOR primary antibody was used, and for the second blot an anti mTOR C-terminal primary antibody was utilised. The blots are shown in **Fig. 5.8**. In **Fig. 5.8(A)**, large quantities of mTORβ/NTAP(GS) were purified using protein G sepharose beads in lanes 3 and 4, demonstrating that the affinity purification was successful and that the fusion protein was expressed. No protein of similar MW was detected in lanes 1 and 2, proving that the 100kDa protein in lanes 3 and 4 was not merely the result of non specific binding. Far more fusion protein was visible compared to mTORβ, which again showed that affinity purification was effective. In **Fig. 5.8(B)** even larger quantities of mTORβ/NTAP(GS) were detected using anti mTOR C-terminal primary antibody. This blot also demonstrated that affinity purification with Protein G sepharose beads was successful and that the fusion protein was expressed in transiently transfected HEK293 cells.

A)

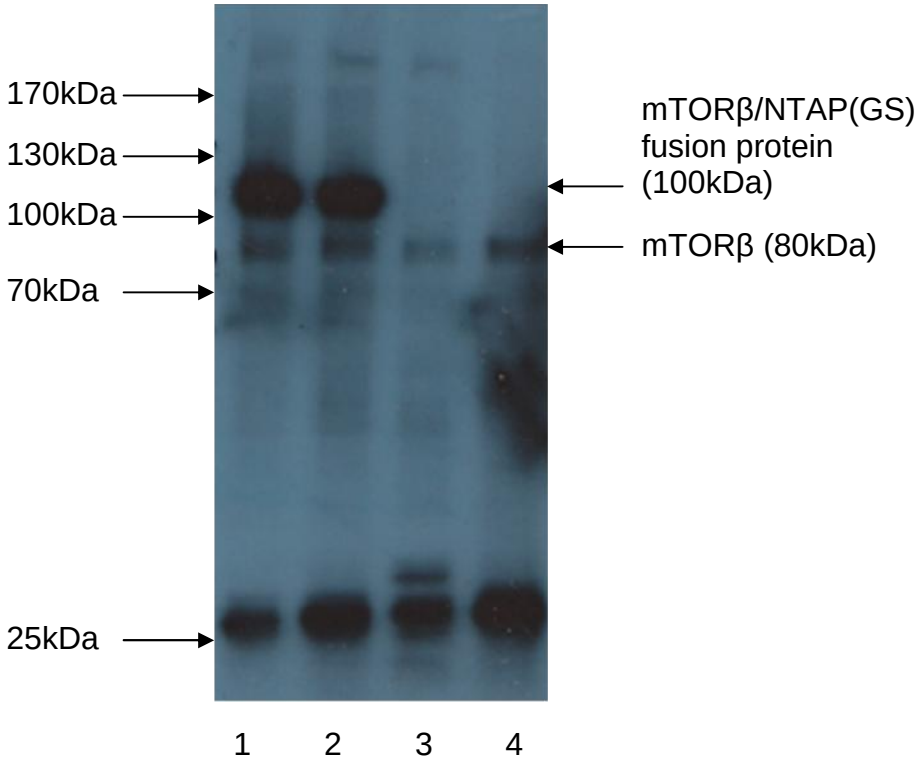

B)

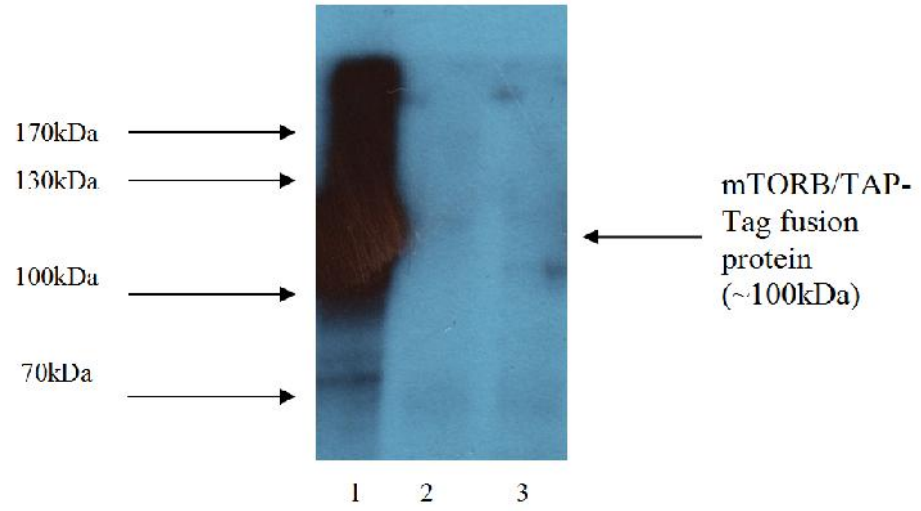

Fig. 5.8, Affinity purification of mTORβ/NTAP(GS) Protein G Sepharose beads and subsequent Western blots using Anti-Phospho-mTOR S2448 (A) and anti-mTOR C-terminal (B) primary ABs to detect mTORβ/NTAP(GS) fusion protein in transiently transfected HEK293 cells. (A) Lanes 1 and 2 contained mTORβ/pCeMM-NTAP(GS) clones 1 and 2. Lanes 3 and 4 contained pCeMM-NTAP(GS) and mTORβ-myc/pcDNA3.1(+) respectively. **(B)** Lane 1 contained mTORβ/pCeMM-NTAP(GS) Clone 1. Lanes 2 and 3 were pCeMM-NTAP(GS) and mTORβ-myc/pcDNA3.1(+) respectively.

5.6 Discussion

The full coding sequence of mTORβ was successfully cloned into the pCeMM-NTAP(GS) vector, with the N-terminal TAP-tag positioned at the N-terminus of mTORβ. Expression of the fusion protein in transiently transfected HEK293 cells was also confirmed. Affinity purification with Protein G sepharose beads appeared to be efficient, owing to the copious amounts of proteins that could be detected by Western blotting. Future work would involve testing whether known mTORβ binding partners such as Rictor and Raptor, (Panasyuk et al. 2009) can be efficiently co-purified using the mTORβ/NTAP(GS) fusion protein that has been created. It is my hope that new binding partners are subsequently discovered and their functions in the mTOR signalling pathway elucidated.

Chapter 6

General Discussion

Chapter 6: General Discussion

Advances in the understanding of mTOR function have been hampered by the lack of a mTOR crystal structure. The principal problem encountered has been the difficulty in obtaining sufficient quantities of soluble protein for crystallisation studies. In order to overcome this challenge it was decided to make a departure from conventional practice. Instead of expressing mTOR protein in mammalian cells which has been the accepted methodology, insect cells were transfected. In addition, insect cells were co-transfected with plasmids containing Rictor and Raptor. It was hoped that co-expression of either Rictor or Raptor with mTOR would increase its solubility, and hence the quantity of protein that would be available for crystallographic analysis. With regard to the first objective, we were not disappointed. Rictor, Raptor and mTOR were all successfully purified from cellular lysates using immunoprecipitation and Western Blotting confirmed their expression. However, solubilising adequate mTOR protein still proved to be elusive. Although the results from this work have not been presented in this thesis, they did influence the direction of my subsequent studies. Consequently, it was decided to model the Kinase domain of mTORβ using in silico methods. This approach would be rapid, cheap and offer a reasonably accurate model of mTORβ's active region.

A 3D model of mTOR's kinase domain, with the FRB domain positioned in an adjacent location was created using the technique of comparative modelling. This model allowed us to visualise the ATP binding pocket of mTOR. Furthermore, the model also allowed me to visualise the location of the S2215Y and 12del mutations in mTOR with respect to the catalytic pocket. Hence the model could be used as a tool to understand experimental results. However, the additional experiments that have been

proposed in the discussion for chapter 4 would most certainly be necessary before sufficient data had been generated to propose potential regulatory mechanisms. Time did not permit me to model the full length mTOR protein or any of the proteins that are components of the mTOR complexes. Provided that suitable homologue proteins exist for each domain, it would be useful to model both mTORα and mTORβ in their entirety. This would potentially give us greater insight into the protein's function and inhibition. Molecular docking studies with FKBP12-rapamycin, rapalogues and ATP-competitive inhibitors also offer scope for future work. A full-length mTOR model might also be useful for understanding the interaction of novel mTORβ binding partners with mTORβ, if any should be discovered in the future using the mTORβ-NTAP(GS) fusion protein that I have created.

The S2215Y and 12del mutations were also introduced into mTORβ. The point mutation S2215Y has been shown to convey constitutive activation on mTORα. In contrast the 12del mutation removes the entire kbeta5 strand from the catalytic site, which includes the critical Lys2187 residue. This amino acid is thought to interact with the α-phosphate of ATP. Consequently, it is thought that the 12del mutation disrupts mTOR activity. The effects that these mutations had on the phosphorylation of the mTOR substrates Akt, S6K1 and 4E-BP1 following starvation was assessed. It was shown that under the initial starvation conditions employed (overnight serum starvation and 1hr nutrient starvation), mTOR activity was unimpaired. However, when the HEK293 cells were starved for an extended period (24hr serum starvation and 3hr nutrient starvation) and then stimulated (incubation in complete medium for 1hr), the results conformed to expectations. Augmenting the duration of starvation had the desired effect of inhibiting mTOR activity. This also lent further weight to my previous supposition that the original starvation conditions employed were

insufficient to inhibit mTOR activity. Stimulation fully restored mTORC1 activity, as shown by the detection of P-4E-BP1 in cells transiently transfected with just empty vector. It would also be interesting to assess the effect that stimulation would have on cells that were transfected with mTORβWT and the mTORβ mutant plasmids. Also of interest, would be to repeat the experiments with the addition of a sample of cells that had been transfected with a plasmid containing mTORαS2215Y. Isolation of the mutant and WT proteins by immunoprecipitation followed by in vitro kinase assays would also be informative. The benefit of conducting these experiments would be that any mTOR activity present could only be attributed to the purified protein. A disadvantage would be that intracellular mTOR complex components that are requisite for mTOR activity may be lost in the immunoprecipitation.

A mTORβ-NTAP(GS) fusion protein was also successfully created. Unfortunately, there was not enough time for me to perform a preliminary tandem affinity purification. Nevertheless, the student that continues my work will be able to use the bait protein that I have generated to search for novel mTORβ binding partners.

Bibliography

Adami, A., Garcia-Alvarez, B., Arias-Palomo, E., Barford, D., & Llorca, O. 2007, "Structure of TOR and its complex with KOG1", *Mol.Cell*, vol. 27, no. 3, pp. 509-516.

Alarcon, C. M., Heitman, J., & Cardenas, M. E. 1999, "Protein kinase activity and identification of a toxic effector domain of the target of rapamycin TOR proteins in yeast", *Mol.Biol.Cell*, vol. 10, no. 8, pp. 2531-2546.

Altschul, S. F., Madden, T. L., Schaffer, A. A., Zhang, J., Zhang, Z., Miller, W., & Lipman, D. J. 1997, "Gapped BLAST and PSI-BLAST: a new generation of protein database search programs", *Nucleic Acids Res.* , vol. 25, no. 17, pp. 3389-3402.

Andrade, M. A. & Bork, P. 1995, "HEAT repeats in the Huntington's disease protein", *Nat.Genet.*, vol. 11, no. 2, pp. 115-116.

Arsham, A. M., Howell, J. J., & Simon, M. C. 2003, "A novel hypoxia-inducible factor-independent hypoxic response regulating mammalian target of rapamycin and its targets", *J.Biol.Chem.*, vol. 278, no. 32, pp. 29655-29660.

Ballif, B. A., Roux, P. P., Gerber, S. A., MacKeigan, J. P., Blenis, J., & Gygi, S. P. 2005, "Quantitative phosphorylation profiling of the ERK/p90 ribosomal S6 kinase-signaling cassette and its targets, the tuberous sclerosis tumor suppressors", *Proc.Natl.Acad.Sci.U.S.A*, vol. 102, no. 3, pp. 667-672.

Bentzinger, C. F., Romanino, K., Cloetta, D., Lin, S., Mascarenhas, J. B., Oliveri, F., Xia, J., Casanova, E., Costa, C. F., Brink, M., Zorzato, F., Hall, M. N., & Ruegg, M. A. 2008, "Skeletal muscle-specific ablation of raptor, but not of rictor, causes metabolic changes and results in muscle dystrophy", *Cell Metab*, vol. 8, no. 5, pp. 411-424.

Berchtold, D. & Walther, T. C. 2009, "TORC2 plasma membrane localization is essential for cell viability and restricted to a distinct domain", *Mol.Biol.Cell*, vol. 20, no. 5, pp. 1565-1575.

Bernardi, R., Guernah, I., Jin, D., Grisendi, S., Alimonti, A., Teruya-Feldstein, J., Cordon-Cardo, C., Simon, M. C., Rafii, S., & Pandolfi, P. P. 2006, "PML inhibits HIF-1alpha translation and neoangiogenesis through repression of mTOR", *Nature*, vol. 442, no. 7104, pp. 779-785.

Berndt, A., Miller, S., Williams, O., Le, D. D., Houseman, B. T., Pacold, J. I., Gorrec, F., Hon, W. C., Liu, Y., Rommel, C., Gaillard, P., Ruckle, T., Schwarz, M. K., Shokat, K. M., Shaw, J. P., & Williams, R. L. 2010, "The p110delta structure: mechanisms for selectivity and potency of new PI(3)K inhibitors", *Nat.Chem.Biol.*, vol. 6, no. 3, p. 244.

Bhaskar, P. T. & Hay, N. 2007, "The two TORCs and Akt", *Dev.Cell*, vol. 12, no. 4, pp. 487-502.

Biondi, R. M., Kieloch, A., Currie, R. A., Deak, M., & Alessi, D. R. 2001, "The PIF-binding pocket in PDK1 is essential for activation of S6K and SGK, but not PKB", *EMBO J.*, vol. 20, no. 16, pp. 4380-4390.

Brachmann, S., Fritsch, C., Maira, S. M., & Garcia-Echeverria, C. 2009, "PI3K and mTOR inhibitors: a new generation of targeted anticancer agents", *Curr.Opin.Cell Biol.*, vol. 21, no. 2, pp. 194-198.

Brugarolas, J., Lei, K., Hurley, R. L., Manning, B. D., Reiling, J. H., Hafen, E., Witters, L. A., Ellisen, L. W., & Kaelin, W. G., Jr. 2004, "Regulation of mTOR function in response to hypoxia by REDD1 and the TSC1/TSC2 tumor suppressor complex", *Genes Dev.*, vol. 18, no. 23, pp. 2893-2904.

Budanov, A. V. & Karin, M. 2008, "p53 target genes sestrin1 and sestrin2 connect genotoxic stress and mTOR signaling", *Cell*, vol. 134, no. 3, pp. 451-460.

Byfield, M. P., Murray, J. T., & Backer, J. M. 2005, "hVps34 is a nutrient-regulated lipid kinase required for activation of p70 S6 kinase", *J.Biol.Chem.*, vol. 280, no. 38, pp. 33076-33082.

Calnan, D. R. & Brunet, A. 2008, "The FoxO code", *Oncogene*, vol. 27, no. 16, pp. 2276-2288.

Castilho, R. M., Squarize, C. H., Chodosh, L. A., Williams, B. O., & Gutkind, J. S. 2009, "mTOR mediates Wnt-induced epidermal stem cell exhaustion and aging", *Cell Stem Cell*, vol. 5, no. 3, pp. 279-289.

Chen, C., Liu, Y., Liu, R., Ikenoue, T., Guan, K. L., Liu, Y., & Zheng, P. 2008, "TSC-mTOR maintains quiescence and function of hematopoietic stem cells by repressing mitochondrial biogenesis and reactive oxygen species", *J.Exp.Med.*, vol. 205, no. 10, pp. 2397-2408.

Choi, J., Chen, J., Schreiber, S. L., & Clardy, J. 1996, "Structure of the FKBP12-rapamycin complex interacting with the binding domain of human FRAP", *Science*, vol. 273, no. 5272, pp. 239-242.

Christie, G. R., Hajduch, E., Hundal, H. S., Proud, C. G., & Taylor, P. M. 2002, "Intracellular sensing of amino acids in Xenopus laevis oocytes stimulates p70 S6 kinase in a target of rapamycin-dependent manner", *J.Biol.Chem.*, vol. 277, no. 12, pp. 9952-9957.

Ciccia, A. & Elledge, S. J. 2010, "The DNA damage response: making it safe to play with knives", *Mol.Cell*, vol. 40, no. 2, pp. 179-204.

Codogno, P. & Meijer, A. J. 2005, "Autophagy and signaling: their role in cell survival and cell death", *Cell Death.Differ.*, vol. 12 Suppl 2, pp. 1509-1518.

Collins, B. J., Deak, M., Arthur, J. S., Armit, L. J., & Alessi, D. R. 2003, "In vivo role of the PIF-binding docking site of PDK1 defined by knock-in mutation", *EMBO J.*, vol. 22, no. 16, pp. 4202-4211.

Corradetti, M. N., Inoki, K., Bardeesy, N., DePinho, R. A., & Guan, K. L. 2004, "Regulation of the TSC pathway by LKB1: evidence of a molecular link between tuberous sclerosis complex and Peutz-Jeghers syndrome", *Genes Dev.*, vol. 18, no. 13, pp. 1533-1538.

Cunningham, J. T., Rodgers, J. T., Arlow, D. H., Vazquez, F., Mootha, V. K., & Puigserver, P. 2007, "mTOR controls mitochondrial oxidative function through a YY1-PGC-1alpha transcriptional complex", *Nature*, vol. 450, no. 7170, pp. 736-740.

Dazert, E. & Hall, M. N. 2011, "mTOR signaling in disease", *Curr.Opin.Cell Biol.*, vol. 23, no. 6, pp. 744-755.

Desai, B. N., Myers, B. R., & Schreiber, S. L. 2002, "FKBP12-rapamycin-associated protein associates with mitochondria and senses osmotic stress via mitochondrial dysfunction", *Proc.Natl.Acad.Sci.U.S.A*, vol. 99, no. 7, pp. 4319-4324.

DeYoung, M. P., Horak, P., Sofer, A., Sgroi, D., & Ellisen, L. W. 2008, "Hypoxia regulates TSC1/2-mTOR signaling and tumor suppression through REDD1-mediated 14-3-3 shuttling", *Genes Dev.*, vol. 22, no. 2, pp. 239-251.

Dorrello, N. V., Peschiaroli, A., Guardavaccaro, D., Colburn, N. H., Sherman, N. E., & Pagano, M. 2006, *Science*, vol. 314, no. 5798, pp. 467-471.

Drenan, R. M., Liu, X., Bertram, P. G., & Zheng, X. F. 2004, "FKBP12-rapamycin-associated protein or mammalian target of rapamycin (FRAP/mTOR) localization in the endoplasmic reticulum and the Golgi apparatus", *J.Biol.Chem.*, vol. 279, no. 1, pp. 772-778.

Dunlop, E. A. & Tee, A. R. 2009, "Mammalian target of rapamycin complex 1: signalling inputs, substrates and feedback mechanisms", *Cell Signal.*, vol. 21, no. 6, pp. 827-835.

Edinger, A. L. & Thompson, C. B. 2002, "Akt maintains cell size and survival by increasing mTOR-dependent nutrient uptake", *Mol.Biol.Cell*, vol. 13, no. 7, pp. 2276-2288.

Ellisen, L. W., Ramsayer, K. D., Johannessen, C. M., Yang, A., Beppu, H., Minda, K., Oliner, J. D., McKeon, F., & Haber, D. A. 2002, "REDD1, a developmentally regulated transcriptional target of p63 and p53, links p63 to regulation of reactive oxygen species", *Mol.Cell*, vol. 10, no. 5, pp. 995-1005.

Engelman, J. A., Chen, L., Tan, X., Crosby, K., Guimaraes, A. R., Upadhyay, R., Maira, M., McNamara, K., Perera, S. A., Song, Y., Chirieac, L. R., Kaur, R., Lightbown, A., Simendinger, J., Li, T., Padera, R. F., Garcia-Echeverria, C., Weissleder, R., Mahmood, U., Cantley, L. C., & Wong, K. K. 2008, "Effective use of PI3K and MEK inhibitors to treat mutant Kras G12D and PIK3CA H1047R murine lung cancers", *Nat.Med.*, vol. 14, no. 12, pp. 1351-1356.

Facchinetti, V., Ouyang, W., Wei, H., Soto, N., Lazorchak, A., Gould, C., Lowry, C., Newton, A. C., Mao, Y., Miao, R. Q., Sessa, W. C., Qin, J., Zhang,

P., Su, B., & Jacinto, E. 2008, "The mammalian target of rapamycin complex 2 controls folding and stability of Akt and protein kinase C", *EMBO J.*, vol. 27, no. 14, pp. 1932-1943.

Feldman, M. E., Apsel, B., Uotila, A., Loewith, R., Knight, Z. A., Ruggero, D., & Shokat, K. M. 2009, "Active-site inhibitors of mTOR target rapamycin-resistant outputs of mTORC1 and mTORC2", *PLoS.Biol.*, vol. 7, no. 2, p. e38.

Feng, Z., Zhang, H., Levine, A. J., & Jin, S. 2005, "The coordinate regulation of the p53 and mTOR pathways in cells", *Proc.Natl.Acad.Sci.U.S.A*, vol. 102, no. 23, pp. 8204-8209.

Findlay, G. M., Yan, L., Procter, J., Mieulet, V., & Lamb, R. F. 2007, "A MAP4 kinase related to Ste20 is a nutrient-sensitive regulator of mTOR signalling", *Biochem.J.*, vol. 403, no. 1, pp. 13-20.

Foster, D. A. 2007, "Regulation of mTOR by phosphatidic acid?", *Cancer Res.*, vol. 67, no. 1, pp. 1-4.

Frias, M. A., Thoreen, C. C., Jaffe, J. D., Schroder, W., Sculley, T., Carr, S. A., & Sabatini, D. M. 2006, "mSin1 is necessary for Akt/PKB phosphorylation, and its isoforms define three distinct mTORC2s", *Curr.Biol.*, vol. 16, no. 18, pp. 1865-1870.

Ganley, I. G., Lam, d. H., Wang, J., Ding, X., Chen, S., & Jiang, X. 2009, "ULK1.ATG13.FIP200 complex mediates mTOR signaling and is essential for autophagy", *J.Biol.Chem.*, vol. 284, no. 18, pp. 12297-12305.

Garami, A., Zwartkruis, F. J., Nobukuni, T., Joaquin, M., Roccio, M., Stocker, H., Kozma, S. C., Hafen, E., Bos, J. L., & Thomas, G. 2003, "Insulin activation of Rheb, a mediator of mTOR/S6K/4E-BP signaling, is inhibited by TSC1 and 2", *Mol.Cell*, vol. 11, no. 6, pp. 1457-1466.

Garcia-Martinez, J. M. & Alessi, D. R. 2008, "mTOR complex 2 (mTORC2) controls hydrophobic motif phosphorylation and activation of serum- and glucocorticoid-induced protein kinase 1 (SGK1)", *Biochem.J.*, vol. 416, no. 3, pp. 375-385.

Garcia-Martinez, J. M., Moran, J., Clarke, R. G., Gray, A., Cosulich, S. C., Chresta, C. M., & Alessi, D. R. 2009, "Ku-0063794 is a specific inhibitor of the mammalian target of rapamycin (mTOR)", *Biochem.J.* , vol. 421, no. 1, pp. 29-42.

Ghosh, S., Tergaonkar, V., Rothlin, C. V., Correa, R. G., Bottero, V., Bist, P., Verma, I. M., & Hunter, T. 2006, "Essential role of tuberous sclerosis genes TSC1 and TSC2 in NF-kappaB activation and cell survival", *Cancer Cell*, vol. 10, no. 3, pp. 215-226.

Groves, M. R., Hanlon, N., Turowski, P., Hemmings, B. A., & Barford, D. 1999, "The structure of the protein phosphatase 2A PR65/A subunit reveals the conformation of its 15 tandemly repeated HEAT motifs", *Cell*, vol. 96, no. 1, pp. 99-110.

Guertin, D. A., Stevens, D. M., Thoreen, C. C., Burds, A. A., Kalaany, N. Y., Moffat, J., Brown, M., Fitzgerald, K. J., & Sabatini, D. M. 2006, "Ablation in mice of the mTORC components raptor, rictor, or mLST8 reveals that mTORC2 is required for signaling to Akt-FOXO and PKCalpha, but not S6K1", *Dev.Cell*, vol. 11, no. 6, pp. 859-871.

Guertin, D. A. & Sabatini, D. M. 2007, "Defining the role of mTOR in cancer", *Cancer Cell*, vol. 12, no. 1, pp. 9-22.

Gwinn, D. M., Shackelford, D. B., Egan, D. F., Mihaylova, M. M., Mery, A., Vasquez, D. S., Turk, B. E., & Shaw, R. J. 2008, "AMPK phosphorylation of raptor mediates a metabolic checkpoint", *Mol.Cell*, vol. 30, no. 2, pp. 214-226.

Hall, M. N. 2008, "mTOR-what does it do?", *Transplant.Proc.*, vol. 40, no. 10 Suppl, p. S5-S8.

Hannan, K. M., Brandenburger, Y., Jenkins, A., Sharkey, K., Cavanaugh, A., Rothblum, L., Moss, T., Poortinga, G., McArthur, G. A., Pearson, R. B., & Hannan, R. D. 2003, "mTOR-dependent regulation of ribosomal gene transcription requires S6K1 and is mediated by phosphorylation of the carboxy-terminal activation domain of the nucleolar transcription factor UBF", *Mol.Cell Biol.*, vol. 23, no. 23, pp. 8862-8877.

Hara, K., Yonezawa, K., Weng, Q. P., Kozlowski, M. T., Belham, C., & Avruch, J. 1998, "Amino acid sufficiency and mTOR regulate p70 S6 kinase and eIF-4E BP1 through a common effector mechanism", *J.Biol.Chem.* , vol. 273, no. 23, pp. 14484-14494.

Hara, K., Maruki, Y., Long, X., Yoshino, K., Oshiro, N., Hidayat, S., Tokunaga, C., Avruch, J., & Yonezawa, K. 2002, "Raptor, a binding partner of target of rapamycin (TOR), mediates TOR action", *Cell*, vol. 110, no. 2, pp. 177-189.

Hardie, D. G. 2007, "AMP-activated/SNF1 protein kinases: conserved guardians of cellular energy", *Nat.Rev.Mol.Cell Biol.*, vol. 8, no. 10, pp. 774-785.

Harrington, L. S., Findlay, G. M., Gray, A., Tolkacheva, T., Wigfield, S., Rebholz, H., Barnett, J., Leslie, N. R., Cheng, S., Shepherd, P. R., Gout, I., Downes, C. P., & Lamb, R. F. 2004, "The TSC1-2 tumor suppressor controls insulin-PI3K signaling via regulation of IRS proteins", *J.Cell Biol.*, vol. 166, no. 2, pp. 213-223.

Harris, T. E. & Lawrence, J. C., Jr. 2003, "TOR signaling", *Sci.STKE.*, vol. 2003, no. 212, p. re15.

Harris, T. E. & Lawrence, J. C., Jr. 2003, "TOR signaling", *Sci.STKE.*, vol. 2003, no. 212, p. re15.

Hay, N. & Sonenberg, N. 2004, "Upstream and downstream of mTOR", *Genes Dev.*, vol. 18, no. 16, pp. 1926-1945.

Hershey, J. W. 1991, "Translational control in mammalian cells", *Annu.Rev.Biochem.*, vol. 60, pp. 717-755.

Holz, M. K., Ballif, B. A., Gygi, S. P., & Blenis, J. 2005, "mTOR and S6K1 mediate assembly of the translation preinitiation complex through dynamic protein interchange and ordered phosphorylation events", *Cell*, vol. 123, no. 4, pp. 569-580.

Horton, L. E., Bushell, M., Barth-Baus, D., Tilleray, V. J., Clemens, M. J., & Hensold, J. O. 2002, "p53 activation results in rapid dephosphorylation of the eIF4E-binding protein 4E-BP1, inhibition of ribosomal protein S6 kinase and inhibition of translation initiation", *Oncogene*, vol. 21, no. 34, pp. 5325-5334.

Hosokawa, N., Hara, T., Kaizuka, T., Kishi, C., Takamura, A., Miura, Y., Iemura, S., Natsume, T., Takehana, K., Yamada, N., Guan, J. L., Oshiro, N., & Mizushima, N. 2009, "Nutrient-dependent mTORC1 association with the ULK1-Atg13-FIP200 complex required for autophagy", *Mol.Biol.Cell*, vol. 20, no. 7, pp. 1981-1991.

Huffman, T. A., Mothe-Satney, I., & Lawrence, J. C., Jr. 2002, "Insulin-stimulated phosphorylation of lipin mediated by the mammalian target of rapamycin", *Proc.Natl.Acad.Sci.U.S.A*, vol. 99, no. 2, pp. 1047-1052.

Ihle, N. T., Lemos, R., Jr., Wipf, P., Yacoub, A., Mitchell, C., Siwak, D., Mills, G. B., Dent, P., Kirkpatrick, D. L., & Powis, G. 2009, "Mutations in the phosphatidylinositol-3-kinase pathway predict for antitumor activity of the inhibitor PX-866 whereas oncogenic Ras is a dominant predictor for resistance", *Cancer Res.*, vol. 69, no. 1, pp. 143-150.

Ikenoue, T., Inoki, K., Yang, Q., Zhou, X., & Guan, K. L. 2008, "Essential function of TORC2 in PKC and Akt turn motif phosphorylation, maturation and signalling", *EMBO J.*, vol. 27, no. 14, pp. 1919-1931.

Inoki, K., Zhu, T., & Guan, K. L. 2003, "TSC2 mediates cellular energy response to control cell growth and survival", *Cell*, vol. 115, no. 5, pp. 577-590.

Inoki, K., Li, Y., Xu, T., & Guan, K. L. 2003, "Rheb GTPase is a direct target of TSC2 GAP activity and regulates mTOR signaling", *Genes Dev.*, vol. 17, no. 15, pp. 1829-1834.

Inoki, K., Ouyang, H., Li, Y., & Guan, K. L. 2005, "Signaling by target of rapamycin proteins in cell growth control", *Microbiol.Mol.Biol.Rev.*, vol. 69, no. 1, pp. 79-100.

Inoki, K., Ouyang, H., Zhu, T., Lindvall, C., Wang, Y., Zhang, X., Yang, Q., Bennett, C., Harada, Y., Stankunas, K., Wang, C. Y., He, X., MacDougald, O. A., You, M., Williams, B. O., & Guan, K. L. 2006, "TSC2 integrates Wnt and energy signals via a coordinated phosphorylation by AMPK and GSK3 to regulate cell growth", *Cell*, vol. 126, no. 5, pp. 955-968.

Jacinto, E., Loewith, R., Schmidt, A., Lin, S., Ruegg, M. A., Hall, A., & Hall, M. N. 2004, "Mammalian TOR complex 2 controls the actin cytoskeleton and is rapamycin insensitive", *Nat.Cell Biol.*, vol. 6, no. 11, pp. 1122-1128.

Jacinto, E., Facchinetti, V., Liu, D., Soto, N., Wei, S., Jung, S. Y., Huang, Q., Qin, J., & Su, B. 2006, "SIN1/MIP1 maintains rictor-mTOR complex integrity and regulates Akt phosphorylation and substrate specificity", *Cell*, vol. 127, no. 1, pp. 125-137.

Jung, C. H., Jun, C. B., Ro, S. H., Kim, Y. M., Otto, N. M., Cao, J., Kundu, M., & Kim, D. H. 2009, "ULK-Atg13-FIP200 complexes mediate mTOR signaling to the autophagy machinery", *Mol.Biol.Cell*, vol. 20, no. 7, pp. 1992-2003.

Kabsch, W. & Sander, C. 1983, "Dictionary of protein secondary structure: pattern recognition of hydrogen-bonded and geometrical features", *Biopolymers*, vol. 22, no. 12, pp. 2577-2637.

Kim, D. H., Sarbassov, D. D., Ali, S. M., King, J. E., Latek, R. R., Erdjument-Bromage, H., Tempst, P., & Sabatini, D. M. 2002, "mTOR interacts with raptor to form a nutrient-sensitive complex that signals to the cell growth machinery", *Cell*, vol. 110, no. 2, pp. 163-175.

Kim, D. H., Sarbassov, D. D., Ali, S. M., Latek, R. R., Guntur, K. V., Erdjument-Bromage, H., Tempst, P., & Sabatini, D. M. 2003, "GbetaL, a positive regulator of the rapamycin-sensitive pathway required for the nutrient-sensitive interaction between raptor and mTOR", *Mol.Cell*, vol. 11, no. 4, pp. 895-904.

Kim, E., Goraksha-Hicks, P., Li, L., Neufeld, T. P., & Guan, K. L. 2008, "Regulation of TORC1 by Rag GTPases in nutrient response", *Nat.Cell Biol.*, vol. 10, no. 8, pp. 935-945.

Laplante, M. & Sabatini, D. M. 2009, "mTOR signaling at a glance", *J.Cell Sci.*, vol. 122, no. Pt 20, pp. 3589-3594.

Laplante, M. & Sabatini, D. M. 2012, "mTOR signaling in growth control and disease", *Cell*, vol. 149, no. 2, pp. 274-293.

Lee, D. F., Kuo, H. P., Chen, C. T., Hsu, J. M., Chou, C. K., Wei, Y., Sun, H. L., Li, L. Y., Ping, B., Huang, W. C., He, X., Hung, J. Y., Lai, C. C., Ding, Q., Su, J. L., Yang, J. Y., Sahin, A. A., Hortobagyi, G. N., Tsai, F. J., Tsai, C. H., & Hung, M. C. 2007, "IKK beta suppression of TSC1 links inflammation and tumor angiogenesis via the mTOR pathway", *Cell*, vol. 130, no. 3, pp. 440-455.

Lee, D. F., Kuo, H. P., Chen, C. T., Wei, Y., Chou, C. K., Hung, J. Y., Yen, C. J., & Hung, M. C. 2008, "IKKbeta suppression of TSC1 function links the mTOR pathway with insulin resistance", *Int.J.Mol.Med.*, vol. 22, no. 5, pp. 633-638.

Leone, M., Crowell, K. J., Chen, J., Jung, D., Chiang, G. G., Sareth, S., Abraham, R. T., & Pellecchia, M. 2006, "The FRB domain of mTOR: NMR

solution structure and inhibitor design", *Biochemistry*, vol. 45, no. 34, pp. 10294-10302.

Li, Y., Inoki, K., Vacratsis, P., & Guan, K. L. 2003, "The p38 and MK2 kinase cascade phosphorylates tuberin, the tuberous sclerosis 2 gene product, and enhances its interaction with 14-3-3", *J.Biol.Chem.*, vol. 278, no. 16, pp. 13663-13671.

Li, Y., Wang, Y., Kim, E., Beemiller, P., Wang, C. Y., Swanson, J., You, M., & Guan, K. L. 2007, "Bnip3 mediates the hypoxia-induced inhibition on mammalian target of rapamycin by interacting with Rheb", *J.Biol.Chem.*, vol. 282, no. 49, pp. 35803-35813.

Li, Y. 2011, "The tandem affinity purification technology: an overview", *Biotechnol.Lett.*, vol. 33, no. 8, pp. 1487-1499.

Liu, L., Cash, T. P., Jones, R. G., Keith, B., Thompson, C. B., & Simon, M. C. 2006, "Hypoxia-induced energy stress regulates mRNA translation and cell growth", *Mol.Cell*, vol. 21, no. 4, pp. 521-531.

Liu, X. & Zheng, X. F. 2007, "Endoplasmic reticulum and Golgi localization sequences for mammalian target of rapamycin", *Mol.Biol.Cell*, vol. 18, no. 3, pp. 1073-1082.

Loewith, R., Jacinto, E., Wullschleger, S., Lorberg, A., Crespo, J. L., Bonenfant, D., Oppliger, W., Jenoe, P., & Hall, M. N. 2002, "Two TOR complexes, only one of which is rapamycin sensitive, have distinct roles in cell growth control", *Mol.Cell*, vol. 10, no. 3, pp. 457-468.

Long, X., Lin, Y., Ortiz-Vega, S., Yonezawa, K., & Avruch, J. 2005, "Rheb binds and regulates the mTOR kinase", *Curr.Biol.*, vol. 15, no. 8, pp. 702-713.

Ma, L., Chen, Z., Erdjument-Bromage, H., Tempst, P., & Pandolfi, P. P. 2005, "Phosphorylation and functional inactivation of TSC2 by Erk implications for tuberous sclerosis and cancer pathogenesis", *Cell*, vol. 121, no. 2, pp. 179-193.

Ma, X. M., Yoon, S. O., Richardson, C. J., Julich, K., & Blenis, J. 2008, "SKAR links pre-mRNA splicing to mTOR/S6K1-mediated enhanced translation efficiency of spliced mRNAs", *Cell*, vol. 133, no. 2, pp. 303-313.

Ma, X. M. & Blenis, J. 2009, "Molecular mechanisms of mTOR-mediated translational control", *Nat.Rev.Mol.Cell Biol.*, vol. 10, no. 5, pp. 307-318.

Manning, B. D. & Cantley, L. C. 2007, "AKT/PKB signaling: navigating downstream", *Cell*, vol. 129, no. 7, pp. 1261-1274.

Mayer, C., Zhao, J., Yuan, X., & Grummt, I. 2004, "mTOR-dependent activation of the transcription factor TIF-IA links rRNA synthesis to nutrient availability", *Genes Dev.*, vol. 18, no. 4, pp. 423-434.

Napoli, K. L. & Taylor, P. J. 2001, "From beach to bedside: history of the development of sirolimus", *Ther.Drug Monit.*, vol. 23, no. 5, pp. 559-586.

Nave, B. T., Ouwens, M., Withers, D. J., Alessi, D. R., & Shepherd, P. R. 1999, "Mammalian target of rapamycin is a direct target for protein kinase B: identification of a convergence point for opposing effects of insulin and amino-acid deficiency on protein translation", *Biochem.J.*, vol. 344 Pt 2, pp. 427-431.

Needleman, S. B. & Wunsch, C. D. 1970, "A general method applicable to the search for similarities in the amino acid sequence of two proteins", *J.Mol.Biol.*, vol. 48, no. 3, pp. 443-453.

Nicklin, P., Bergman, P., Zhang, B., Triantafellow, E., Wang, H., Nyfeler, B., Yang, H., Hild, M., Kung, C., Wilson, C., Myer, V. E., MacKeigan, J. P., Porter, J. A., Wang, Y. K., Cantley, L. C., Finan, P. M., & Murphy, L. O. 2009, "Bidirectional transport of amino acids regulates mTOR and autophagy", *Cell*, vol. 136, no. 3, pp. 521-534.

Nobukuni, T., Joaquin, M., Roccio, M., Dann, S. G., Kim, S. Y., Gulati, P., Byfield, M. P., Backer, J. M., Natt, F., Bos, J. L., Zwartkruis, F. J., & Thomas, G. 2005, "Amino acids mediate mTOR/raptor signaling through activation of class 3 phosphatidylinositol 3OH-kinase", *Proc.Natl.Acad.Sci.U.S.A*, vol. 102, no. 40, pp. 14238-14243.

Nojima, H., Tokunaga, C., Eguchi, S., Oshiro, N., Hidayat, S., Yoshino, K., Hara, K., Tanaka, N., Avruch, J., & Yonezawa, K. 2003, "The mammalian target of rapamycin (mTOR) partner, raptor, binds the mTOR substrates p70 S6 kinase and 4E-BP1 through their TOR signaling (TOS) motif", *J.Biol.Chem.*, vol. 278, no. 18, pp. 15461-15464.

Oshiro, N., Takahashi, R., Yoshino, K., Tanimura, K., Nakashima, A., Eguchi, S., Miyamoto, T., Hara, K., Takehana, K., Avruch, J., Kikkawa, U., & Yonezawa, K. 2007, "The proline-rich Akt substrate of 40 kDa (PRAS40) is a physiological substrate of mammalian target of rapamycin complex 1", *J.Biol.Chem.*, vol. 282, no. 28, pp. 20329-20339.

Panasyuk, G., Nemazanyy, I., Zhyvoloup, A., Filonenko, V., Davies, D., Robson, M., Pedley, R. B., Waterfield, M., & Gout, I. 2009, "mTORbeta splicing isoform promotes cell proliferation and tumorigenesis", *J.Biol.Chem.*, vol. 284, no. 45, pp. 30807-30814.

Peterson, T. R. & Sabatini, D. M. 2005, "eIF3: a connecTOR of S6K1 to the translation preinitiation complex", *Mol.Cell*, vol. 20, no. 5, pp. 655-657.

Peterson, T. R., Laplante, M., Thoreen, C. C., Sancak, Y., Kang, S. A., Kuehl, W. M., Gray, N. S., & Sabatini, D. M. 2009, "DEPTOR is an mTOR inhibitor frequently overexpressed in multiple myeloma cells and required for their survival", *Cell*, vol. 137, no. 5, pp. 873-886.

Polak, P. & Hall, M. N. 2009, "mTOR and the control of whole body metabolism", *Curr.Opin.Cell Biol.*, vol. 21, no. 2, pp. 209-218.

Potter, C. J., Pedraza, L. G., & Xu, T. 2002, "Akt regulates growth by directly phosphorylating Tsc2", *Nat.Cell Biol.*, vol. 4, no. 9, pp. 658-665.

Proud, C. G. 2006, "Regulation of protein synthesis by insulin", *Biochem.Soc.Trans.*, vol. 34, no. Pt 2, pp. 213-216.

Puig, O., Caspary, F., Rigaut, G., Rutz, B., Bouveret, E., Bragado-Nilsson, E., Wilm, M., & Seraphin, B. 2001, "The tandem affinity purification (TAP) method: a general procedure of protein complex purification", *Methods*, vol. 24, no. 3, pp. 218-229.

Reiling, J. H. & Hafen, E. 2004, "The hypoxia-induced paralogs Scylla and Charybdis inhibit growth by down-regulating S6K activity upstream of TSC in Drosophila", *Genes Dev.*, vol. 18, no. 23, pp. 2879-2892.

Reiling, J. H. & Sabatini, D. M. 2006, "Stress and mTORture signaling", *Oncogene*, vol. 25, no. 48, pp. 6373-6383.

Rigaut, G., Shevchenko, A., Rutz, B., Wilm, M., Mann, M., & Seraphin, B. 1999, "A generic protein purification method for protein complex characterization and proteome exploration", *Nat.Biotechnol.*, vol. 17, no. 10, pp. 1030-1032.

Rosner, M., Fuchs, C., Siegel, N., Valli, A., & Hengstschlager, M. 2009, "Functional interaction of mammalian target of rapamycin complexes in regulating mammalian cell size and cell cycle", *Hum.Mol.Genet.*, vol. 18, no. 17, pp. 3298-3310.

Roux, P. P., Ballif, B. A., Anjum, R., Gygi, S. P., & Blenis, J. 2004, "Tumor-promoting phorbol esters and activated Ras inactivate the tuberous sclerosis tumor suppressor complex via p90 ribosomal S6 kinase", *Proc.Natl.Acad.Sci.U.S.A*, vol. 101, no. 37, pp. 13489-13494.

Ryazanov, A. G., Pavur, K. S., & Dorovkov, M. V. 1999, "Alpha-kinases: a new class of protein kinases with a novel catalytic domain", *Curr.Biol.*, vol. 9, no. 2, p. R43-R45.

Sabatini, D. M., Barrow, R. K., Blackshaw, S., Burnett, P. E., Lai, M. M., Field, M. E., Bahr, B. A., Kirsch, J., Betz, H., & Snyder, S. H. 1999, "Interaction of RAFT1 with gephyrin required for rapamycin-sensitive signaling", *Science*, vol. 284, no. 5417, pp. 1161-1164.

Sali, A. & Overington, J. P. 1994, "Derivation of rules for comparative protein modeling from a database of protein structure alignments", *Protein Sci.*, vol. 3, no. 9, pp. 1582-1596.

Sali, A., Potterton, L., Yuan, F., van, V. H., & Karplus, M. 1995, "Evaluation of comparative protein modeling by MODELLER", *Proteins*, vol. 23, no. 3, pp. 318-326.

Sancak, Y., Thoreen, C. C., Peterson, T. R., Lindquist, R. A., Kang, S. A., Spooner, E., Carr, S. A., & Sabatini, D. M. 2007, "PRAS40 is an insulin-

regulated inhibitor of the mTORC1 protein kinase", *Mol.Cell* , vol. 25, no. 6, pp. 903-915.

Sancak, Y., Peterson, T. R., Shaul, Y. D., Lindquist, R. A., Thoreen, C. C., Bar-Peled, L., & Sabatini, D. M. 2008, "The Rag GTPases bind raptor and mediate amino acid signaling to mTORC1", *Science*, vol. 320, no. 5882, pp. 1496-1501.

Sancak, Y., Bar-Peled, L., Zoncu, R., Markhard, A. L., Nada, S., & Sabatini, D. M. 2010, "Ragulator-Rag complex targets mTORC1 to the lysosomal surface and is necessary for its activation by amino acids", *Cell*, vol. 141, no. 2, pp. 290-303.

Sarbassov, D. D., Ali, S. M., Kim, D. H., Guertin, D. A., Latek, R. R., Erdjument-Bromage, H., Tempst, P., & Sabatini, D. M. 2004, "Rictor, a novel binding partner of mTOR, defines a rapamycin-insensitive and raptor-independent pathway that regulates the cytoskeleton", *Curr.Biol.*, vol. 14, no. 14, pp. 1296-1302.

Sarbassov, D. D., Guertin, D. A., Ali, S. M., & Sabatini, D. M. 2005, "Phosphorylation and regulation of Akt/PKB by the rictor-mTOR complex", *Science*, vol. 307, no. 5712, pp. 1098-1101.

Sato, T., Nakashima, A., Guo, L., Coffman, K., & Tamanoi, F. 2010, "Single amino-acid changes that confer constitutive activation of mTOR are discovered in human cancer", *Oncogene*, vol. 29, no. 18, pp. 2746-2752.

Sayle, R. A. & Milner-White, E. J. 1995, "RASMOL: biomolecular graphics for all", *Trends Biochem.Sci.*, vol. 20, no. 9, p. 374.

Schalm, S. S. & Blenis, J. 2002, "Identification of a conserved motif required for mTOR signaling", *Curr.Biol.*, vol. 12, no. 8, pp. 632-639.

Schalm, S. S., Fingar, D. C., Sabatini, D. M., & Blenis, J. 2003, "TOS motif-mediated raptor binding regulates 4E-BP1 multisite phosphorylation and function", *Curr.Biol.*, vol. 13, no. 10, pp. 797-806.

Schieke, S. M., Phillips, D., McCoy, J. P., Jr., Aponte, A. M., Shen, R. F., Balaban, R. S., & Finkel, T. 2006, "The mammalian target of rapamycin (mTOR) pathway regulates mitochondrial oxygen consumption and oxidative capacity", *J.Biol.Chem.*, vol. 281, no. 37, pp. 27643-27652.

Schroder, W. A., Buck, M., Cloonan, N., Hancock, J. F., Suhrbier, A., Sculley, T., & Bushell, G. 2007, "Human Sin1 contains Ras-binding and pleckstrin homology domains and suppresses Ras signalling", *Cell Signal.*, vol. 19, no. 6, pp. 1279-1289.

Scott, P. H., Brunn, G. J., Kohn, A. D., Roth, R. A., & Lawrence, J. C., Jr. 1998, "Evidence of insulin-stimulated phosphorylation and activation of the mammalian target of rapamycin mediated by a protein kinase B signaling pathway", *Proc.Natl.Acad.Sci.U.S.A*, vol. 95, no. 13, pp. 7772-7777.

Sekulic, A., Hudson, C. C., Homme, J. L., Yin, P., Otterness, D. M., Karnitz, L. M., & Abraham, R. T. 2000, "A direct linkage between the phosphoinositide 3-kinase-AKT signaling pathway and the mammalian target of rapamycin in mitogen-stimulated and transformed cells", *Cancer Res.*, vol. 60, no. 13, pp. 3504-3513.

Sengupta, S., Peterson, T. R., & Sabatini, D. M. 2010, "Regulation of the mTOR complex 1 pathway by nutrients, growth factors, and stress", *Mol.Cell*, vol. 40, no. 2, pp. 310-322.

Serra, V., Markman, B., Scaltriti, M., Eichhorn, P. J., Valero, V., Guzman, M., Botero, M. L., Llonch, E., Atzori, F., Di, C. S., Maira, M., Garcia-Echeverria, C., Parra, J. L., Arribas, J., & Baselga, J. 2008, "NVP-BEZ235, a dual PI3K/mTOR inhibitor, prevents PI3K signaling and inhibits the growth of cancer cells with activating PI3K mutations", *Cancer Res.*, vol. 68, no. 19, pp. 8022-8030.

Shah, O. J. & Hunter, T. 2006, "Turnover of the active fraction of IRS1 involves raptor-mTOR- and S6K1-dependent serine phosphorylation in cell culture models of tuberous sclerosis", *Mol.Cell Biol.*, vol. 26, no. 17, pp. 6425-6434.

Shaw, R. J., Bardeesy, N., Manning, B. D., Lopez, L., Kosmatka, M., DePinho, R. A., & Cantley, L. C. 2004, "The LKB1 tumor suppressor negatively regulates mTOR signaling", *Cancer Cell*, vol. 6, no. 1, pp. 91-99.

Sofer, A., Lei, K., Johannessen, C. M., & Ellisen, L. W. 2005, "Regulation of mTOR and cell growth in response to energy stress by REDD1", *Mol.Cell Biol.*, vol. 25, no. 14, pp. 5834-5845.

Stambolic, V., MacPherson, D., Sas, D., Lin, Y., Snow, B., Jang, Y., Benchimol, S., & Mak, T. W. 2001, "Regulation of PTEN transcription by p53", *Mol.Cell*, vol. 8, no. 2, pp. 317-325.

Sturgill, T. W. & Hall, M. N. 2009, "Activating mutations in TOR are in similar structures as oncogenic mutations in PI3KCalpha", *ACS Chem.Biol.*, vol. 4, no. 12, pp. 999-1015.

Takahashi, T., Hara, K., Inoue, H., Kawa, Y., Tokunaga, C., Hidayat, S., Yoshino, K., Kuroda, Y., & Yonezawa, K. 2000, "Carboxyl-terminal region conserved among phosphoinositide-kinase-related kinases is indispensable for mTOR function in vivo and in vitro", *Genes Cells*, vol. 5, no. 9, pp. 765-775.

Tee, A. R. & Proud, C. G. 2002, "Caspase cleavage of initiation factor 4E-binding protein 1 yields a dominant inhibitor of cap-dependent translation and reveals a novel regulatory motif", *Mol.Cell Biol.*, vol. 22, no. 6, pp. 1674-1683.

Tee, A. R., Anjum, R., & Blenis, J. 2003, "Inactivation of the tuberous sclerosis complex-1 and -2 gene products occurs by phosphoinositide 3-kinase/Akt-dependent and -independent phosphorylation of tuberin", *J.Biol.Chem.*, vol. 278, no. 39, pp. 37288-37296.

Tee, A. R. & Blenis, J. 2005, "mTOR, translational control and human disease", *Semin.Cell Dev.Biol.*, vol. 16, no. 1, pp. 29-37.

Thedieck, K., Polak, P., Kim, M. L., Molle, K. D., Cohen, A., Jeno, P., Arrieumerlou, C., & Hall, M. N. 2007, "PRAS40 and PRR5-like protein are new mTOR interactors that regulate apoptosis", *PLoS.One.*, vol. 2, no. 11, p. e1217.

Thompson, J. D., Higgins, D. G., & Gibson, T. J. 1994, "CLUSTAL W: improving the sensitivity of progressive multiple sequence alignment through sequence weighting, position-specific gap penalties and weight matrix choice", *Nucleic Acids Res.*, vol. 22, no. 22, pp. 4673-4680.

Thoreen, C. C., Kang, S. A., Chang, J. W., Liu, Q., Zhang, J., Gao, Y., Reichling, L. J., Sim, T., Sabatini, D. M., & Gray, N. S. 2009, "An ATP-competitive mammalian target of rapamycin inhibitor reveals rapamycin-resistant functions of mTORC1", *J.Biol.Chem.*, vol. 284, no. 12, pp. 8023-8032.

Tirado, O. M., Mateo-Lozano, S., Sanders, S., Dettin, L. E., & Notario, V. 2003, "The PCPH oncoprotein antagonizes the proapoptotic role of the mammalian target of rapamycin in the response of normal fibroblasts to ionizing radiation", *Cancer Res.*, vol. 63, no. 19, pp. 6290-6298.

Torbett, N. E., Luna-Moran, A., Knight, Z. A., Houk, A., Moasser, M., Weiss, W., Shokat, K. M., & Stokoe, D. 2008, "A chemical screen in diverse breast cancer cell lines reveals genetic enhancers and suppressors of sensitivity to PI3K isoform-selective inhibition", *Biochem.J.*, vol. 415, no. 1, pp. 97-110.

Toschi, A., Lee, E., Xu, L., Garcia, A., Gadir, N., & Foster, D. A. 2009, "Regulation of mTORC1 and mTORC2 complex assembly by phosphatidic acid: competition with rapamycin", *Mol.Cell Biol.*, vol. 29, no. 6, pp. 1411-1420.

Tremblay, F., Brule, S., Hee, U. S., Li, Y., Masuda, K., Roden, M., Sun, X. J., Krebs, M., Polakiewicz, R. D., Thomas, G., & Marette, A. 2007, "Identification of IRS-1 Ser-1101 as a target of S6K1 in nutrient- and obesity-induced insulin resistance", *Proc.Natl.Acad.Sci.U.S.A*, vol. 104, no. 35, pp. 14056-14061.

Tzatsos, A. 2009, "Raptor binds the SAIN (Shc and IRS-1 NPXY binding) domain of insulin receptor substrate-1 (IRS-1) and regulates the phosphorylation of IRS-1 at Ser-636/639 by mTOR", *J.Biol.Chem.*, vol. 284, no. 34, pp. 22525-22534.

Vander, H. E., Lee, S. I., Bandhakavi, S., Griffin, T. J., & Kim, D. H. 2007, "Insulin signalling to mTOR mediated by the Akt/PKB substrate PRAS40", *Nat.Cell Biol.*, vol. 9, no. 3, pp. 316-323.

Vega-Rubin-de-Celis, S., Abdallah, Z., Kinch, L., Grishin, N. V., Brugarolas, J., & Zhang, X. 2010, "Structural analysis and functional implications of the negative mTORC1 regulator REDD1", *Biochemistry*, vol. 49, no. 11, pp. 2491-2501.

Walker, E. H., Pacold, M. E., Perisic, O., Stephens, L., Hawkins, P. T., Wymann, M. P., & Williams, R. L. 2000, "Structural determinants of phosphoinositide 3-kinase inhibition by wortmannin, LY294002, quercetin, myricetin, and staurosporine", *Mol.Cell*, vol. 6, no. 4, pp. 909-919.

Wang, L., Harris, T. E., Roth, R. A., & Lawrence, J. C., Jr. 2007, "PRAS40 regulates mTORC1 kinase activity by functioning as a direct inhibitor of substrate binding", *J.Biol.Chem.*, vol. 282, no. 27, pp. 20036-20044.

Wang, L., Harris, T. E., & Lawrence, J. C., Jr. 2008, "Regulation of proline-rich Akt substrate of 40 kDa (PRAS40) function by mammalian target of rapamycin complex 1 (mTORC1)-mediated phosphorylation", *J.Biol.Chem.*, vol. 283, no. 23, pp. 15619-15627.

Wang, X., Campbell, L. E., Miller, C. M., & Proud, C. G. 1998, "Amino acid availability regulates p70 S6 kinase and multiple translation factors", *Biochem.J.*, vol. 334 (Pt 1), pp. 261-267.

Wang, X., Beugnet, A., Murakami, M., Yamanaka, S., & Proud, C. G. 2005, "Distinct signaling events downstream of mTOR cooperate to mediate the effects of amino acids and insulin on initiation factor 4E-binding proteins", *Mol.Cell Biol.*, vol. 25, no. 7, pp. 2558-2572.

Wang, Z., Malone, M. H., Thomenius, M. J., Zhong, F., Xu, F., & Distelhorst, C. W. 2003, "Dexamethasone-induced gene 2 (dig2) is a novel pro-survival stress gene induced rapidly by diverse apoptotic signals", *J.Biol.Chem.*, vol. 278, no. 29, pp. 27053-27058.

Withers, D. J., Ouwens, D. M., Nave, B. T., van der Zon, G. C., Alarcon, C. M., Cardenas, M. E., Heitman, J., Maassen, J. A., & Shepherd, P. R. 1997, "Expression, enzyme activity, and subcellular localization of mammalian target of rapamycin in insulin-responsive cells", *Biochem.Biophys.Res.Commun.*, vol. 241, no. 3, pp. 704-709.

Wouters, B. G. & Koritzinsky, M. 2008, "Hypoxia signalling through mTOR and the unfolded protein response in cancer", *Nat.Rev.Cancer*, vol. 8, no. 11, pp. 851-864.

Wullschleger, S., Loewith, R., & Hall, M. N. 2006, "TOR signaling in growth and metabolism", *Cell*, vol. 124, no. 3, pp. 471-484.

Yang, H. S., Jansen, A. P., Komar, A. A., Zheng, X., Merrick, W. C., Costes, S., Lockett, S. J., Sonenberg, N., & Colburn, N. H. 2003, "The transformation suppressor Pdcd4 is a novel eukaryotic translation initiation factor 4A binding protein that inhibits translation", *Mol.Cell Biol.*, vol. 23, no. 1, pp. 26-37.

Yang, Q. & Guan, K. L. 2007, "Expanding mTOR signaling", *Cell Res.*, vol. 17, no. 8, pp. 666-681.

Yip, C. K., Murata, K., Walz, T., Sabatini, D. M., & Kang, S. A. 2010, "Structure of the human mTOR complex I and its implications for rapamycin inhibition", *Mol.Cell*, vol. 38, no. 5, pp. 768-774.

Yoshida, T., Mett, I., Bhunia, A. K., Bowman, J., Perez, M., Zhang, L., Gandjeva, A., Zhen, L., Chukwueke, U., Mao, T., Richter, A., Brown, E., Ashush, H., Notkin, N., Gelfand, A., Thimmulappa, R. K., Rangasamy, T., Sussan, T., Cosgrove, G., Mouded, M., Shapiro, S. D., Petrache, I., Biswal, S., Feinstein, E., & Tuder, R. M. 2010, "Rtp801, a suppressor of mTOR signaling, is an essential mediator of cigarette smoke-induced pulmonary injury and emphysema", *Nat.Med.*, vol. 16, no. 7, pp. 767-773.

Yu, K., Toral-Barza, L., Shi, C., Zhang, W. G., Lucas, J., Shor, B., Kim, J., Verheijen, J., Curran, K., Malwitz, D. J., Cole, D. C., Ellingboe, J., Ayral-Kaloustian, S., Mansour, T. S., Gibbons, J. J., Abraham, R. T., Nowak, P., & Zask, A. 2009, "Biochemical, cellular, and in vivo activity of novel ATP-competitive and selective inhibitors of the mammalian target of rapamycin", *Cancer Res.*, vol. 69, no. 15, pp. 6232-6240.

Zhang, H., Cicchetti, G., Onda, H., Koon, H. B., Asrican, K., Bajraszewski, N., Vazquez, F., Carpenter, C. L., & Kwiatkowski, D. J. 2003, "Loss of Tsc1/Tsc2 activates mTOR and disrupts PI3K-Akt signaling through downregulation of PDGFR", *J.Clin.Invest*, vol. 112, no. 8, pp. 1223-1233.